

EISSN 2979-9139



Official Journal of
TURKISH
THORACIC SOCIETY

Thoracic

Research & Practice

Formerly Turkish Thoracic Journal



Thoracic Research & Practice

Official Journal of the Turkish Thoracic Society

EDITORS in CHIEF

Metin AKGÜN 

Ağrı İbrahim Çeçen University Faculty of Medicine, Department of Pulmonary Medicine, Ağrı, Türkiye

Begüm ERGAN 

Department of Chest Diseases, Dokuz Eylül University Faculty of Medicine, İzmir, Türkiye

EDITORS

Alphabetically in order:

Aylin ÖZGEN ALPAYDIN 

Department of Chest Diseases, Dokuz Eylül University Faculty of Medicine, İzmir, Türkiye

Buğra KERGET 

Department of Chest Diseases, Aksaray University Faculty of Medicine, Aksaray, Türkiye

Canan GÜNDÜZ GÜRKAN 

Department of Chest Diseases, İstanbul Medipol University, İstanbul, Türkiye Hospital, İstanbul, Türkiye

Cüneyt SALTÜRK 

Department of Chest Diseases, İstanbul Medipol University, İstanbul, Türkiye

Ebru DAMADOĞLU 

Department of Chest Diseases, Hacettepe University Faculty of Medicine, Ankara, Türkiye

Ege GÜLEÇ BALBAY 

Department of Chest Diseases, Düzce University Faculty of Medicine, Düzce, Türkiye

İlknur BAŞYİĞİT 

Department of Chest Diseases, Kocaeli University Faculty of Medicine, Kocaeli, Türkiye

İpek ÇAYLI CANDEMİR 

Department of Chest Diseases, Atatürk Chest Diseases and Surgery Training and Research Hospital, Ankara, Türkiye

Nagehan EMİRALİOĞLU ORDUKAYA 

Department of Pediatric Pulmonology, Hacettepe University Faculty of Medicine, Ankara, Türkiye

Necati ÇITAK 

Department of Thoracic Surgery, University of Health Sciences Türkiye, Bakırköy Dr. Sadi Konuk Training and Research Hospital, İstanbul, Türkiye

Özlem KAR KURT 

Department of Occupational Medicine, Yedikule Chest Diseases and Thoracic Surgery Training and Research Hospital, İstanbul, Türkiye

Refika ERSU 

Department of Pediatrics, Division of Respiratory, Children's Hospital of Eastern Ontario (CHEO), University of Ottawa, Ottawa, Ontario, Canada

Tamer ALTINOK 

Department of Chest Diseases, Necmettin Erbakan University Faculty of Medicine, Konya, Türkiye

Tuncay GÖKSEL 

Department of Pulmonary Medicine, Ege University Faculty of Medicine, İzmir, Türkiye
Department of Translational Pulmonology, Ege University Institute of Health Sciences, İzmir, Türkiye

BIostatistical CONSULTANT

Ahmet Uğur DEMİR 

Department of Chest Diseases, Hacettepe University School of Medicine, Ankara, Türkiye

Seval KUL 

Department of Biostatistics and Medical Informatics, Gaziantep University School of Medicine, Gaziantep, Türkiye

PUBLICATION COORDINATOR

Oğuz KILINÇ 

İzmir University of Economics, School of Medicine, İzmir, Türkiye



Publisher Contact

Address: Molla Gürani Mah. Kaçamak Sk.

No: 21/1 34093 İstanbul, Türkiye

Phone: +90 (530) 177 30 97

E-mail: info@galenos.com.tr Web: www.galenos.com.tr

Publisher Certificate Number: 14521

Online Publication Date: May 2026

E-ISSN: 2979-9139

International scientific journal published bimonthly.



Thoracic Research & Practice

Official Journal of the Turkish Thoracic Society

EDITORIAL BOARD

A. Fuat Kalyoncu

Department of Chest Diseases, Hacettepe University
Faculty of Medicine, Ankara, Türkiye

Arzu Yorgancıoğlu

Department of Chest Diseases, Manisa Celal Bayar
University Faculty of Medicine, Manisa, Türkiye

Aslı Görek Dilektaşlı

Department of Chest Diseases, Bursa Uludağ University
Faculty of Medicine, Bursa, Türkiye

Benoit Nemery

Department of Public Health and Primary Care, Centre
for Environment and Health, KU Leuven Faculty of
Medicine, Leuven, Belgium

David Koh

Saw Swee Hock School of Public Health, National
University of Singapore, Singapore; University of
Occupational and Environmental Health, Kitakyushu,
Japan

Eyüp Sabri Uçan

Department of Chest Diseases, Dokuz Eylül University
Faculty of Medicine, İzmir, Türkiye

Hasan Bayram

University Research Center for Translational Medicine
(KUTTAM), Koç University Faculty of Medicine;
Department of Pulmonary Medicine, Koç University
Faculty of Medicine, İstanbul, Türkiye

İpek Kivılcım Oğuzülgen

Department of Pulmonary Diseases, Gazi University
Faculty of Medicine, Ankara, Türkiye

Joao Winck

Cardiovascular R&D Centre, Faculdade de Medicina da
Universidade do Porto, Portugal

Kent E. Pinkerton

University of California, Davis, Center for Health and the
Environment, Davis, USA

Lara Pisani

Respiratory and Critical Care Unit, IRCCS Azienda
Ospedaliero-Universitaria di Bologna; Alma Mater
Studiorum, Department of Medical and Surgical
Sciences (DIMEC), University of Bologna, Bologna, Italy

Leyla Pur Özyiğit

Department of Allergy and Immunology, University
Hospitals of Leicester, Leicester, United Kingdom

Nurdan Köktürk

Department of Chest Diseases, Gazi University Faculty
of Medicine, Ankara, Türkiye

Özge Yılmaz

Department of Pediatrics, Celal Bayar University Faculty
of Medicine, Manisa, Türkiye

Richard Casaburi

Rehabilitation Clinical Trials Center, Los Angeles
Biomedical Research Institute at Harbor-UCLA Medical
Center, Torrance, California, USA

Ufuk Çağırıcı

Department of Chest Surgery, Ege University Faculty of
Medicine, İzmir, Türkiye

Zuhal Karakurt

Respiratory Intensive Care Unit, Süreyyapaşa Chest
Diseases and Surgery Training and Research Hospital,
İstanbul, Türkiye



Thoracic Research & Practice

Official Journal of the Turkish Thoracic Society

ABOUT

About the Thoracic Research and Practice

Thoracic Research and Practice is a peer reviewed, open access, online-only journal published by the Turkish Thoracic Society.

Thoracic Research and Practice is a bimonthly journal that is published in English in January, March, May, July, September, and November.

Journal History

Thoracic Research and Practice started its publication life following the merger of two journals which were published under the titles "Turkish Respiratory Journal" and "Toraks Journal" until 2008. From 2008 to 2022, the journal was published under the title "Turkish Thoracic Journal". Archives of the journals were transferred to Thoracic Research and Practice.

Abstracting and Indexing

Thoracic Research and Practice is covered in the following abstracting and indexing databases; PubMed Central, Web of Science - Emerging Sources Citation Index, Scopus, EMBASE, EBSCO, CINAHL, Gale/Cengage Learning, ProQuest, DOAJ, CNKI, TUBITAK ULAKBIM TR Index.

Aims, Scope, and Audience

Thoracic Research and Practice aims to publish studies of the highest scientific and clinical value, and encourages the submission of high-quality research that advances the understanding and treatment of pulmonary diseases.

Thoracic Research and Practice covers a wide range of topics related to adult and pediatric pulmonary diseases, as well as thoracic imaging, environmental and occupational disorders, intensive care, sleep disorders and thoracic surgery, including diagnostic methods, treatment techniques, and prevention strategies. The journal is interested in publishing original research that addresses important clinical questions and advances the understanding and treatment of these conditions. This may include studies on the effectiveness of different treatments, new diagnostic tools or techniques, and novel approaches to preventing or managing pulmonary diseases.

Thoracic Research and Practice publishes clinical and basic research articles, reviews, statements of agreement or disagreement on controversial issues, national and international consensus reports, systematic reviews and meta-analyses, letters to the editor and editorials. Conference proceedings may also be considered for publication.

The target audience of the journal includes healthcare professionals and researchers who are interested in or working in the pulmonary diseases field, and related disciplines.

Open Access Policy

Thoracic Research and Practice is an open access publication.

Starting on January 2022 issue, all content published in the journal is licensed under the Creative Commons Attribution-NonCommercial (CC BY-NC) 4.0 International License which allows third parties to use the content for non-commercial purposes as long as they give credit to the original work. This license allows for the content to be shared and adapted for non-commercial purposes, promoting the dissemination and use of the research published in the journal.

The content published before January 2022 was licensed under a traditional copyright, but the archive is still available for free access.

All published content is available online, free of charge at thoracrespract.org.

When using previously published content, including figures, tables, or any other material in both print and electronic formats, authors must obtain permission from the copyright holder. Legal, financial and criminal liabilities in this regard belong to the author(s).



Thoracic Research & Practice

Official Journal of the Turkish Thoracic Society

Copyright Policy

A Copyright Agreement and Acknowledgement of Authorship form should be submitted with all manuscripts. By signing this form, authors transfer the copyright of their work to the Turkish Thoracic Society and agree that the article, if accepted for publication by the Thoracic Research and Practice will be licensed under a Creative Commons Attribution-Non Commercial 4.0 International License (CC BY-NC 4.0) which permits third parties to share and adapt the content for non-commercial purposes by giving the appropriate credit to the original work.

When using previously published content, including figures, tables, or any other material in both print and electronic formats, authors must obtain permission from the copyright holder. Legal, financial and criminal liabilities in this regard belong to the author(s).

Authors retain the copyright of their published work in the Thoracic Research and Practice.

Publication Fee Policy

Thoracic Research and Practice is funded by the Turkish Thoracic Society. Authors are not required to pay any fees during the evaluation and publication process.

You can find the current version of the Instructions to Authors at <https://thoracrespract.org/instructions-to-authors>.



Thoracic Research & Practice

Official Journal of the Turkish Thoracic Society

CONTENTS

ORIGINAL ARTICLES

- 132 Prognostic Significance of Computed Tomography Severity Score for Machine Learning Prediction of Intensive Care Unit Admission in COVID-19 Patients**
Seyed Salman Zakariaee, Ali Sohrabnejad, Mostafa Shanbehzadeh, Negar Naderi; Ilam, Tehran, Iran
- 141 Seasonal Oxidative Stress and Airway Reactivity in Rhinitis: Distinct Patterns in Allergic vs. Non-allergic Individuals**
Sümeysra Alan Yalım, Ayşe Füsün Kalpaklıoğlu, Ayşe Baççioğlu; Afyonkarahisar, Kırıkkale, Türkiye
- 148 Reliability and Validity of the Turkish Version of the Lung Transplant-specific Valued Life Activities Scale**
Ulaş Ar, Erdal Yekeler, Ebru Çalık, Fatmanur Çelik Başaran, Sinan Türkkın; Ankara, Türkiye
- 155 Compliance of Aerosol Therapy with Evidence-based Guideline and Cost Incurred in Adult Critically-ill Patients: A Prospective Observational Study**
Ayushi R. Verma, Jignesh Shah, Sulochana Kumari, Asavari L. Raut, Steffi Abraham, Ritu Priya, Kinjal K. Patil; Maharashtra, India
- 165 Cost Analysis of Tuberculosis Disease in the Case of Tuberculosis Control Dispensary**
Dolunay Özlem Zeybek, Mustafa Zeybek, İskender Çetintürk, Yasemin Aslan, Filiz Özyiğit; Balıkesir, Bilecik, Isparta, Türkiye
- 173 Clinical Characteristics of Moderate-to-Severe Obstructive Sleep Apnea: A Cross-sectional Analysis of 12,715 Adults from the TURKAPNE Cohort**
Baran Balcan, Aylin Phtılı, Esen Kıyan, Mehmet Sezai Taşbakan, Özen K. Başoğlu, Şenay Aydın, Aykut Çilli, Neşe Dursunoğlu, Nur Aleyna Yetkin, Yüksel Peker, TURKAPNE Study Group; İstanbul, İzmir, Antalya, Denizli, Kayseri, Bursa, Düzce, Erzurum, Afyon, Edirne, Eskişehir, Ankara, Balıkesir, Diyarbakır, Isparta, Adana, Ağrı, Tekirdağ, Kocaeli, Türkiye; Gothenburg, Lund, Sweden; PA, USA

REVIEW

- 182 The Impact of the Exposome on Epithelial Barriers: New Approach Methodologies for Translational Research**
Pelın Sağlam-Metiner-, Ebru Calkan-Yıldırım, Basar Dogan, R. Dilara Vaizoglu, Cigdem Elif Celik, Ozlem Goksel, Ozlem Yesil-Celiktas, Levent Pelit, Yasin Kaymaz, Henrik Kløverpris-, Douglas S. Kwon, Carla F. Kim, Petros Koutrakis, Cezmi Akdis, Omer H. Yilmaz, Tuncay Goksel; İzmir, Ankara, Türkiye; Copenhagen, Denmark; Durban, South Africa; MA, Massachusetts, USA; Respiratory Diseases, Boston; Davos, Switzerland




LETTERS TO THE EDITOR

- 195 Comment on: Letter to the Editor Regarding CT-based Prediction of Lung Cancer Histology**
Fani Tsolaki; Thessaloniki, Greece
- 196 Response to: Letter to the Editor Regarding CT-based Prediction of Lung Cancer Histology**
Fadlan Adima Adrianta, Dini Rachma Erwati, Suryanti Dwi Pratiwi, Nanik Setijowati; Malang, Indonesia

Original Article



Prognostic Significance of Computed Tomography Severity Score for Machine Learning Prediction of Intensive Care Unit Admission in COVID-19 Patients

 Seyed Salman Zakariaee¹,  Ali Sohrabnejad²,  Mostafa Shanbehzadeh³,  Negar Naderi⁴

¹Department of Medical Physics, Faculty of Paramedical Sciences, Ilam University of Medical Sciences, Ilam, Iran

²Department of Health Services Management, School of Health Management and Information Sciences, Iran University of Medical Sciences, Tehran, Iran

³Department of Health Information Management, Faculty of Paramedical Sciences, Ilam University of Medical Sciences, Ilam, Iran

⁴Department of Midwifery, Faculty of Nursing and Midwifery, Ilam University of Medical Sciences, Ilam, Iran

Cite this article as: Zakariaee SS, Sohrabnejad A, Shanbehzadeh M, Naderi N. Prognostic significance of computed tomography severity score for machine learning prediction of intensive care unit admission in COVID-19 patients. *Thorac Res Pract.* 2026;27(3):132-140

ABSTRACT

OBJECTIVE: The computed tomography-severity score (CT-SS) quantifies the severity of pulmonary involvement and is significantly associated with disease severity, intensive care unit (ICU) admissions, and mortality in coronavirus disease-2019 (COVID-19) patients. There is very limited information on the prognostic value of CT-SS when used in machine learning (ML) models to predict ICU admission in COVID-19 patients. In this study, the prognostic significance of CT-SS in ML model-based prediction of ICU admission among COVID-19 patients was evaluated.

MATERIAL AND METHODS: In this retrospective study, a hospital-based database from 6,854 COVID-19 patients was reviewed. To evaluate the prognostic significance of CT-SS in predicting ICU admission in patients, seven ML methods were trained separately using the most important features, with and without CT-SS data, and their performances were compared.

RESULTS: After applying exclusion criteria, 815 COVID-19 patients remained. Just over half of the patients (54.85%) were male, and the mean age was 57.22 ± 16.76 years. The CT-SS index was the strongest predictor among the parameters examined, and integrating this index into the training dataset enhanced ML model performance. The k-nearest neighbors model with 93.3% accuracy, 97.3% sensitivity, 89.4% specificity, and an area under the curve of approximately 98.8% showed the best performance for predicting ICU admission in COVID-19 patients.

CONCLUSION: The results showed that CT-SS is a key predictor for ML models of ICU admission in COVID-19 patients. The ML models developed using a dataset including CT-SS are efficient risk stratification tools for identifying critical COVID-19 patients, thereby facilitating optimal allocation of limited hospital resources.

KEYWORDS: CT severity score, COVID-19, CT-SS, machine learning, ICU admission

Received: 30.07.2025

Revision Requested: 22.09.2025

Last Revision Received: 14.10.2025

Accepted: 12.11.2025

Epub: 15.01.2026

Publication Date: 12.05.2026

INTRODUCTION

The coronavirus disease-2019 (COVID-19) pandemic presented unprecedented challenges to healthcare systems, leading to an overwhelming influx of patients and a critical shortage of resources.^{1,2} Since the initial reports of the COVID-19 outbreak emerged in mid-December 2019, over 689 million individuals have been infected globally as of May 23, 2023.³ The COVID-19 virus exhibits high transmissibility and complex, heterogeneous, and evolving clinical features, resulting in a significant increase in patient morbidity and mortality.⁴⁻⁶

Corresponding author: Seyed Salman Zakariaee, MD, e-mail: salman_zakariaee@yahoo.com

Among patients diagnosed with COVID-19, approximately 14% to 20% experience severe or critical illness,⁷ characterized by clinical manifestations, including acute respiratory distress syndrome, myocarditis, cardiac or septic shock, and multi-organ failure. These manifestations often necessitate hospitalization in intensive care units (ICUs) and can lead to death.^{4,8} Given the high mortality among COVID-19 patients hospitalized in the ICU, reported to be as high as 50%,⁷ early risk stratification is essential for effective patient management and optimal allocation of medical resources. It is estimated that 20% to 30% of hospitalized patients require ICU admission,⁹ with this rate varying based on the specific characteristics of the study population.⁸

ICU resources are severely limited, with more than 50% of them frequently occupied under normal conditions.^{8,9} Therefore, there is an urgent need for effective tools to predict patient outcomes and to facilitate appropriate triage of patients. Numerous clinical and demographic parameters associated with disease severity and ICU admission have been documented.^{7,8,10-19} These prognostic variables are critical for identifying patients at high-risk who require intensive care during hospitalization. Identifying relevant predictors ultimately leads to enhanced management of high-risk COVID-19 patients and optimal use of ICU capacity. Artificial intelligence (AI) offers a useful approach to develop an effective clinical risk-prediction tool for ICU admission among COVID-19 patients.^{4,9} Machine learning (ML) models, as a subset of AI, leverage vast datasets to identify patterns and predict outcomes with high precision. Using ML algorithms, clinicians can stratify patients based on their risk of deterioration, allowing for timely interventions that may improve survival rates and reduce the burden on ICUs.^{1,2}

Previous studies have employed ML methods that were developed using demographic data, risk factors, clinical symptoms, and laboratory results to predict ICU admissions among hospitalized COVID-19 patients. Notably, most of these studies did not include radiological indicators in their

datasets.^{4,9,20-23} The computed tomography-severity score (CT-SS) is a key predictor that measures the severity of pulmonary involvement and is significantly correlated with disease severity, ICU admissions, and mortality in COVID-19 patients.^{5,6,14,18,24-27} Therefore, adding CT-SS to other predictors could improve the predictive power of ML models for clinical outcomes in COVID-19 patients and aid their clinical management. There is very limited information on the prognostic value of CT-SS for predicting ICU admission of COVID-19 patients using ML models. In this study, the prognostic significance of CT-SS for predicting ICU admission in COVID-19 patients was evaluated using the ML method. For this purpose, ML models were developed separately using datasets with and without CT-SS data, and their performances were compared.

MATERIAL AND METHODS

Dataset Description

In this retrospective study, a hospital-based database of COVID-19 patient information was analyzed. During initial screening of individuals referred to the COVID-19 referral center between 9 February and 20 December 2020, 6,854 suspected cases were identified. Out of these registered cases, 1,853 were confirmed as positive for COVID-19 through reverse transcriptase–polymerase chain reaction (RT-PCR) testing. The exclusion criteria for the study included: 1) a negative RT-PCR COVID-19 result, 2) absence of laboratory or CT-SS results, 3) age under 18 years, 4) discharge or death without ICU admission, and 5) unknown patient disposition. After applying these criteria, 815 records were retained for analysis. The patient selection flowchart is shown in Figure 1.

The dataset comprised 54 primary features derived from patient information that included 5 demographic variables, 14 clinical presentations, 7 medical histories, 26 laboratory results, 1

Main Points

- For predicting intensive care unit (ICU) admission of coronavirus disease-2019 (COVID-19) patients, computed tomography-severity score (CT-SS) is a highly relevant predictor: it differs significantly between patients admitted to the ICU and those not admitted, highlighting the necessity of including this parameter in machine learning (ML) models.
- The prognostic performance of the ML models for predicting ICU admission in COVID-19 patients was improved by integrating CT-SS data with other prognostic parameters.
- The k-nearest neighbors model, with 93.3% accuracy, 97.3% sensitivity, 89.4% specificity, 90.1% precision, 93.6% F-measure, and an area under the curve of 98.8%, had the best performance in predicting ICU admission in patients with COVID-19.
- The ML models developed using a dataset that includes CT-SS can more effectively identify vulnerable and critical patients, thereby optimizing the allocation of limited hospital resources.

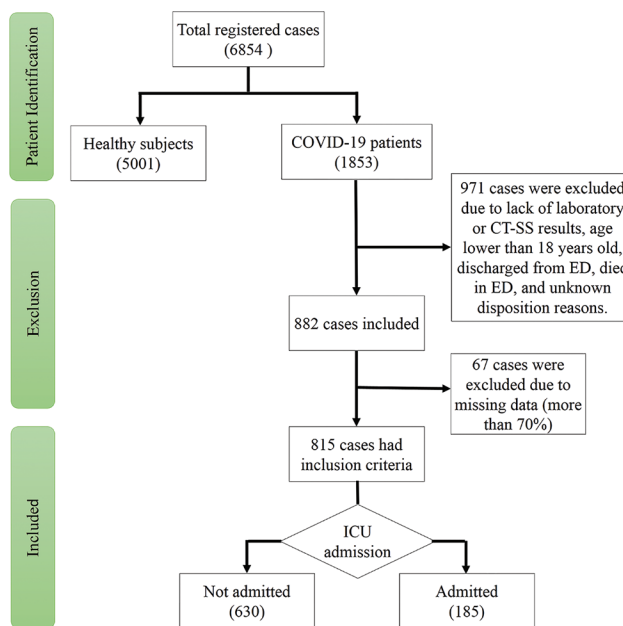


Figure 1. Flow chart describing patient selection

COVID-19: coronavirus disease-2019, CT-SS: computed tomography-severity score, ED: emergency department, ICU: intensive care unit

radiological measure (CT-SS), and 1 outcome variable (0 for non-ICU-admitted patients and 1 for ICU-admitted patients). The CT-SS index evaluates the severity of pulmonary involvement across five lung lobes, with each lobe assigned a visual score ranging from 0 to 5 based on the extent of involvement. The total CT-SS, ranging from 0 to 25, was derived by summing these scores.^{1,2,5,27} Two thoracic radiologists, each with a minimum of 10 years of experience, reviewed the high-resolution chest CT images. In the event of disagreement between the two observers, discrepancies were resolved by consulting a senior radiologist. Figure 2 illustrates CT images of COVID-19 patients with different degrees of pulmonary involvement.

Data Pre-processing

Records with more than 70% missing data were excluded. Abnormal, noisy, and irrelevant data were reviewed and corrected in consultation with an infectious disease specialist. Missing values for continuous and discrete variables were imputed using mean and mode values, respectively.

The refined dataset included 185 ICU-admitted patients and 630 non-ICU patients, highlighting a significant imbalance that could bias the results toward non-ICU patients. This imbalance was addressed using the synthetic minority over-sampling technique (SMOTE) (<https://imbalanced-learn.org/stable/>). The SMOTE technique is an advanced algorithm designed to address data imbalance commonly encountered in data mining. SMOTE operates by generating synthetic examples of the minority class rather than merely duplicating existing instances. It identifies

instances of the minority class and, for each instance, calculates the distances to its k-nearest neighbors (k-NN) within the same class. By interpolating between a minority instance and its neighbors, SMOTE creates synthetic data points that enrich the minority-class distribution. This process not only balances the class distribution but also enhances the model’s ability to learn the decision boundaries between classes, leading to improved predictive performance.^{1,2}

Feature Selection

The feature selection process aimed to identify parameters that were highly correlated with the target outcome, thereby significantly reducing the risk of overfitting in ML algorithms. In this study, the Boruta feature selection package was used to assess the significance of features in predicting ICU admission in COVID-19 patients. This methodology functions as a wrapper around a random forest (RF) algorithm. The Boruta algorithm evaluates the importance of features in predicting the target outcome. It determines the significance of each feature using importance values derived from shadow attributes created by randomly shuffling original attribute values across subjects. The importance of a feature is quantified using a Z-score, calculated as the mean loss in classification accuracy divided by the feature’s standard deviation. The maximum Z-score of the shadow attributes (MZSA) is identified; any attribute with an importance value exceeding this score is considered relevant. On the other hand, attributes with importance values lower than the MZSA are deemed insignificant. This iterative process continues with the elimination of shadow attributes

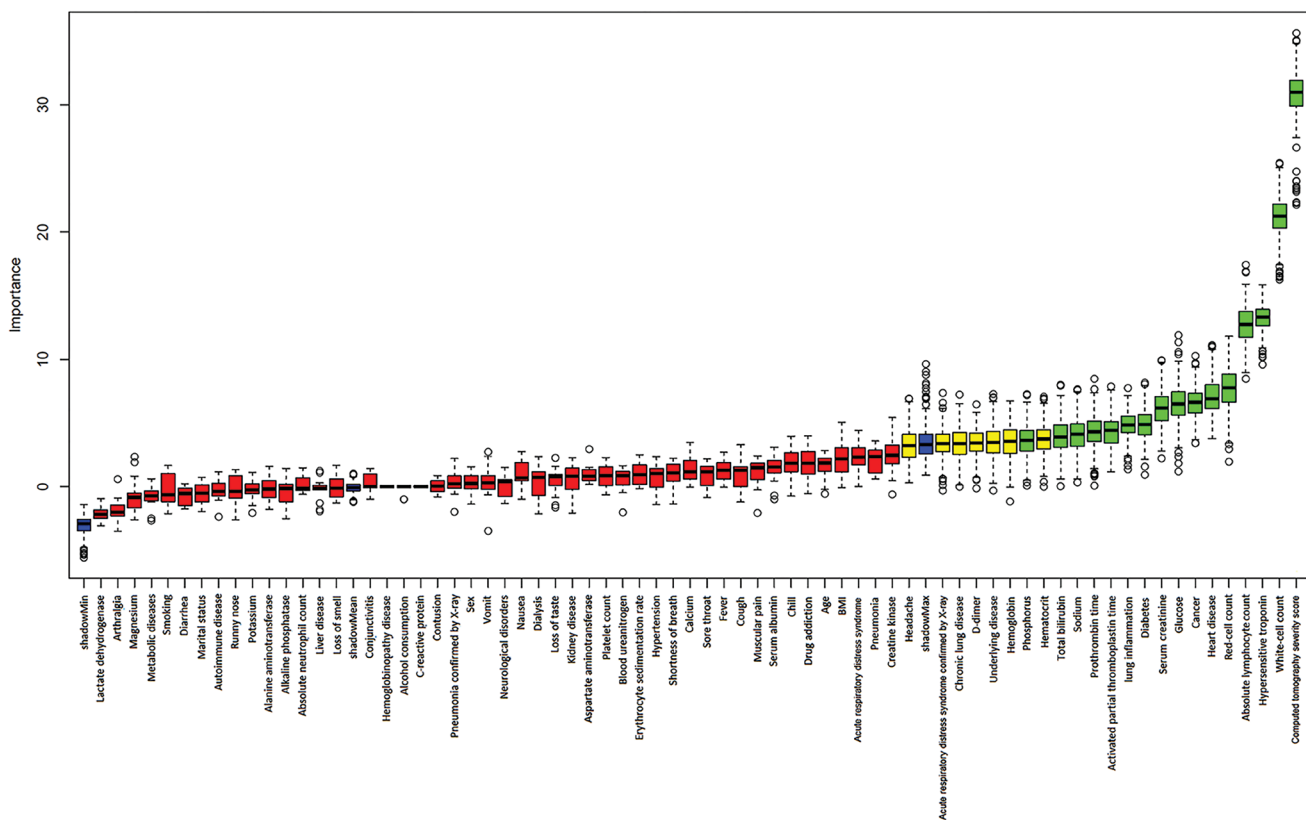


Figure 2. Chart of the Boruta algorithm for feature selection in predicting ICU admission of COVID-19 patients. Green, yellow, and red boxes show the confirmed, tentative, and irrelevant features. Blue boxes represent the minimum, average, and maximum of shadow variables

until the significance of all features is reliably determined. The maximum number of importance source runs and the verbosity level (doTrace) were set to 500 and 2, respectively.^{1,2}

Model Development

To evaluate the prognostic significance of CT-SS for ICU admission among COVID-19 patients, seven ML methods were used: logistic regression (LR), k-NN, multilayer perceptron (MLP), support vector machines (SVM), eXtreme gradient boosting (XGB), RF, and C4.5 decision tree (DT). These ML models were developed using Waikato Environment for Knowledge Analysis software (version 3.9.2, University of Waikato, New Zealand). The attributes selected in the feature selection step were used as input for training and testing ML models.

To optimize the performance of each ML model, hyperparameter tuning was performed using random search. Random search explores the hyperparameter space by sampling values from predefined distributions or ranges. Random search offers great flexibility and efficiency when dealing with a large number of hyperparameters or when the optimal parameter values are less intuitive or not known. The hyperparameters tuned for each ML model are listed in Table 1.

The ML models were trained separately on datasets with and without CT-SS to evaluate the prognostic role of CT-SS in ML-based prediction of ICU admissions among patients with COVID-19. A 10-fold cross-validation method was used to examine the performance of the developed classifiers. The classification performance of each model in predicting ICU admission among COVID-19 patients was assessed using sensitivity, specificity, accuracy, and area under the receiver operating characteristic (ROC) curve (AUC).

Ethical Considerations

This article is extracted from a research project supported by Ilam University of Medical Sciences, and all experimental protocols were approved by the Ethical Committee of Ilam University of Medical Sciences (approved number: IR.MEDILAM.REC.1402.294, approval date: 11.03.2024). All methods used in the study were performed in accordance with the relevant guidelines and regulations of the Ethics Committee

of Ilam University of Medical Sciences. This study used information from a hospital-based registry, and no intervention was performed on patients’ treatment procedures. Patient identification information was anonymized to protect patient confidentiality and privacy. All data generated and analyzed during the current study are not publicly available but will be shared by the corresponding author upon reasonable request.

RESULTS

After applying inclusion/exclusion criteria, a total of 815 COVID-19 patients were included in the study. Slightly more than half of the patients (447, 54.85%) were male, and the mean age was 57.22±16.76 years. Among the included patients, 185 (22.7%) were admitted to the ICU, increasing the number of records in this class to 630 after balancing the dataset.

Feature Selection

In the feature-selection step, the most important features for predicting ICU admission in COVID-19 patients were identified using the Boruta algorithm. Twenty-three variables were selected as the most important features for output prediction. The variable importance diagram for predicting ICU admission among COVID-19 patients is shown in Figure 3. In this diagram, the parameters shown in green, yellow, and red boxes are the confirmed, tentative, and irrelevant features, respectively. The confirmed or most important features selected in this step were used to develop ML models.

Evaluation of the Developed Models

The prediction of ICU admission in COVID-19 patients was performed using seven ML models, including LR, k-NN, MLP, SVM, XGB, RF, and C4.5 DT algorithm. These models were trained separately using the most important features, with and without CT-SS data, and their performance was compared to assess the prognostic significance of CT-SS for ML-based prediction of ICU admission among COVID-19 patients. The sensitivity, specificity, accuracy, precision, F-measure, and AUC indices for the ML models developed using datasets with and without CT-SS data are summarized in Table 2. Among all the models evaluated, the k-NN algorithm demonstrated the best predictive performance for ICU admission in COVID-19

Table 1. The hyperparameters tuned for ML models

| ML algorithm | Tuned hyperparameters |
|---------------------------|---|
| Logistic regression | The regularization strength (L1 and L2), and the ridge value in the log-likelihood (ridge) |
| Support vector machines | The complexity parameter C, and the type of kernel function |
| Multilayer perceptron | The amount the weights are updated (learningRate), the number of hidden layers, the momentum applied to the weights during updating, and the number of epochs to train |
| k-nearest neighbors | The number of neighbors to use (k), the distance weighting method, and the nearest neighbor search algorithm |
| EXtreme gradient boosting | The number of trees, the maximum depth, and the learning rate. |
| C4.5 decision tree | The number of trees, maximum depth, the confidence factor used for pruning (confidenceFactor), the amount of data used for reduced-error pruning, and the minimum number of instances per leaf |
| Random forest | The number of trees, maximum depth, size of each bag as a percentage of the training set size, the number of iterations to be performed, the number of execution slots (threads) to use for constructing the ensemble, the number of randomly chosen attributes, and minimum samples required to split a node |

ML: machine learning

Table 2. Performances of ML models for predicting ICU admission of COVID-19 patients

| ML algorithm | Sensitivity (%) | | Specificity (%) | | Accuracy (%) | | Precision (%) | | F-measure(%) | | AUC (%) | |
|---------------------------|-----------------------|--------------------|-----------------------|--------------------|-----------------------|--------------------|-----------------------|--------------------|-----------------------|--------------------|-----------------------|--------------------|
| | Dataset without CT-SS | Dataset with CT-SS | Dataset without CT-SS | Dataset with CT-SS | Dataset without CT-SS | Dataset with CT-SS | Dataset without CT-SS | Dataset with CT-SS | Dataset without CT-SS | Dataset with CT-SS | Dataset without CT-SS | Dataset with CT-SS |
| Logistic regression | 72.2 | 75.9 | 76.3 | 81.0 | 74.3 | 78.4 | 75.3 | 79.9 | 73.7 | 77.9 | 81.3 | 85.5 |
| Support vector machines | 73.3 | 76.3 | 77.0 | 80.5 | 75.2 | 78.4 | 76.1 | 79.6 | 74.7 | 78.0 | 75.2 | 78.4 |
| Multilayer perceptron | 96.5 | 94.9 | 80.5 | 83.5 | 88.5 | 89.2 | 83.2 | 85.2 | 89.3 | 89.8 | 93.3 | 93.4 |
| k-nearest neighbors | 96.2 | 97.3 | 86.8 | 89.4 | 91.5 | 93.3 | 88.0 | 90.1 | 91.9 | 93.6 | 98.4 | 98.8 |
| C4.5 decision tree | 87.8 | 87.3 | 77.3 | 80.5 | 82.5 | 83.9 | 79.5 | 81.7 | 83.4 | 84.4 | 87.1 | 88.6 |
| Random forest | 96.5 | 97.8 | 86.0 | 87.5 | 91.3 | 92.6 | 87.4 | 88.6 | 91.7 | 93.0 | 97.7 | 98.3 |
| EXtreme gradient boosting | 95.7 | 97.2 | 84.3 | 85.3 | 89.9 | 91.1 | 85.6 | 86.5 | 90.3 | 91.5 | 94.6 | 95.4 |

ML: machine learning, ICU: intensive care unit, COVID-19: coronavirus disease-2019, CT-SS: computed tomography-severity score, AUC: area under the curve

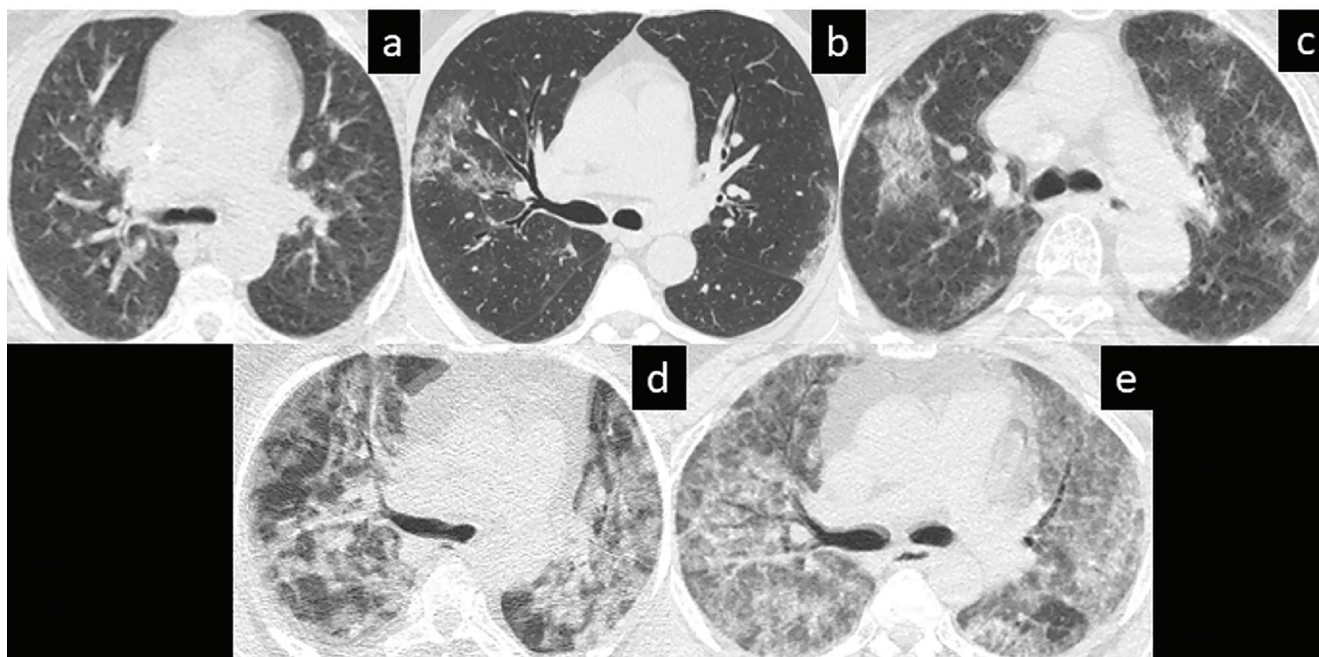


Figure 3. The exemplary chest CT images of COVID-19 patients with CT-SSs of 5 (a), 10 (b), 15 (c), 20 (d), and 25 (e). These CT images show less than 5% involvement, 5%-25% involvement, 25%-50% involvement, 50%-75% involvement, and more than 75% involvement, respectively

CT: computed tomography, COVID-19: coronavirus disease-2019, SS: severity score

patients. The RF, XGB, and MLP models (AUC >93%) were ranked next and demonstrated performance comparable to that of the k-NN model.

The sensitivity, specificity, accuracy, precision, F-measure, and AUC indices for the k-NN algorithm developed using the dataset without CT-SS data were 96.2%, 86.8%, 91.5%, 88.0%, 91.9%, and 98.4%, respectively. For the CT-SS dataset, the k-NN algorithm yielded 97.3% sensitivity, 89.4% specificity,

93.3% accuracy, 90.1% precision, 93.6% F-measure, and an AUC of 98.8%.

Figure 4 compares ROC curves of ML models developed using datasets with and without CT-SS data.

The integration of CT-SS data into the training dataset, consisting of demographic data, clinical symptoms, and laboratory results, enhanced the performance of the ML models.

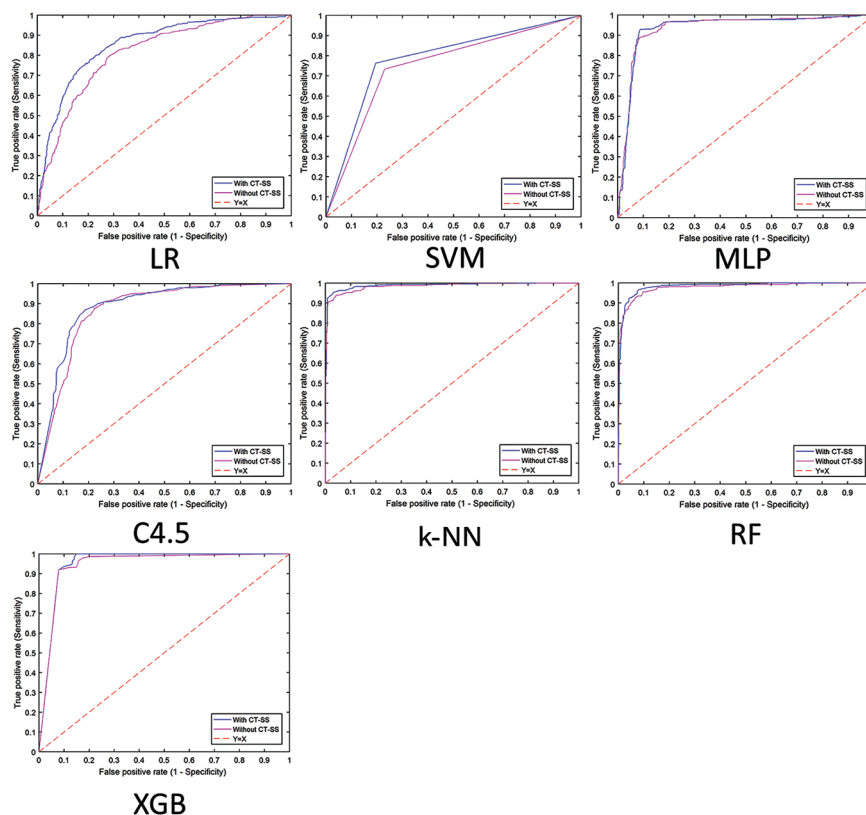


Figure 4. ROC curves of ML models developed using the datasets with and without CT-SS data

ROC: receiver operating characteristic, ML: machine learning, CT-SS: computed tomography-severity score, LR: logistic regression, SVM: support vector machines, MLP: multilayer perceptron, k-NN: k-nearest neighbors, RF: random forest, XGB: eXtreme gradient boosting

DISCUSSION

In disease outbreaks such as the COVID-19 pandemic, healthcare systems face a growing influx of patients and significant constraints on hospital resources.⁹ Therefore, identifying disease-related risk factors and developing an effective predictive model to evaluate the risk of adverse outcomes can help healthcare systems optimize patient management and efficiently allocate limited medical resources. Pioneering studies have demonstrated that chest CT is a robust tool for identifying and monitoring the disease progression of COVID-19 because of its high sensitivity in depicting the severity of pulmonary involvement.^{6,14,18,24-26} Although a significant correlation between CT-SS and COVID-19 severity and the likelihood of ICU admission has been established, its prognostic value in ML model-based prediction of ICU admission among COVID-19 patients has not yet been evaluated. In this study, the prognostic significance of CT-SS in predicting ICU admission of COVID-19 patients was evaluated using the ML method. The results showed that CT-SS data are a strong predictor of ICU admission among COVID-19 patients, and that integrating this index with other predictors improves ML models' performance in predicting ICU hospitalization. Among the models studied, the k-NN model yielded the best performance for predicting ICU admission of COVID-19 patients.

In the first step, the importance of demographic characteristics, underlying diseases, clinical symptoms, laboratory results, and the CT-SS index for predicting ICU admission among COVID-19

patients was evaluated using the Boruta method. The results of the feature-selection step indicated that the CT-SS index was the strongest predictor among the parameters examined. COVID-19 patients admitted to the ICU had a higher mean CT-SS than those not admitted (13.9 ± 6.6 vs. 10.4 ± 4.6); this difference was statistically significant ($P < 0.001$). Therefore, CT-SS is a strong predictor of ICU admission among COVID-19 patients, and integrating this index with other predictors could improve ML models' performance in predicting ICU hospitalization.

Twenty-three features, including white blood cell count, blood glucose level, creatinine, bilirubin, lung inflammation, heart disease, diabetes, and CT-SS, were selected as the most relevant parameters to predict ICU admission in COVID-19 patients using the Boruta method. The importance of these parameters in predicting ICU admission among COVID-19 patients has also been confirmed by other studies. Previous studies have indicated that elderly COVID-19 patients exhibiting abnormal laboratory results (such as hemoglobin, hematocrit, lymphocyte count, creatinine levels, etc.) and multiple comorbidities (such as diabetes, heart disease, chronic obstructive pulmonary disease, and chest tightness), along with radiological manifestations of extensive pulmonary involvement, are at an elevated risk of developing severe illness, leading to ICU admission.^{7,8,12,14-17,19,28,29}

The selected predictors were used as input for training the ML models. The models were separately developed using

datasets with and without CT-SS data. The performance of the ML models was then compared to determine the role of CT-SS parameters in predicting ICU hospitalization among patients. Across all ML models studied, integrating CT-SS parameters into the input dataset improved the models' prognostic performance for identifying COVID-19 patients admitted to the ICU. The best classification performance in predicting ICU admission in COVID-19 patients was achieved by the k-NN model. The sensitivity, specificity, accuracy, precision, F1-measure, and AUC indices of the k-NN model developed using the dataset with CT-SS were 97.3%, 89.4%, 93.3%, 90.1%, 93.6%, and 98.8%, respectively.

Prior studies have also evaluated ML techniques for predicting ICU admission of COVID-19 patients. Shanbehzadeh et al.⁹ employed artificial neural network, DT, k-NN, SVM, and RF algorithms to predict ICU admissions among 1,225 laboratory-confirmed COVID-19 patients. Their findings indicated that the RF model outperformed other techniques. The mean accuracy, mean specificity, mean sensitivity, and root mean square error of the RF model were 99.5%, 99.7%, 99.4%, and 0.015 respectively. The k-NN algorithm, ranked next, achieved a mean accuracy of 94.1%, a mean sensitivity of 99.5%, and a mean specificity of 88.7%. The dataset used to develop the ML models in this study did not include imaging data, and the study aimed to investigate the performance of ML models in predicting the likelihood that COVID-19 patients would be admitted to the ICU. Overall, the performance of the ML models developed in this study for predicting the likelihood of COVID-19 patients being admitted to the ICU was in very close agreement with that of models developed in our research. The slight differences in results could be attributed to variations in the study population and the type of information used as input for model development. The results of this study confirm our findings.

In the study by Zakariaee et al.¹, ML models were developed to predict ICU admission and length of stay (LOS) of COVID-19 patients using a dataset comprising demographics, risk factors, clinical manifestations, laboratory results, and CT-SS. For predicting ICU admission of COVID-19 patients, the performance comparison of eight ML models indicates that the k-NN model, with 97.0% sensitivity, 89.7% specificity, 93.3% accuracy, 90.4% precision, 93.6% F-measure, and 99.1% AUC, yields the best results. The RF, MLP, and XGB models (with AUC >91%) were ranked next and had performance comparable to that of the k-NN model. The advantage of this study over similar studies was that the dataset used to develop ML models included radiological manifestations. In this study, the performance of ML models for predicting the likelihood of patient admission to the ICU was examined. However, the prognostic value of the CT-SS parameter was not evaluated. The performance of our models was similar to that of the models developed in this study, which confirms our findings.

The prognostic value of CT-SS parameters for predicting mortality and clinical outcomes in patients with COVID-19 has been investigated in studies by Zakariaee et al.^{2,5} In study designs similar to ours, the prognostic value of CT-SS for predicting mortality, hospital LOS, and ICU LOS among COVID-19 patients was investigated using four ML models:

k-NN, MLP, SVM, and the C4.5 DT. In these studies, ML models were also developed separately using datasets with and without CT data, and their performances were compared to determine the prognostic value of the CT-SS index. The results of these studies showed that the CT-SS index is among the strongest predictors of COVID-19 progression and related complications, and that integrating this parameter into the datasets used to develop ML models improves their predictive performance.

These studies highlight the potential of ML methods to facilitate the timely and accurate identification of patients at risk for severe illness. An efficient risk stratification tool to predict ICU admissions of COVID-19 patients could significantly mitigate severe complications and associated mortality. Our findings indicate that the integration of CT-SS data with the input dataset for the ML models improves the performance of these models in predicting ICU admission among COVID-19 patients. Consequently, ML models developed using a dataset including CT-SS data can more effectively identify vulnerable and critical patients, thereby optimizing the allocation of limited hospital resources.

Study Limitations

This study has several limitations that should be acknowledged. First, the sample sizes across the data classes were significantly imbalanced. The number of patients not admitted to the ICU was much higher than that of those admitted (630 vs. 185). The SMOTE technique was used to address the dataset's imbalance. In most data mining studies, class imbalance in sample sizes is a persistent problem. Many solutions, including oversampling of minority-class data, undersampling of majority-class data, and advanced methods such as SMOTE have been proposed to address this problem. In healthcare scenarios, many conditions are underrepresented in datasets due to their rarity, which can lead to biased models that fail to accurately predict outcomes for minority populations. Solutions such as oversampling the minority class cannot solve this problem, but the SMOTE method simulates real-world situations to generate examples. This method certainly has limitations in simulating real-world conditions, but it has advantages over other approaches because new samples are generated from existing ones rather than merely repeating them. By augmenting these datasets using synthetic examples, SMOTE enables more robust training of ML models, thereby improving their ability to generalize across diverse patient populations. This enhanced model performance can lead to more accurate risk assessments, timely interventions, and ultimately better patient outcomes. Furthermore, the use of synthetic data can facilitate the development of predictive models in clinical settings where data collection is constrained by privacy concerns or logistical challenges.

Second, prior studies developed ML models that utilized demographics, risk factors, clinical manifestations, and laboratory predictors but did not integrate radiological imaging data. In our study, the integration of CT-SS data with other predictors enriched the input dataset for developing ML models. Third, the study's design was retrospective and limited to a single center. Further research with larger sample sizes and multicenter datasets is required to enhance the generalizability of the results. Finally, the prediction of ICU admission for COVID-19 patients was based on clinical predictors at the time

of admission. Consequently, the selected features, as relevant predictors, and the developed models may be employed to predict ICU admissions at initial hospitalization of COVID-19 patients.

Conclusion

In this study, the prognostic significance of CT-SS in predicting ICU admissions for COVID-19 patients was evaluated using ML models. Our results showed that the integration of CT-SS data with other clinical predictors enhanced the prognostic performance of ML algorithms for ICU admission among COVID-19 patients. The k-NN algorithm yielded the best predictive performance among the evaluated ML techniques. The ML models developed from datasets including demographics, risk factors, clinical manifestations, laboratory results, and CT-SS data are effective tools for risk stratification to identify critically ill COVID-19 patients, thereby facilitating optimal allocation of limited hospital resources. ML predictive models can significantly enhance the timely and accurate identification of patients at risk for severe illness, ultimately reducing the incidence of severe complications and associated mortality.

Ethics

Ethics Committee Approval: Ethical committee of Ilam University of Medical Sciences (approved number: IR.MEDILAM.REC.1402.294, approval date: 11.03.2024).

Informed Consent: Informed consent was waived because of the retrospective nature of the study and anonymous data was used in the data analysis.

Acknowledgements

The authors would like to thank the Research Deputy of Ilam University of Medical Sciences and we also would like to thank all experts who participated in this study.

Footnotes

Authorship Contributions

Surgical and Medical Practices: S.S.Z., M.S., N.N., Concept: S.S.Z., Design: S.S.Z., Data Collection or Processing: S.S.Z., A.S., M.S., N.N., Analysis or Interpretation: S.S.Z., A.S., M.S., Literature Search: S.S.Z., A.S., M.S., N.N., Writing: S.S.Z., A.S., M.S., N.N.

Conflict of Interest: No conflict of interest was declared by the authors.

Financial Disclosure: This article is extracted from a research project supported by Ilam University of Medical Sciences (grant no: 2004/7).

REFERENCES

- Zakariaee SS, Naderi N, Kazemi-Arpanahi H. Development of machine learning prediction models to predict ICU admission and the length of stay in ICU for COVID-19 patients using a clinical dataset including chest computed tomography severity score data. *Gazi Med J.* 2025;36(3):278-286. [\[Crossref\]](#)
- Zakariaee SS, Molazadeh M, Salmanipour H, Naderi N. Additive value of computed tomography severity scores to predict lengths of stay in hospital and ICU for COVID-19 patients: a machine learning study. *J Biostat Epidemiol.* 2025;10(4):469-483. [\[Crossref\]](#)
- Worldometer COVID-19 Data [Internet]. Accessed May 23, 2023. [\[Crossref\]](#)
- Orooji A, Kazemi-Arpanahi H, Kaffashian M, Kalvandi G, Shanbehzadeh M. Comparing of machine learning algorithms for predicting ICU admission in COVID-19 hospitalized patients. *Health Promot Pract.* 2021;9(3):229-236. [\[Crossref\]](#)
- Zakariaee SS, Abdi AI, Naderi N, Babashahi M. Prognostic significance of chest CT severity score in mortality prediction of COVID-19 patients, a machine learning study. *Egypt J Radiol Nucl Med.* 2023;54(1):73. [\[Crossref\]](#)
- Zakariaee SS, Naderi N, Rezaee D. Prognostic accuracy of visual lung damage computed tomography score for mortality prediction in patients with COVID-19 pneumonia: a systematic review and meta-analysis. *Egypt J Radiol Nucl Med.* 2022;53(1):1-9. [\[Crossref\]](#)
- Pan P, Li Y, Xiao Y, et al. Prognostic assessment of COVID-19 in the intensive care unit by machine learning methods: model development and validation. *J Med Internet Res.* 2020;22(11):e23128. [\[Crossref\]](#)
- Sadeghi A, Eslami P, Dooghaie Moghadam A, et al. COVID-19 and ICU admission associated predictive factors in Iranian patients. *Caspian J Intern Med.* 2020;11(Suppl 1):512-519. [\[Crossref\]](#)
- Shanbehzadeh M, Haghiri H, Afrash MR, Amraei M, Erfannia L, Kazemi-Arpanahi H. Comparison of machine learning tools for the prediction of ICU admission in COVID-19 hospitalized patients. *Shiraz E-Med J.* 2022;23(5):e117849. [\[Crossref\]](#)
- Halacli B, Kaya A, Topeli A. Critically-ill COVID-19 patient. *Turk J Med Sci.* 2020;50(SI-1):585-591. [\[Crossref\]](#)
- Phua J, Weng L, Ling L, et al. Intensive care management of coronavirus disease 2019 (COVID-19): challenges and recommendations. *Lancet Respir Med.* 2020;8(5):506-517. [\[Crossref\]](#)
- Assaf D, Gutman Y, Neuman Y, et al. Utilization of machine-learning models to accurately predict the risk for critical COVID-19. *Intern Emerg Med.* 2020;15(8):1435-1443. [\[Crossref\]](#)
- Foieni F, Sala G, Mognarelli JG, et al. Derivation and validation of the clinical prediction model for COVID-19. *Intern Emerg Med.* 2020;15(8):1409-1414. [\[Crossref\]](#)
- Wu G, Yang P, Xie Y, et al. Development of a clinical decision support system for severity risk prediction and triage of COVID-19 patients at hospital admission: an international multicentre study. *Eur Respir J.* 2020;56(2):2001104. [\[Crossref\]](#)
- Agieb R. Machine learning models for the prediction the necessity of resorting to icu of COVID-19 patients. *Int J Adv Trends Comput Sci Eng.* 2020;9(5):6980-6984. [\[Crossref\]](#)
- Liang W, Liang H, Ou L, et al. Development and validation of a clinical risk score to predict the occurrence of critical illness in hospitalized patients with COVID-19. *JAMA Intern Med.* 2020;180(8):1081-1089. [\[Crossref\]](#)
- Zhou Y, He Y, Yang H, et al. Exploiting an early warning nomogram for predicting the risk of ICU admission in patients with COVID-19: a multi-center study in China. *Scand J Trauma Resusc Emerg Med.* 2020;28(1):106. [\[Crossref\]](#)
- Allenbach Y, Saadoun D, Maalouf G, et al. Development of a multivariate prediction model of intensive care unit transfer or death: a French prospective cohort study of hospitalized COVID-19 patients. *PLoS One.* 2020;15(10):e0240711. [\[Crossref\]](#)

19. Zhao Z, Chen A, Hou W, et al. Prediction model and risk scores of ICU admission and mortality in COVID-19. *PLoS One*. 2020;15(7):e0236618. [\[Crossref\]](#)
20. Shanbehzadeh M, Nopour R, Kazemi-Arpanahi H. Using decision tree algorithms for estimating ICU admission of COVID-19 patients. *Inform Med Unlocked*. 2022;30:100919. [\[Crossref\]](#)
21. Crowley G, Kwon S, Mengling L, Nolan A. ICU Admission and mortality prediction in severe COVID-19: a machine learning approach. *Am J Respir Crit Care Med*. 2021;203:A2564. [\[Crossref\]](#)
22. Saadatmand S, Salimifard K, Mohammadi R, Kuiper A, Marzban M, Farhadi A. Using machine learning in prediction of ICU admission, mortality, and length of stay in the early stage of admission of COVID-19 patients. *Ann Oper Res*. 2022:1-29. [\[Crossref\]](#)
23. Subudhi S, Verma A, Patel AB, et al. Comparing machine learning algorithms for predicting ICU admission and mortality in COVID-19. *NPJ Digit Med*. 2021;4(1):87. [\[Crossref\]](#)
24. Zakariaee SS, Salmanipour H, Naderi N, Kazemi-Arpanahi H, Shanbehzadeh M. Association of chest CT severity score with mortality of COVID-19 patients: a systematic review and meta-analysis. *Clin Transl Imaging*. 2022;10(6):663-676. [\[Crossref\]](#)
25. Galzin E, Roche L, Vlachomitrou A, et al. Additional value of chest CT AI-based quantification of lung involvement in predicting death and ICU admission for COVID-19 patients. *Res Diagn Interv Imaging*. 2022;4:100018. [\[Crossref\]](#)
26. Laino ME, Ammirabile A, Lofino L, et al. Prognostic findings for ICU admission in patients with COVID-19 pneumonia: baseline and follow-up chest CT and the added value of artificial intelligence. *Emerg Radiol*. 2022;29(2):243-262. [\[Crossref\]](#)
27. Zakariaee SS, Naderi N, Ebrahimi M, Kazemi-Arpanahi H. Comparing machine learning algorithms to predict COVID-19 mortality using a dataset including chest computed tomography severity score data. *Sci Rep*. 2023;13(1):1-12. [\[Crossref\]](#)
28. Li X, Ge P, Zhu J, et al. Deep learning prediction of likelihood of ICU admission and mortality in COVID-19 patients using clinical variables. *PeerJ*. 2020;8:e10337. [\[Crossref\]](#)
29. Ryan L, Lam C, Mataraso S, et al. Mortality prediction model for the triage of COVID-19, pneumonia, and mechanically ventilated ICU patients: a retrospective study. *Ann Med Surg (Lond)*. 2020;59:207-216. [\[Crossref\]](#)

Original Article

Seasonal Oxidative Stress and Airway Reactivity in Rhinitis: Distinct Patterns in Allergic vs. Non-allergic Individuals

Sümeýra Alan Yalým¹, Ayşe Füsün Kalpaklıođlu², Ayşe Baççíođlu²¹Department of Immunology and Allergic Diseases, Afyonkarahisar Health Sciences University, Afyonkarahisar, Türkiye²Department of Immunology and Allergic Diseases, Kırıkkale University Faculty of Medicine, Kırıkkale, Türkiye

Cite this article as: Alan Yalým S, Kalpaklıođlu AF, Baççíođlu A. Seasonal oxidative stress and airway reactivity in rhinitis: distinct patterns in allergic vs. non-allergic individuals. *Thorac Res Pract.* 2026;27(3):141-147

ABSTRACT

OBJECTIVE: Rhinitis is a common upper airway disorder, classified as either allergic rhinitis (AR) or non-allergic rhinitis (NAR). While the association between air pollution and AR airway diseases has been well documented, its specific effects on NAR remain poorly understood. This study aimed to evaluate the seasonal impact of air pollution on pulmonary function, oxidative stress biomarkers, and bronchial hyperresponsiveness in patients with AR, patients with NAR, and healthy controls.

MATERIAL AND METHODS: In this prospective case-control study, 58 participants (23 AR, 22 NAR, 13 controls) were evaluated during periods of low pollution (summer) and high pollution (winter). Assessments included symptom questionnaires, pulmonary function tests, bronchial provocation tests (BPT), serum total antioxidant status (TAS), and total oxidative status.

RESULTS: In the high pollution period, the NAR group exhibited significantly lower TAS levels compared to summer (1.51 ± 0.15 , 1.60 ± 0.2 , $P = 0.041$), indicating an increased oxidative stress. A significant decrease in post-bronchodilator forced expiratory volume in 1 second (FEV_1) was also observed in the NAR group, suggesting heightened airway reactivity. The AR group demonstrated a higher frequency of BPT reactivity. Pulmonary function declined across all groups in winter, with the greatest reduction observed in AR patients. Within-group analyses revealed seasonal reductions in both FEV_1 and post-BPT FEV_1 in AR and NAR groups.

CONCLUSION: Seasonal air pollution exerts phenotype-specific effects on oxidative stress and airway reactivity in rhinitis. AR patients exhibited increased bronchial hyperresponsiveness, whereas NAR individuals showed a marked decline in antioxidant capacity. These findings highlight the importance of phenotype-based monitoring and management during periods of high environmental exposure.

KEYWORDS: Rhinitis, allergic rhinitis, non-allergic rhinitis, asthma, oxidative stress, air pollution, allergy

Received: 08.10.2025

Revision Requested: 02.12.2025

Last Revision Received: 22.12.2025

Accepted: 22.01.2026

Epub: 31.03.2026

Publication Date: 12.05.2026

INTRODUCTION

Rhinitis is a common inflammatory disorder of the upper airways and is classified as allergic rhinitis (AR) or non-allergic rhinitis (NAR) depending on the presence or absence of allergen-specific immunoglobulin E (IgE).¹ AR frequently coexists with asthma and other atopic diseases, forming part of a broader allergic spectrum.² Both AR and NAR phenotypes are increasingly influenced by environmental factors, particularly air pollution.³ Although genetic predisposition contributes to susceptibility, the rapid increase in rhinitis prevalence underscores the importance of environmental exposures, especially urbanization and air pollutants such as particulate matter (PM), nitrogen dioxide (NO₂), and ozone.⁴

Fine PM_{2.5} is of particular concern because it disrupts epithelial barrier integrity and promotes inflammatory responses through the excessive generation of reactive oxygen species (ROS).^{5,6} Oxidative stress, defined as an imbalance between

Corresponding author: Assoc. Prof. Sümeýra Alan Yalým, e-mail: alansumeyra@gmail.com



ROS production and antioxidant defense systems, is considered a key mechanism underlying pollutant-induced airway damage. Biomarkers such as total antioxidant status (TAS) and total oxidant status (TOS) provide integrative measures of systemic redox homeostasis.⁷ While these have been studied in asthma and AR,⁸ data regarding their relevance in NAR are sparse. Furthermore, limited research has examined how these biomarkers vary seasonally among different rhinitis phenotypes.

Recent evidence suggests that AR patients readily generate ROS in response to environmental triggers,⁹ whereas the oxidative profile and airway reactivity of NAR patients under pollution stress remain poorly understood. Some studies suggest a potential link between air pollution and increased bronchial hyperresponsiveness, even in non-asthmatic individuals.¹⁰ This study investigates the seasonal impact of air pollution on oxidative stress and bronchial responsiveness in patients with AR and NAR, and in healthy controls. By evaluating TAS, TOS, and pulmonary parameters during both low-pollution (summer) and high-pollution (winter) seasons, we aim to delineate phenotype-specific responses to environmental oxidative burden.

Study Design

This prospective, observational, case-control study was conducted at a tertiary allergy and immunology clinic in Kırıkkale, Türkiye between January 2022 and June 2023. A total of 58 participants (23 AR, 22 NAR, 13 controls) were enrolled. Each participant was evaluated at two time points corresponding to seasonal variations in air pollution: summer (low-pollution season; June–August) and winter (high-pollution season; December–February). All procedures were carried out in accordance with the Declaration of Helsinki. The study protocol was approved by the Kırıkkale University Clinical Research Ethics Committee (date/approval no: 12.09.2022/07-02), and supported by a Kırıkkale University Scientific Research Grant (BAP project no: 2022/108). Written informed consent was obtained from all participants prior to enrollment.

Kırıkkale is a mid-sized industrial city characterized by substantial seasonal fluctuations in ambient air quality. During winter, average concentrations of sulfur dioxide and PM₁₀ exceeded World Health Organization thresholds, reaching 340 µg/m³ and 220 µg/m³, respectively.¹¹ These natural seasonal variations provided a real-world context to explore pollution-associated respiratory effects.¹²

Main Points

- Air pollution affects allergic rhinitis and non-allergic rhinitis (NAR) through different pathways.
- Winter pollution causes a significant antioxidant drop, specifically in NAR.
- Both phenotypes show higher bronchial hyperresponsiveness in winter.
- Monitoring total antioxidant status levels may help manage rhinitis during high pollution.

The sample size for the study group was determined using G*Power 3.1.9.7. The mean TAS and TOS values and standard deviations of the patient and control groups in the study by Pekince and Baccioglu¹³ were used to determine the sample size. As a result of these analyzes, it was determined that a power of 95% and a type 1 error level of 5% could be achieved with at least 56 cases.

Participants

Eligibility criteria included adults aged 18–60 years who were lifelong non-smokers and long-term residents of Kırıkkale. This age range was selected to minimize age-related comorbidities, polypharmacy and age-dependent variability in lung function that might confound spirometric and bronchial responsiveness measurements. Prior to enrollment, a detailed survey was conducted to assess residence, education level, home heating methods, proximity to industrial zones, and daily outdoor exposure. Based on these data, participants were selected to represent the average environmental exposure profile of the region. Healthy controls were recruited from the same catchment area and with the same characteristics as the patients (hospital staff and hospital visitors without respiratory or allergic disease). To ensure comparability, frequency matching based on age and sex was employed rather than individual matching. Specifically, only non-smokers were included in all three groups. Recruitment was aimed at achieving an age range and female predominance similar to those in the rhinitis groups. All participants resided in the same urban area.

AR was diagnosed based on symptoms and a positive skin prick test (SPT) to common aeroallergens. NAR was defined as chronic rhinitis symptoms with negative SPT results and non-IgE-mediated triggers. Controls had no respiratory disease, no history of allergy, atopy, or chronic illness. Exclusion criteria included pregnancy, a diagnosis of asthma, chronic systemic diseases, recent use of corticosteroids or immunosuppressives, and occupational exposure to inhaled pollutants.

Clinical and Environmental Assessments

Participants underwent comprehensive evaluations during both visits. They completed standardized questionnaires that captured rhinitis symptom severity (total nasal symptom score, TNSS), environmental exposure history, indoor irritant sources, heating type, and duration of outdoor exposure. Physical examinations and pulmonary assessments were performed under standardized clinical conditions during both seasonal visits.

SPT was performed during the initial visit using a panel of standardized aeroallergens. Pulmonary function testing (PFT) included spirometry measurements of forced expiratory volume in 1 second (FEV₁), forced vital capacity (FVC), and FEV₁/FVC ratio in accordance with American Thoracic Society/European Respiratory Society guidelines.¹⁴ Bronchial hyperresponsiveness was evaluated using a methacholine challenge test, with PD₂₀ calculated when feasible.¹⁵

Blood samples were obtained at both visits for complete blood count, C-reactive protein (CRP), total IgE, and oxidative stress markers. Serum TAS and TOS were quantified using a fully automated spectrophotometric method described by Erel.⁷ TAS values were expressed as mmol Trolox equivalents/L and

TOS as $\mu\text{mol H}_2\text{O}_2$ equivalents/L. The oxidative stress index (OSI) was calculated as the TOS/TAS ratio. All measurements were performed in a single central laboratory using the same analyzer, calibrators, and internal controls. Replicate values with discrepancies greater than 10% were retested, and outliers were compared with the original sample and clinical data.

Environmental exposure was further assessed through air quality data from the Turkish National Monitoring Network.¹² Variables such as outdoor exposure duration, home heating type, and passive smoke exposure were also recorded. These data were matched to the corresponding seasonal visits for each participant.

Statistical Analysis

Statistical analyses were performed using SPSS version 23. Data distribution was assessed using the Shapiro–Wilk test. Depending on the normality assumptions, two-group comparisons were performed using t-tests or the Mann–Whitney U test. Additionally, three groups were analyzed using ANOVA and Kruskal–Wallis test, and post-hoc adjustments. In post-hoc analyses, significant differences were confirmed using Bonferroni and Tamhane's T2 tests, as appropriate for their distributions; for comparisons involving three variables, the alpha value was set at 0.0167. Seasonal within-group changes were assessed using paired t-tests or Wilcoxon signed-rank tests. Categorical variables were analyzed via chi-square or Fisher's exact tests. Correlation analyses were performed using Pearson or Spearman methods, depending on the data distribution. The P value <0.05 was considered statistically significant.

RESULTS

Participant Characteristics

A total of 58 participants were included in the study: 23 with AR, 22 with NAR, and 13 healthy controls. The mean age of participants was 30.4 ± 9.4 years, and the majority were female (79.7%). Educational level was generally high across all groups, and the majority of participants (93.2%) resided in urban apartment settings in the city center. Evaluation of environmental factors showed a high rate of indoor irritant exposure: approximately 50% of cases reported exposure to detergents, air fresheners, and cigarette smoke. Similarly, approximately 50% of the patients lived on main streets or in areas of heavy traffic. No statistically significant differences were detected between the AR and NAR groups with respect to these exposure characteristics.

Environmental Exposures and Trigger Factors

Environmental and exposure characteristics were similar between the AR and NAR groups. The majority of patients with rhinitis (77%) reported identifiable symptom triggers, most commonly air pollution, dust, and cold air. Only one-third of symptomatic participants reported symptom control during the study period. Indoor irritants, particularly detergents and air fresheners, were frequently reported and did not differ significantly across groups.

Pulmonary Function and Seasonal Variation

Baseline pulmonary function values, including FEV₁, were similar among the three groups during both seasonal visits. A general decline in FEV₁ was observed during the winter period, although differences were not statistically significant in intergroup comparisons. Mean winter declines in FEV₁ were -3.2% in the NAR group, -2.8% in the AR group, and -1.9% in the control group. This seasonal decrease in pulmonary function is illustrated in Figure 1.

Oxidative Stress Markers

TAS, TOS, and OSI were evaluated in all participants. Intergroup comparisons revealed no significant seasonal differences in oxidative stress parameters (Table 1). However, within-group analysis in the NAR group showed a significant reduction in TAS levels during winter ($P < 0.05$), suggesting an increased oxidative burden during periods of high air pollution. This decline is depicted in Figure 2.

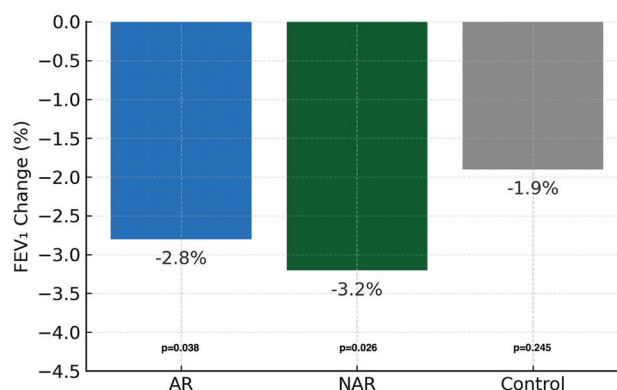


Figure 1. Seasonal changes in FEV₁ values across allergic rhinitis (AR), non-allergic rhinitis (NAR) and control groups

FEV₁: forced expiratory volume in 1 second

Table 1. Baseline demographic characteristics and oxidative stress of study groups

| Parameter | AR (n = 23) | NAR (n = 22) | Control (n = 13) | P value |
|---|-------------|--------------|------------------|---------|
| Age | 28.5±9.3 | 34±12.2 | 29.3±5.8 | 0.105 |
| Sex, female | 16 (69.6%) | 19 (86.4%) | 24 (82.8%) | 0.327 |
| BMI (kg/m ²) | 24.2±3.1 | 24.6±3.5 | 23.9±2.8 | 0.753 |
| TAS (mmol Trolox equiv./L) | 1.59±0.22 | 1.58±0.17 | 1.56±0.15 | 0.819 |
| TOS ($\mu\text{mol H}_2\text{O}_2$ equiv./L) | 8.4±4.8 | 9.2±5.6 | 10.1±6.5 | 0.570 |
| OSI (arbitrary units) | 0.52±0.30 | 0.58±0.33 | 0.69±0.49 | 0.295 |

Control participants were presented with the average of both summer and winter period data

The ANOVA test and the Kruskal–Wallis test were used according to distributions

AR: allergic rhinitis, NAR: non-allergic rhinitis, BMI: body mass index, TAS: total antioxidant status, TOS: total oxidant status, OSI: oxidative stress index, FEV₁: forced expiratory volume in 1 second

TOS and OSI values did not exhibit significant changes in any group (Tables 2 and 3). Collectively, these findings suggest that NAR patients may be more susceptible to pollutant-associated oxidative imbalance, whereas AR participants may exhibit relatively stable systemic oxidative profiles.

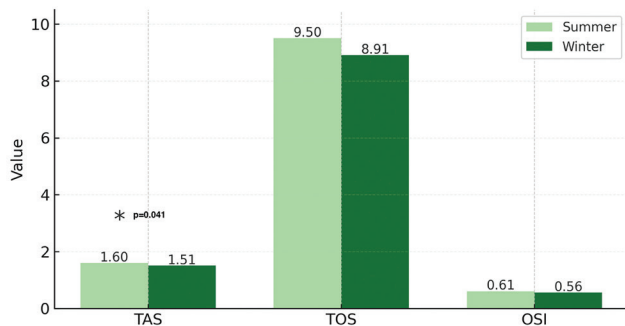


Figure 2. Seasonal comparison of TAS, TOS, and OSI levels in the NAR group

TAS: total antioxidant status, TOS: total oxidant status, OSI: oxidative stress index, NAR: non-allergic rhinitis

Bronchial Hyperresponsiveness

Bronchial provocation testing (BPT) results indicated seasonal changes in airway responsiveness. In winter, the NAR group showed a significant reduction in post-BPT FEV₁ (% change from baseline), indicating increased bronchial hyperresponsiveness (P = 0.02). The AR group also showed seasonal reductions in both FEV₁ (P = 0.038) and post-BPT FEV₁ (P = 0.009), though to a lesser extent. These findings are visualized in Figure 3 and detailed in Table 3.

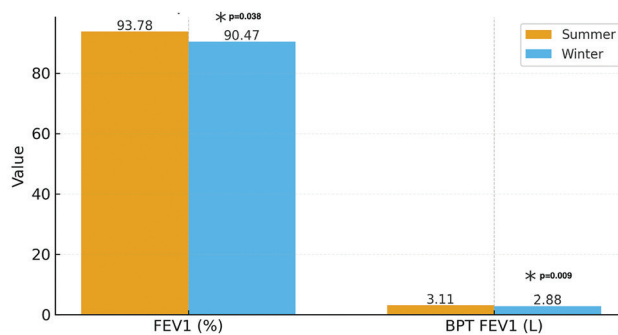


Figure 3. Seasonal changes in forced expiratory volume in 1 second (FEV₁) and post-bronchial provocation test (BPT) FEV₁ values in the allergic rhinitis (AR) group

Table 2. Comparison of the variables examined during the summer visit of the study patients

| Parameter | AR (n = 23) | NAR (n = 22) | Control (n = 13) | P value |
|---|-------------|--------------|------------------|---------|
| TAS (mmol Trolox equiv./L) | 1.6±0.23 | 1.6±0.2 | 1.55±0.19 | 0.737 |
| TOS (µmol H ₂ O ₂ equiv./L) | 9.6±8.3 | 9.5±7.2 | 11.8±8.2 | 0.668 |
| OSI (arbitrary units) | 0.581±0.51 | 0.61±0.48 | 0.803±0.6 | 0.455 |
| TNSS | 6.7±3.1 | 6.1±2.5 | 0.2±0.8 | <0.001* |
| FEV ₁ (L) | 3.51±0.75 | 2.93±0.5 | 3.19±0.45 | 0.009 |
| FEV ₁ (%) | 93.7±8.5 | 93.9±10.4 | 98.7±9.4 | 0.270 |
| BPT FEV ₁ (L) | 3.11±0.55 | 2.6±0.57 | 3.01±0.58 | 0.011 |
| BPT FEV ₁ change | -9.3±7.6 | -9.8±9.06 | -5.94±8.7 | 0.395 |

*A significant difference was observed between the control and AR/NAR groups. The ANOVA test and the Kruskal–Wallis test were used according to distributions
AR: allergic rhinitis, NAR: non-allergic rhinitis, TAS: total antioxidant status, TOS: total oxidant status, OSI: oxidative stress index, TNSS: total nasal symptom score, BPT: bronchial provocation test, FEV₁: forced expiratory volume in 1 second

Table 3. Comparison of the variables examined during the winter visit of the study patients

| Parameter | AR (n = 23) | NAR (n = 22) | Control (n = 13) | P value |
|---|-------------|--------------|------------------|---------|
| TAS (mmol Trolox equiv./L) | 1.58±0.22 | 1.51±0.15 | 1.45±0.17 | 0.123 |
| TOS (µmol H ₂ O ₂ equiv./L) | 7.27±3.58 | 8.91±7.83 | 8.04±8.20 | 0.658 |
| OSI (arbitrary units) | 0.47±0.25 | 0.57±0.41 | 0.56±0.41 | 0.594 |
| TNSS | 6.5±3.2 | 6.6±2.7 | 0.8±1.6 | <0.001* |
| FEV ₁ (L) | 3.40±0.71 | 2.87±0.54 | 3.24±0.80 | 0.036** |
| FEV ₁ (% predicted) | 90.4±9.7 | 90.6±11.3 | 93.4±9.3 | 0.629 |
| BPT FEV ₁ (L) | 2.88±0.69 | 2.42±0.56 | 2.90±0.72 | 0.036** |
| BPT FEV ₁ change (%) | -11.6±11.2 | -12.9±11.7 | -7.1±9.3 | 0.254 |

*A significant difference was observed between the control and AR/NAR groups.
**A significant difference was observed between the NAR and AR/control groups.
The ANOVA test and the Kruskal–Wallis test were used according to distributions
AR: allergic rhinitis, NAR: non-allergic rhinitis, TAS: total antioxidant status, TOS: total oxidant status, OSI: oxidative stress index, BPT: bronchial provocation test, TNSS: total nasal symptom score, FEV₁: forced expiratory volume in 1 second

Notably, the AR group maintained stable TAS levels despite the functional decline in FEV₁. The control group showed no significant seasonal variation in oxidative or pulmonary markers. These findings suggest that while both rhinitis phenotypes experience functional impairment in winter, the underlying mechanisms may differ, with oxidative stress being more pronounced in NAR and airway hyperresponsiveness (AHR) being more evident in AR.

Intergroup and Seasonal Comparisons

During the summer and winter visits, no statistically significant differences were observed in TAS, TOS, or body mass index among the three groups. However, TNSS was significantly higher in both rhinitis groups compared to controls ($P < 0.001$). FEV₁ values were lower in the NAR group than in the AR group and the controls ($P = 0.009$). These results are summarized in Tables 2, 3.

A more detailed comparison of the groups during winter is presented in Table 4a. While OSI and TOS remained stable across phenotypes, TAS showed a significantly greater reduction in the NAR group than in AR ($P = 0.041$). No significant seasonal differences were noted in OSI or post-BPT FEV₁ between AR and NAR. These comparisons are shown in Table 4a, 4b.

Correlation Analyses

A moderate inverse correlation was observed between seasonal changes in TAS and TNSS ($r: -0.337, P = 0.012$), suggesting that reduced antioxidant capacity is associated with increased nasal symptom severity. No significant correlations were found between OSI or TOS and symptom scores.

Inflammatory markers, such as CRP and white blood cell counts, showed no significant variation between groups. However, neutrophil counts were significantly higher in the AR group than in the NAR group during winter ($P < 0.05$), potentially indicating differing inflammatory responses to pollution exposure.

Further correlation analyzes demonstrated associations between environmental pollutant levels and clinical parameters. Elevated PM_{2.5}, NO₂, and CO levels were significantly correlated with higher TOS and OSI values, and with lower FEV₁ (change from baseline) ($P < 0.05$). These findings support a link between ambient air pollution and systemic oxidative stress and pulmonary impairment, particularly among patients with rhinitis.

Table 4a. Comparison of changes in respiratory function test and laboratory parameters of NAR group patients in winter (W) and summer (S)

| Variables | Mean (W) | Mean (S) | P value |
|-----------------------------|--------------|----------------|---------|
| TAS | 1.51±0.1576 | 1.60±0.20 | 0.041 |
| TOS | 8.91±7.8345 | 9.50±7.29 | 0.782 |
| OSI | 0.56±0.4112 | 0.61±0.48 | 0.747 |
| TNSS | 6.63±2.73 | 6.18±2.59 | 0.116 |
| FEV ₁ (L) | 2.87±0.54 | 2.93±0.50 | 0.314 |
| FEV ₁ (%) | 90.63±11.31 | 93.95±10.40 | 0.026 |
| BPT FEV ₁ (L) | 2.42±0.56 | 2.6005±0.5708 | 0.110 |
| FEV ₁ change (%) | -12.99±11.76 | -9.8273±9.0653 | 0.234 |

Paired t-tests or Wilcoxon signed-rank tests were used according to distributions. The P value < 0.05 is considered statistically significant
NAR: non-allergic rhinitis, TAS: total antioxidant status, TOS: total oxidant status, OSI: oxidative stress index, BPT: bronchial provocation test, TNSS: total nasal symptom score, FEV₁: forced expiratory volume in 1 second

Table 4b. Comparison of changes in respiratory function test and laboratory parameters of AR group patients in winter (W) and summer (S)

| Variables | Mean (W) | Mean (S) | P value |
|-----------------------------|--------------|-------------|---------|
| TAS | 1.58±0.22 | 1.60±0.23 | 0.559 |
| TOS | 7.27±3.58 | 9.60±8.36 | 0.201 |
| OSI | 0.46±0.25 | 0.58±0.51 | 0.322 |
| TNSS | 6.52±3.21 | 6.78±3.19 | 0.299 |
| FEV ₁ (L) | 3.40±0.72 | 3.51±0.75 | 0.115 |
| FEV ₁ (%) | 90.47±9.76 | 93.78±8.58 | 0.038 |
| BPT FEV ₁ (L) | 2.88±0.69 | 3.11±0.55 | 0.009 |
| FEV ₁ change (%) | -11.60±11.22 | -9.308±7.60 | 0.174 |

Paired t-tests or Wilcoxon signed-rank tests were used according to distributions. The P value < 0.05 is considered statistically significant
AR: allergic rhinitis, TAS: total antioxidant status, TOS: total oxidant status, OSI: oxidative stress index, BPT: bronchial provocation test, TNSS: total nasal symptom score, FEV₁: forced expiratory volume in 1 second

DISCUSSION

This study investigated the seasonal effects of air pollution on oxidative stress and airway responsiveness in patients with AR and NAR, revealing distinct pathophysiological responses. In winter, when pollutant concentrations were elevated, the NAR group exhibited a significant decline in TAS and an increase in bronchial hyperresponsiveness, whereas the AR group showed greater functional impairment on spirometry but maintained stable antioxidant profiles.

These findings suggest phenotype-specific vulnerability to environmental stressors. Previous studies have shown that PM and gaseous pollutants such as NO₂ and CO contribute to epithelial barrier dysfunction and oxidative stress via excessive ROS production.^{5,6} Oxidative imbalance has been well documented in asthma and AR,⁸ but data regarding NAR remain limited. Our results demonstrate that NAR patients, despite lacking IgE-mediated inflammation, may exhibit impaired redox balance during high-exposure periods, consistent with emerging studies on non-atopic airway diseases.¹⁶

Interestingly, TAS levels declined significantly only in the NAR group, while TOS and OSI remained stable across all phenotypes. This may suggest that antioxidant depletion, rather than oxidant excess, is a key driver of seasonal redox shifts in NAR. Li et al.¹⁷ reported similar patterns in asthmatic children exposed to air pollution, noting stronger oxidative biomarker responses in non-allergic subtypes. Pekince and Baccioglu¹³ also demonstrated that oxidative impairment due to pollution was more prominent in non-allergic asthma patients, paralleling our observations in NAR. However, the wide standard deviation observed in TOS values likely reflects inter-individual biological heterogeneity, potentially driven by genetic *polymorphisms* in antioxidant enzyme systems (e.g. GSTM1, GSTP1), which are known to modulate individual responses to oxidative triggers¹⁸ rather than methodological limitations. This suggests that antioxidant capacity (TAS) might be a more sensitive marker for detecting pollution-induced redox shifts in this cohort.

AHR, classically associated with asthma and AR¹⁵ was also significantly increased in NAR during winter. Crucially, although seasonal AHR was observed in both groups, the underlying mechanisms appear to diverge. The specific reduction in TAS observed in NAR suggests that airway reactivity in this phenotype may be driven by failure of antioxidant defenses, whereas in AR it likely results from aggravation of established allergic inflammation, independent of systemic redox shifts. This raises the possibility that NAR patients may have heightened reactivity to non-allergic stimuli, such as air pollutants, through non-IgE pathways involving neurogenic inflammation or epithelial-derived mediators.^{19,20} The modest inverse correlation between TAS and TNSS further supports the hypothesis that oxidative stress contributes to symptom exacerbation.

Environmental pollutant levels (PM_{2.5}, NO₂, CO) were significantly associated with reduced pulmonary function and elevated TOS/OSI values, corroborating previous research linking air pollution to systemic inflammation and respiratory morbidity.^{4,5} These findings emphasize that ambient exposures

can impact both upper and lower airway physiology, even in individuals without classic allergic sensitization.

This study contributes to the growing recognition that NAR is not a benign or “residual” diagnosis, but rather may represent a distinct inflammatory endotype with environmental susceptibility. The observed functional and biochemical impairments highlight the need for individualized clinical management, including environmental exposure counseling and possibly antioxidant strategies.

While this study has several strengths, including seasonal design and the use of validated clinical and biochemical markers, some limitations must be acknowledged. The sample size was modest, and individual exposure levels were not directly measured. The methacholine challenge, although standardized, may not capture all dimensions of AHR in rhinitis patients. TAS and TOS are systemic markers and may not fully reflect local nasal or bronchial oxidative status. Air pollution exposure was estimated using city-level data from fixed monitoring stations, without personal exposure monitoring or time-activity diaries. Therefore, individual exposure misclassification is possible. Indoor air pollutant levels and detailed home microenvironment characteristics were not systematically measured. The study was conducted in a single center with a modest sample size, which limits generalizability to populations with different genetic, dietary, or pollution profiles. Multicenter studies in diverse settings are needed to confirm these phenotype-specific patterns. These limitations may introduce bias and should be considered when interpreting our findings.

In summary, our findings support a model in which seasonal air pollution induces distinct oxidative and functional responses in AR and NAR phenotypes. The disproportionate impact on NAR patients suggests that environmental monitoring, phenotype-specific evaluation, and tailored interventions are critical for optimal disease management in polluted settings.

CONCLUSION

Seasonal air pollution exerts differential effects on patients with AR and NAR. While AR patients exhibited greater bronchial hyperresponsiveness, individuals with NAR demonstrated significant reductions in antioxidant capacity during the winter months, highlighting a potential vulnerability to an oxidative imbalance. These findings underscore the need for phenotype-specific management strategies that incorporate environmental exposure assessment. Monitoring redox biomarkers and implementing protective interventions during high-pollution periods may improve clinical outcomes in susceptible populations.

Ethics

Ethics Committee Approval: The study protocol was approved by the Kırıkkale University Clinical Research Ethics Committee (date/approval no: 12.09.2022/07-02).

Informed Consent: Written informed consent was obtained from all participants prior to enrollment.

Footnotes

Authorship Contributions

Concept: S.A.Y., A.F.K., A.B., Design: S.A.Y., A.F.K., A.B., Data Collection or Processing: S.A.Y., A.B., Analysis or Interpretation: S.A.Y., A.B., Literature Search: S.A.Y., A.B., Writing: S.A.Y.

Conflict of Interest: No conflict of interest was declared by the authors.

Financial Disclosure: The study was supported by a Kırıkkale University Scientific Research Grant (BAP project no: 2022/108).

REFERENCES

- Bousquet J, Schünemann HJ, Togias A, et al. Next-generation Allergic Rhinitis and Its Impact on Asthma (ARIA) guidelines for allergic rhinitis based on Grading of Recommendations Assessment, Development and Evaluation (GRADE) and real-world evidence. *J Allergy Clin Immunol.* 2020;145(1):70-80.e3. [\[Crossref\]](#)
- Leynaert B, Neukirch C, Liard R, Bousquet J, Neukirch F. Quality of life in allergic rhinitis and asthma: a population-based study of young adults. *Am J Respir Crit Care Med.* 2000;162(4):1391-1396. [\[Crossref\]](#)
- Bauchau V, Durham SR. Prevalence and rate of diagnosis of allergic rhinitis in Europe. *Eur Respir J.* 2004;24(5):758-764. [\[Crossref\]](#)
- D'Amato G, Cecchi L, D'amato M, Liccardi G. Urban air pollution and climate change as environmental risk factors of respiratory allergy: an update. *J Investig Allergol Clin Immunol.* 2010;20(2):95-102. [\[Crossref\]](#)
- Schraufnagel DE, Balmes JR, Cowl CT, et al. Air pollution and noncommunicable diseases: a review by the forum of international respiratory societies' environmental committee, part 2: air pollution and organ systems. *Chest.* 2019;155(2):417-426. [\[Crossref\]](#)
- Zhang Z, Guo C, Lau AKH, et al. Long-term exposure to fine particulate matter, blood pressure, and incident hypertension in Taiwanese adults. *Environ Health Perspect.* 2018;126(1):17008. [\[Crossref\]](#)
- Erel O. A novel automated method to measure total antioxidant response against potent free radical reactions. *Clin Biochem.* 2004;37(2):112-119. [\[Crossref\]](#)
- Ai S, Liu L, Xue Y, Cheng X, Li M, Deng Q. Prenatal exposure to air pollutants associated with allergic diseases in children: which pollutant, when exposure, and what disease? A systematic review and meta-analysis. *Clin Rev Allergy Immunol.* 2024;66(2):149-163. [\[Crossref\]](#)
- Riedl M, Diaz-Sanchez D. Biology of diesel exhaust effects on respiratory function. *J Allergy Clin Immunol.* 2005;115(2):221-228. [\[Crossref\]](#)
- Liu L, Poon R, Chen L, et al. Acute effects of air pollution on pulmonary function, airway inflammation, and oxidative stress in asthmatic children. *Environ Health Perspect.* 2009;117(4):668-674. [\[Crossref\]](#)
- Organization WH. *WHO Global Air Quality Guidelines: Particulate Matter (PM_{2.5} and PM₁₀), Ozone, Nitrogen Dioxide, Sulfur Dioxide and Carbon Monoxide.* World Health Organization; 2021. [\[Crossref\]](#)
- Turkish Ministry of Environment and Urbanization. National Air Quality Monitoring Network. Accessed March 15 2025. [\[Crossref\]](#)
- Pekince B, Baccioglu A. Allergic and non-allergic asthma phenotypes and exposure to air pollution. *J asthma.* 2022;59(8):1509-1520. [\[Crossref\]](#)
- Graham BL, Steenbruggen I, Miller MR, et al. Standardization of Spirometry 2019 Update. An Official American Thoracic Society and European Respiratory Society Technical Statement. *Am J Respir Crit Care Med.* 2019;200(8):e70-e88. [\[Crossref\]](#)
- Cockcroft D, Davis B. Direct and indirect challenges in the clinical assessment of asthma. *Ann Allergy Asthma Immunol.* 2009;103(5):363-370. [\[Crossref\]](#)
- Ciprandi G, Cirillo I, Tosca MA, Vizzaccaro A. Bronchial hyperreactivity and spirometric impairment in patients with seasonal allergic rhinitis. *Respir Med.* 2004;98(9):826-831. [\[Crossref\]](#)
- Li J, Wu H, Xing W, et al. Air pollution mixture associated with oxidative stress exacerbation and symptoms deterioration in allergic rhinitis patients: evidence from a panel study. *Sci Total Environ.* 2024;930:172688. [\[Crossref\]](#)
- Minelli C, Wei I, Sagoo G, Jarvis D, Shaheen S, Burney P. Interactive effects of antioxidant genes and air pollution on respiratory function and airway disease: a HuGE review. *Am J Epidemiol.* 2011;173(6):603-620. [\[Crossref\]](#)
- Rondón C, Campo P, Togias A, et al. Local allergic rhinitis: concept, pathophysiology, and management. *J Allergy Clin Immunol.* 2012;129(6):1460-1467. [\[Crossref\]](#)
- Shusterman, Dennis. The effects of air pollutants and irritants on the upper airway. *Proc Am Thorac Soc.* 2011;8(1):101-105. [\[Crossref\]](#)

Original Article

Reliability and Validity of the Turkish Version of the Lung Transplant-specific Valued Life Activities Scale

Ulaş Ar¹, Erdal Yekeler², Ebru Çalık³, Fatmanur Çelik Başaran², Sinan Türkkan²¹Clinic of Physical Therapy and Rehabilitation, Ankara Bilkent City Hospital, Physical Medicine and Rehabilitation Hospital, Ankara, Türkiye²Clinic of Thoracic Surgery, Ankara Bilkent City Hospital, Ankara, Türkiye³Department of Cardiorespiratory Physiotherapy and Rehabilitation, Hacettepe University Faculty of Physical Therapy and Rehabilitation, Ankara, Türkiye**Cite this article as:** Ar U, Yekeler E, Çalık E, Çelik Başaran F, Türkkan S. Reliability and validity of the Turkish version of the lung transplant-specific valued life activities scale. *Thorac Res Pract.* 2026;27(3):148-154

ABSTRACT

OBJECTIVE: The lung transplantation-specific valued life activities (LT-VLA) is a 15-item questionnaire developed to assess limitations in activities of daily living in LT recipients. This study aimed to evaluate the validity and reliability of its Turkish version.**MATERIAL AND METHODS:** Twenty-two LT recipients participated in this single-center cross-sectional study. Test-retest reliability was assessed using intraclass correlation coefficients (ICC), and internal consistency was measured with Cronbach's alpha (α). Criterion validity was examined by comparing LT-VLA scores with the Saint George Respiratory Questionnaire, Short Form-12 (SF-12), London Chest Activity of Daily Living Scale (LCADL), and modified Medical Research Council (mMRC) scale.**RESULTS:** Cronbach's α values for the mean difficulty, activities affected, and activities unable subscales were 0.945, 0.906, and 0.934, respectively. ICC values ranged from 0.828 to 0.897. The mean difficulty score showed a moderate correlation with LCADL self-care ($r = 0.543$, $P = 0.009$) and SF-12 physical ($r = -0.532$, $P = 0.011$). The activities affected subscale was correlated with SF-12 physical ($r = -0.587$, $P = 0.004$) and with mMRC ($r = 0.563$, $P = 0.006$).**CONCLUSION:** The Turkish version of the LT-VLA is a reliable and valid tool for assessing activity limitations in LT recipients. It will be a useful and feasible tool for rehabilitation professionals to assess activity limitations in LT recipients undergoing pulmonary rehabilitation.**KEYWORDS:** Lung Transplantation, rehabilitation, activities of daily living, quality of life, treatment outcome**Received:** 08.10.2025**Revision Requested:** 15.12.2025**Last Revision Received:** 16.12.2025**Accepted:** 21.01.2026**Epub:** 24.03.2026**Publication Date:** 12.05.2026

INTRODUCTION

Lung transplantation (LT) is a life-saving therapeutic intervention for patients with end-stage lung disease that also enhances health-related quality of life (HRQL) and improves patient-centered outcomes (PCOs).¹ Reported survival rates in lung transplant recipients are 85% at one year and 59% at five years.² These improved survival outcomes have increased the importance of evaluating HRQL and activities of daily living (ADLs) in this patient group, according to the framework of the International Classification of Functioning (ICF), Disability and Health.^{3,4}

The poorer quality of life and limitations in ADLs of lung transplant recipients are multifactorial in origin.⁵ Graft-related complications such as chronic lung allograft dysfunction and bronchiolitis obliterans syndrome may lead to functional limitations due to deterioration in pulmonary function.⁶ Corticosteroid-induced myopathy, infectious disorders, and tacrolimus-related neurotoxicity impair functional capacity and are recognized adverse effects of immunosuppressive therapy.⁷ This progressive deterioration frequently results in clinically significant limitations in ADLs.⁸ Furthermore,

Corresponding author: Ulaş Ar, MSc, e-mail: ulas12ar@gmail.com

post-transplant complications, including critical illness polyneuromyopathy, inactivity-induced sarcopenia, and post-transplant diabetes mellitus, may substantially compromise ADLs.⁹

In the literature, patients' ability to perform ADLs and patients' quality of life are considered essential metrics of post-lung transplant outcomes.¹⁰ Furthermore, the assessment of HRQL and ADLs is a critical parameter for evaluating the effectiveness of pulmonary rehabilitation programs for transplant recipients.¹¹ The LT-specific valued life activities (VLA) scale, developed by Singer et al.¹², is a brief and practical tool designed to assess limitations in ADLs among lung transplant candidates and recipients. The LT-VLA was designed to assess not only basic ADLs but also more complex and personally valued activities that contribute to enjoyment and overall quality of life, such as social interaction, travel, and leisure pursuits. This broader scope represents a key feature that distinguishes the LT-VLA from traditional ADL-based measures. In the original validation study of the LT-VLA, the 15-item LT-VLA demonstrated high internal consistency [Cronbach's alpha (α) = 0.92] in the lung transplant population and showed moderate correlations with objective clinical measures such as pulmonary function tests and 6-minute walk distance. Furthermore, the LT-VLA scale has proven to be a sensitive measure of clinical improvements after transplantation.¹² PCOs developed for specific disease states outperform generic instruments because of their disease-specific content validity, greater sensitivity to clinical changes, and improved patient compliance achieved through appropriately tailored questions.¹³ There are chronic lung disease-specific ADLs assessment tools or questionnaires that evaluate effects of respiratory diseases on activity but none of them corresponds to specific needs for lung transplant populations.^{14,15} There is also a lack of knowledge about the most appropriate ADL evaluation tools for patients with chronic respiratory disorders.¹⁶

Therefore, the cultural and linguistic adaptation of the LT-VLA scale into Turkish can enable the objective assessment of disability levels in patients' ADLs in both clinical practice and research, providing a valuable ICF-based outcome.¹⁷ The objective of this study is to evaluate the validity and reliability of the Turkish version of the LT-VLA scale to assess limitations in ADLs among lung transplant recipients.

Main Points

- Turkish version of the lung transplant-specific valued life activities (LT-VLA) scale was developed and tested for reliability and validity in LT recipients.
- The scale showed excellent internal consistency with Cronbach's alpha values between 0.906 and 0.945.
- Test-retest reliability was high with intraclass correlation coefficient values ranging from 0.828 to 0.897 and criterion validity was confirmed with moderate correlations to Short Form-12, London Chest Activity of Daily Living Scale, and modified Medical Research Council.
- Turkish LT-VLA is a valid and reliable tool for assessing activity limitations in LT recipients and can be used in pulmonary rehabilitation practice.

MATERIAL AND METHODS

Study Design and Participants

Twenty-two lung transplant recipients who were followed up at the Chest Surgery Clinic of Ankara Bilkent City Hospital were included in this cross-sectional methodological study between February 2024 and March 2025. The inclusion criteria for the study were: at least three months since LT, an acceptable level of cooperation, the ability to read and understand Turkish, an age between 18 and 70 years, and willingness to participate in the study. Patients who underwent single-LT, those unable to read or understand Turkish, and those with difficulties cooperating were excluded from the study. Only bilateral lung transplant recipients were included in the study. The primary reason for excluding single-lung transplant recipients was to ensure methodological homogeneity of the study sample and minimize potential confounding factors. Bilateral and single-lung transplant procedures may differ in terms of postoperative physiological capacity, complication profiles, and long-term functional outcomes. Therefore, in this validation study that evaluated the psychometric properties of the LT-VLA scale, a homogeneous patient group (bilateral lung transplant recipients) was preferred to avoid potential confounding from different functional and symptomatic profiles associated with transplant type that could affect scale performance and validity coefficients. The study was approved by the Ankara Bilkent City Hospital No. 1 Clinical Research Ethics Committee (date: 29.11.2023, approval number: E1-23-4215). The scope and purpose of the study were explained, and written informed consent forms were obtained from all participants.

Sample Size Calculation

The sample size calculation was performed based on the number of items and the minimum acceptable and expected values of Cronbach's α to achieve power $(1-\beta) = 80\%$ using a sample-size calculator for reliability studies.¹⁸ Therefore, the minimum required sample size was 20. Finally, we were able to reach 22 patients with LT.

Data Collection Tools

All questionnaires and scales were administered during clinical follow-up visits by a researcher using face-to-face interviews, and participants' verbal responses were recorded.

Sociodemographic and Clinical Data

The sociodemographic, physical and clinical data, including age, body mass index, the presence of supplemental oxygen support, smoking history, education level, and last lung function test results were recorded for all patients. The assessment data were through face-to-face inter-views with patients during routine follow-up visits.

The Lung Transplantation Specific Valued Living Activities Scale

The LT-VLA scale, developed by Singer et al.¹², is a brief, valid, and practical-to-administer disease-specific assessment tool designed to determine limitations in ADLs among lung transplant candidates and recipients. This tool assesses levels of disability

in three domains: obligatory (e.g., self-care), committed (e.g., work), and discretionary (e.g., social activities). Participants rate the difficulty of performing each activity on a 4-point Likert scale (0 = no difficulty; 3 = unable to perform). They also have the option to mark items as “does not apply”. The LT-VLA scale produces three summary scores: mean difficulty, proportion of activities affected, and proportion of activities not applicable.¹² The LT-VLA scale generates three summary scores to assess disability severity: I) mean difficulty score (range: 0–3), calculated as the sum of item scores divided by total items rated, where scores near 0 indicate minimal disability (activities performed easily), 1.5–2 reflect moderate disability (significant difficulty), and scores approaching 3 denote severe disability (inability to perform activities); II) percentage of affected activities, derived from the proportion of items scored ≥ 1 (any difficulty), with 0–30% indicating mild disability (limited impact), 50–80% moderate-severe disability (broad limitations), and 100% universal difficulty; III) percentage of unable-to-perform activities, based on items scored = 3 (unable to perform), where 0–10% suggests minimal functional loss, 20–50% significant limitations (including basic activities), and >50% profound disability. These metrics collectively quantify disability progression and post-transplant recovery, as validated in the original study.

The Saint George Respiratory Questionnaire

The Saint George Respiratory Questionnaire (SGRQ) was used to assess disease-specific HRQL. The SGRQ consists of 76 items and yields a total score and three domain scores (symptoms, activity, and impacts). The total scores for each domain range from 0 (no effect on HRQL) to a maximum score of 100 (maximum perceived distress), and a higher score reflects lower HRQL.^{15,19}

The Short Form-12

The Short Form-12 (SF-12) was used to assess generic quality of life. SF-12 includes 12 items that generate two summary scores: the physical component summary (PCS) and the mental component summary. The scores for each component range from 0 to 100, with higher scores indicating better health status.^{20,21}

The London Chest Daily Life Activity Scale

The London Chest Daily Life Activity Scale (LCADL) was used to assess dyspnea-related limitations in daily activities in patients with chronic lung disease. This scale consists of 15 items grouped into four domains: self-care, domestic, physical activity, and leisure. Each item is scored based on the degree of dyspnea experienced during the activity. Total LCADL scores range from 0 to 75, with higher scores indicating greater activity limitation due to breathlessness.^{14,22}

The Modified Medical Research Council Dyspnea Scale

The modified Medical Research Council (mMRC) dyspnea scale was used to assess the degree of breathlessness during daily life. The mMRC scale is a single-item, five-point scale (ranging from 0 to 4), which reflects the level of activity that provokes dyspnea. A higher score indicates more severe breathlessness and greater functional limitation.^{23,24}

Translation and Adaptation Procedure of LT-VLA Scale

First, written permission was obtained via email from the original developers of the scale to investigate the validity and reliability of the Turkish version of the LT-VLA scale. As a first step, the LT-VLA scale was translated into Turkish by two native Turkish speakers proficient in English, after obtaining permission from the authors of the original versions to translate and use the questionnaires. The two translators were physiotherapists specializing in cardiopulmonary rehabilitation. The two Turkish translations were synthesized into a single consensus version by the two translators. Two native English-speaking translators back-translated the final Turkish version of the LT-VLA scale during the back-translation step. These two back-translated versions were synthesized into a final version by consensus among the translators. The consensus English version was sent to the corresponding author of the original version (Jonathan Paul Singer) for final review. After the corresponding author's final check and revisions were completed, the final version of the LT-VLA scale was created.¹⁷

The LT-VLA was applied to participants twice, 30 minutes apart, to determine test-retest reliability. Four instruments (mMRC, SGRQ, SF-12, LCADL) were used to evaluate criterion validity.

Statistical Analysis

Statistical analyses were performed using the IBM Statistical Package for the Social Sciences (IBM SPSS Corp., Armonk, NY, USA), version 23.0 for Windows. The data were expressed as mean \pm standard deviation and minimum-maximum values for quantitative variables and as percentage (%) for categorical variables. The criterion validity of the LT-VLA was assessed using Spearman correlation analysis between the Turkish version of the LT-VLA scale and the mMRC score, SF-12 scores, LCADL (total and subscale scores), and SGRQ (total and subscale scores). Correlation strengths were interpreted as very weak ($|r| < 0.1$), weak ($0.1 \leq |r| < 0.3$), moderate ($0.3 \leq |r| < 0.7$), strong ($0.7 \leq |r| < 0.9$), or very strong ($|r| \geq 0.9$) based on Schober et al.²⁵, with all observed correlations in this study falling within the moderate range ($0.3 \leq |r| < 0.7$). The internal consistency of the LT-VLA was assessed using Cronbach's α coefficient. A Cronbach's α value of $0.60 \leq \alpha \leq 0.79$ is considered quite reliable and $\alpha \geq 0.80$ is considered highly reliable.²⁶ The test-retest reliability was measured using the intraclass correlation coefficients (ICC), which indicates excellent reliability of the instrument if $ICC \geq 0.80$.²⁷ The probability of error in the statistical analyses was set at $P < 0.05$.

RESULTS

Twenty-two lung transplant recipients (mean age: 45.63 ± 14.59 years, 36.4% female, 63.6% male) were included in the study. The time since transplantation ranged from 3 to 180 months among patients (mean time: 64.86 ± 43.48 months). The underlying diseases necessitating transplantation were chronic obstructive pulmonary disease (COPD) in 9 patients (40.9%), interstitial lung disease (ILD) in 8 patients (36.4%), cystic fibrosis (CF) in 3 patients (13.6%), and pulmonary hypertension (PH) in 2 patients (9.1%). The sociodemographic and clinical data of the patients in the study are shown in Table 1.

Test-retest Reliability

Internal consistency and test-retest reliability of the LT-VLA scale are shown in Table 2. The Cronbach’s α value of the mean difficulty, activities affected and activities unable subscales of LT-VLA test and retest scores were recorded as ≥ 0.80 indicating that the scale is highly reliable and have excellent internal consistency (0.945, 0.906, 0.934 respectively, Table 2). The test-retest ICC values for each subscale of LT-VLA were above 0.80, indicating excellent reliability, as shown in Table 2. The mean ICC values ranged from 0.828 to 0.897. The LT-VLA subscale scores were also strongly and significantly correlated with their retest scores ($P < 0.001$, Table 2).

Criterion Validity

The correlation coefficients between the LT-VLA score and the criterion questionnaires are presented in Table 3. The correlation analysis revealed that LT-VLA mean difficulty scores were moderately correlated with the SGRQ symptom score and with the LCADL self-care and physical activity scores. Additionally, LT-VLA mean difficulty scores showed a moderate negative correlation with the SF-12 physical scores and a moderate positive correlation with the mMRC scores. Furthermore, LT-VLA mean difficulty score was moderately correlated with waiting time on the transplant list ($r = 0.426$; $P = 0.048$). The LT-VLA activities affected scores showed moderate correlations with the SGRQ symptom scores, LCADL self-care scores, SGRQ total scores, and mMRC scores, as well as a moderate negative correlation with the SF-12 physical scores. Waiting time on the transplant list was moderately correlated with the LT-VLA mean difficulty subscore ($r = 0.426$, $P = 0.048$). Otherwise, all LT-VLA subscales showed no statistically significant associations with spirometric measures ($P > 0.05$). The relationship between SGRQ-symptom score and LT-VLA mean difficulty score and

the relationship between SF-12 physical score and LT-VLA activities affected score are presented in Figures 1 and 2.

DISCUSSION

The main finding of this study was that the Turkish version of the LT-VLA scale had excellent reliability and internal consistency. The Turkish version of LT-VLA is a valid PCO that demonstrates associations with generic and HRQL measures and with dyspnea perception during daily activities. The Turkish version of the LT-VLA is a feasible, practical, reliable, and valid assessment tool for evaluating limitations in daily life activities among lung transplant recipients, and it can be used by health professionals for ICF-based assessments within medical and rehabilitation interventions. The principal strength of the LT-VLA in both clinical and research settings lies in its ability to capture not only limitations in basic physical functioning but also restrictions in activities that add meaning and satisfaction to patients’ lives. In this respect, the LT-VLA provides a more comprehensive perspective than traditional ADL measures for pre-transplant counseling and post-transplant quality of life monitoring.

Table 2. The internal consistency and ICC values of Turkish version of the LT-VLA scale

| | 1 st test Mean \pm SD | 2 nd test Mean \pm SD | |
|-----------------------------|---------------------------------------|---------------------------------------|-----------------------------|
| LT-VLA mean difficulty | 0.53 \pm 0.09 | 0.47 \pm 0.47 | $r = 0.905$ $P = <0.001$ |
| LT-VLA activities affected% | 31.28 \pm 5.49 | 32.50 \pm 31.21 | $r = 0.873$ $P = <0.001$ |
| LT-VLA activities unable% | 3.44 \pm 2.18 | 4.15 \pm 10.86 | $r = 0.749$ $P = <0.001$ |
| | Cronbach’s α | ICC | 95% CI |
| LT-VLA mean difficulty | 0.945 | 0.897 | 0.768–0.956 |
| LT-VLA activities affected% | 0.906 | 0.828 | 0.631–0.925 |
| LT-VLA activities unable% | 0.934 | 0.877 | 0.727–0.947 |

LT-VLA: Lung Transplant Valued Life Activity scale, ICC: intraclass correlation coefficient, CI: confidence interval, SD: standard deviation

Table 1. The demographic and clinical data of the lung transplant recipients

| LT recipients (n = 22) | Mean \pm SD | Min-max |
|--|-------------------|-------------|
| Age (years) | 45.63 \pm 14.59 | 22–69 |
| Height (cm) | 166.64 \pm 7.42 | 153–180 |
| Weight (kg) | 66.95 \pm 12.91 | 42–92 |
| BMI (kg/m ²) | 24.21 \pm 4.01 | 16.82–33.79 |
| Smoking exposure (pack-years) | 22.04 \pm 28.45 | 2–42 |
| FEV ₁ (%) | 71.81 \pm 30.85 | 22–121 |
| FVC (%) | 72.63 \pm 22.84 | 30–115 |
| FEV ₁ /FVC (%) | 79.37 \pm 17.32 | 37.50–99.80 |
| PEF (%) | 6.93 \pm 6.79 | 1.46–36 |
| mMRC score (0–4) | 0.86 \pm 0.88 | 0–3 |
| Time elapsed after transplantation (months) | 64.86 \pm 43.48 | 3–180 |
| Waiting time on the transplant list (months) | 23.81 \pm 18.40 | 3–60 |

LT: lung transplantation, SD: standard deviation, Min: minimum, max: maximum, BMI: body mass index, FEV₁: forced expiratory volume in 1 second, FVC: forced vital capacity, FEV₁/FVC: ratio of forced expiratory volume in 1 second to forced vital capacity, PEF: peak expiratory flow, mMRC: modified Medical Research Council Dyspnea scale

Table 3. The bivariate correlations between the LT-VLA score and scores of the criterion scales for criterion validity

| Questionnaires for criterion validity | Subscores | LT-VLA mean difficulty | | LT-VLA activities affected% | |
|---------------------------------------|-----------|------------------------|---------------|-----------------------------|---------------|
| | | r | P | r | P |
| SGRQ | Symptom | 0.479 | 0.024* | 0.510 | 0.015* |
| | Total | | | 0.455 | 0.033* |
| LCADL | Self-care | 0.543 | 0.009* | 0.476 | 0.025* |
| | Physical | 0.448* | 0.036* | 0.479 | 0.024* |
| SF-12 | Physical | –0.532 | 0.011* | –0.587 | 0.004* |
| mMRC score | | 0.461 | 0.031* | 0.563 | 0.006* |

*Indicates statistically significant difference ($P < 0.05$)

SGRQ: Saint George Respiratory Questionnaire, LCADL: London Chest Activity of Daily Life Scale, mMRC: modified Medical Research Council scale, LT-VLA: Lung Transplant Valued Life Activity scale, SF-12: Short Form-12

To the best of our knowledge, few assessment tools for ADLs in LT recipients and candidates have been adapted for the Turkish population, and most of these are chronic lung disease-specific or generic measures that do not reflect the specific needs of LT patients.^{14,15} The present study demonstrated that the Turkish version of the LT-VLA scale subscale scores have high internal consistency level with Cronbach's α value ≥ 0.80 . The Cronbach's α values for the mean difficulty, activities affected, and activities unable subscores of the LT-VLA were 0.945, 0.906, and 0.934, respectively, indicating excellent internal consistency. This shows us that the LT-VLA scores are stable despite the time interval between test and retest. We also showed high ICC values for test-retest reliability (≥ 0.80) and strong correlation level between test and retest LT-VLA scores for each subscales. Therefore, the Turkish version of the LT-VLA scale demonstrated high reliability for evaluating ADLs among LT recipients. The results obtained with the Turkish version closely resemble those reported in the validation study of the original English version by Singer et al.¹² (Cronbach's α value: 0.92).

We used the mMRC, LCADL, SGRQ, and SF-12 assessment tools to evaluate the criterion validity of the Turkish version

of the LT-VLA scale. A moderate correlation was found between mMRC and the LT-VLA mean difficulty and activities affected subscores in LT recipients. Additionally, Singer et al.¹² demonstrated that patients with higher LT-VLA scores had lower forced vital capacity (FCV) values. Patients had increased FVC% and mMRC scores after LT transplantation.²⁸ As patients' perception of dyspnea during daily life increased, ADL performance was negatively affected. In our study, the dyspnea levels we found to be associated with LT-VLA mean difficulty and activities affected scores are consistent with the literature.²⁹

The LCADL scale is a tool that assesses difficulties in ADLs due to shortness of breath from COPD and other chronic respiratory diseases.²² Because the LT-VLA scale also assesses limitations, we chose to use it in this validation study. Both the mean difficulty and activities affected scores of the LT-VLA show moderate correlations with the self-care and physical activity scores of the LCADL. This finding confirms the impact of shortness of breath on ADLs in LT recipients, particularly on self-care skills (e.g., dressing, washing) and physical activities (e.g., walking, housework). As shortness of breath worsens, patients experience greater difficulty performing daily activities and report more restricted tasks. Since dyspnea is a critical parameter in LT patients, we believe it is valuable to associate the LT-VLA with a scale that specifically reflects the impact of shortness of breath on daily functioning.

Since the ability to perform ADLs is a key determinant of HRQL, our study incorporated assessments of both HRQL and ADLs as parts of the ICF framework.⁵ We found a moderate, significant correlation between the LT-VLA activities affected score and the SGRQ total score. Given that the SGRQ total score reflects a composite of all subparameters, it serves as a comprehensive indicator of overall HRQL. In contrast, the LT-VLA activities affected score specifically indicates limitations in functional activities.¹² This positive correlation suggests that greater functional disability is associated with poorer quality of life. There was a moderate positive correlation among the SGRQ symptom score, LT-VLA mean difficulty score, and activities affected score in our study. This finding indicates that an increased symptom burden-particularly the frequency and severity of respiratory symptoms such as cough, sputum production, wheezing, and dyspnea-negatively affects patients' ability to perform daily activities and increases the number of activities that patients are unable to complete. This result supports the presence of a direct relationship between symptom burden and functional limitation in respiratory diseases.¹⁹ The original English version of the LT-VLA scale was also validated using the SF-12 score.¹² Consistent with the original article, our study found a moderately negative correlation between the SF-12 Physical score and the LT-VLA mean difficulty and activities affected subscale scores. This study demonstrates that when patients perceive themselves as physically healthier, they tend to experience less difficulty in performing daily tasks and report fewer activity limitations. In a study by Seijo et al.³⁰ examining factors affecting quality of life and survival after LT, a 0.3-unit increase in the LT-VLA mean difficulty score was associated with a 4-point improvement in SF-12 physical scores. The current data from these studies indicate that the correlation between LT-VLA scores and the SF-12 PCS scores is not only

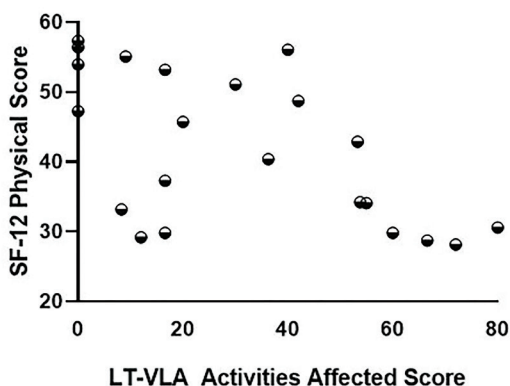


Figure 1. The relationship between SGRQ-symptom score and LT-VLA mean difficulty score
 SGRQ: Saint George Respiratory Questionnaire, LT-VLA: Lung Transplant Valued Life Activity scale, SF-12: Short Form-12

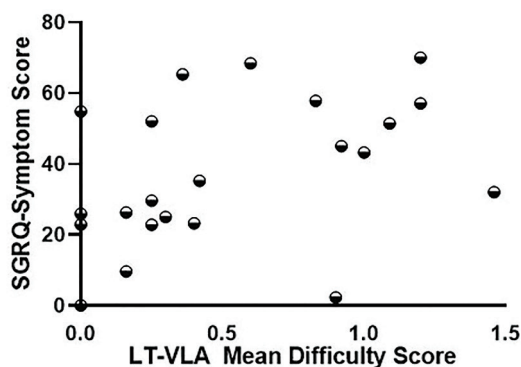


Figure 2. The relationship between SF-12 physical score and LT-VLA activities affected score
 SF-12: Short Form-12, LT-VLA: Lung Transplant Valued Life Activity scale, SGRQ: Saint George Respiratory Questionnaire

cross-sectional but also sensitive to change over time, such as in repeated assessments during the post-transplant period.

There was also a significant positive correlation between the LT-VLA mean difficulty score and the waiting time on the transplant list. This finding suggests that patients who waited longer for LT tended to report greater difficulty in performing daily activities. From a clinical perspective, this is consistent with the progressive nature of end-stage lung diseases, where prolonged waiting times may be associated with further deterioration in physical functioning.³¹ Regarding validity, we consider that this correlation supports the construct validity of the Turkish version of the LT-VLA because it reflects changes in patients' activity limitations over time that are consistent with their clinical status. Therefore, we believe the scale is sensitive to variations in disease burden, further reinforcing its utility in both clinical follow-up and research settings. The lack of significant correlations between LT-VLA scores and spirometric measures suggests that patients' perceived functional limitations may reflect multisystem factors beyond pulmonary function, consistent with the known discordance between objective lung parameters and subjective disability in chronic respiratory diseases.³²

In our Turkish adaptation of the LT-VLA, we noted that male participants frequently selected the response "This does not apply to me" for household activities (e.g., cooking and cleaning) rather than indicating inability or difficulty. Importantly, and in accordance with the original scoring guidelines, these items were correctly excluded from those participants' total scores. This pattern suggests a lack of participation based on culture or gender role, rather than a true functional limitation. This observation is consistent with findings from other LCADL studies, which show that men often receive a zero score not because they are unaffected by dyspnea, but because they do not perform household tasks.¹⁴ Failing to consider this distinction may result in a misrepresentation of their actual functional status.

Study Limitations

The first limitation of our study was the heterogeneity of the sample, which included LT recipients with various pre-transplant diagnoses such as COPD, ILD, CF, and PH. While this reflects the diversity of clinical practice, it may have introduced variability in functional limitations and symptom perception, potentially affecting LT-VLA responses. Future studies should consider evaluating the psychometric properties of the Turkish LT-VLA in more homogeneous subgroups to determine whether disease-specific adaptations or interpretations are warranted. Another limitation of our study is the relatively small sample size. Although the LT-VLA consists of 15 items, our study included only 22 participants. This sample size is below the generally recommended subject-to-item ratio for validation studies, due to the limited number of eligible and available LT recipients during the study period at a single transplant center.³³ Despite the limited number of participants, we conducted robust psychometric analyses that yielded satisfactory results. Given this, future studies should consider

multi-center collaborations to recruit larger and more diverse patient populations, thereby enhancing the generalizability of the findings.

CONCLUSION

In conclusion, the Turkish version of the LT-VLA scale has been validated as a reliable and clinically useful tool for assessing activity limitations in lung transplant recipients. Its practical, self-administered format makes it valuable for multidisciplinary teams, including occupational therapists, physiotherapists, and physicians. For therapists, the scale provides critical insights into patients' challenges with meaningful daily activities, enabling targeted interventions to improve occupational participation and quality of life. Physiotherapists can use the scale to monitor physical function and tailor pulmonary rehabilitation programs, while physicians can integrate patient-reported outcomes with medical assessments to guide comprehensive care. Despite its strengths, limitations, such as the modest sample size and single-center recruitment, suggest the need for further validation in broader populations. Future studies should investigate the scale's responsiveness to various therapeutic interventions, including occupational and physical therapy protocols, to further establish its clinical utility. By offering a standardized measure of functional limitations, the Turkish LT-VLA scale enhances collaborative, patient-centered care and serves as a foundation for developing culturally adapted tools in Türkiye's transplant rehabilitation landscape.

Ethics

Ethics Committee Approval: The study was approved by the Ankara Bilkent City Hospital No. 1 Clinical Research Ethics Committee (date: 29.11.2023, approval number: E1-23-4215).

Informed Consent: The scope and purpose of the study were explained, and written informed consent forms were obtained from all participants.

Footnotes

Authorship Contributions

Surgical and Medical Practices: E.Y., F.Ç.B., S.T., Concept: U.A., E.Ç., Design: U.A., E.Ç., Data Collection or Processing: U.A., Analysis or Interpretation: U.A., E.Ç., Literature Search: U.A., E.Ç., F.Ç.B., S.T., Writing: U.A., E.Ç., F.Ç.B., S.T.

Conflict of Interest: No conflict of interest was declared by the authors.

Financial Disclosure: The authors declared that this study received no financial support.








REFERENCES

1. Singer JP, Singer LG. Quality of life in lung transplantation. *Semin Respir Crit Care Med.* 2013;34(3):421-430. [\[Crossref\]](#)
2. Bos S, Vos R, Van Raemdonck DE, Verleden GM. Survival in adult lung transplantation: where are we in 2020? *Curr Opin Organ Transplant.* 2020;25(3):268-273. [\[Crossref\]](#)

3. Langer D. Rehabilitation in patients before and after lung transplantation. *Respiration*. 2015;89(5):353-362. [\[Crossref\]](#)
4. Ar U, Yekeler E, Calik-Kutukcu E. Body function and structure, activity, and participation limitations of lung transplant recipients within the Scope of the International Classification of Functioning, Disability, and Health. *Exp Clin Transplant*. 2022;18. [\[Crossref\]](#)
5. Takahashi R, Takahashi T, Okada Y, Kohzuki M, Ebihara S. Factors associated with quality of life in patients receiving lung transplantation: a cross-sectional study. *BMC Pulm Med*. 2023;23(1):225. [\[Crossref\]](#)
6. Verleden GM, Glanville AR, Lease ED, et al. Chronic lung allograft dysfunction: definition, diagnostic criteria, and approaches to treatment—a consensus report from the Pulmonary Council of the ISHLT. *J Heart Lung Transplant*. 2019;38(5):493-503. [\[Crossref\]](#)
7. Pantoja JG, Andrade FH, Stokić DS, Frost AE, Eschenbacher WL, Reid MB. Respiratory and limb muscle function in lung allograft recipients. *Am J Respir Crit Care Med*. 1999;160(4):1205-1211. [\[Crossref\]](#)
8. Spiesshoefer J, Henke C, Kabitz HJ, et al. Respiratory muscle and lung function in lung allograft recipients: association with exercise intolerance. *Respiration*. 2020;99(5):398-408. [\[Crossref\]](#)
9. Medical Complications of Lung Transplantation [Internet]. Accessed Jul 8, 2025. [\[Crossref\]](#)
10. Staçel T, Jaworska I, Zawadzki F, et al. Assessment of quality of life among patients after lung transplantation: a single-center study. *Transplant Proc*. 2020;52(7):2165-2172. [\[Crossref\]](#)
11. Hume E, Ward L, Wilkinson M, Manfield J, Clark S, Vogiatzis I. Exercise training for lung transplant candidates and recipients: a systematic review. *Eur Respir Rev*. 2020;29(158):200053. [\[Crossref\]](#)
12. Singer JP, Blanc PD, Dean YM, et al. Development and validation of a lung transplant-specific disability questionnaire. *Thorax*. 2014;69(5):437-442. [\[Crossref\]](#)
13. Rothman M, Burke L, Erickson P, Leidy NK, Patrick DL, Petrie CD. Use of existing patient-reported outcome (PRO) instruments and their modification: the ISPOR Good Research Practices for Evaluating and Documenting Content Validity for the Use of Existing Instruments and Their Modification PRO Task Force Report. *Value Health*. 2009;12(8):1075-1083. [\[Crossref\]](#)
14. Saka S, Savcı S, Kütükcü EÇ, et al. Validity and Reliability of the Turkish Version of the London Chest Activity of Daily Living Scale in Obstructive Lung Diseases. *Turk Thorac J*. 2020;21(2):116-121. [\[Crossref\]](#)
15. Polatlı M, Yorgancıoğlu A, Aydemir Ö, et al. [Validity and reliability of Turkish version of St. George's respiratory questionnaire]. *Tuberk Toraks*. 2013;61(2):81-87. [\[Crossref\]](#)
16. Monjazebi F, Dalvandi A, Ebadi A, Khankeh HR, Rahgozar M, Richter J. Functional status assessment of COPD based on ability to perform daily living activities: a systematic review of paper and pencil instruments. *Glob J Health Sci*. 2015;8(3):210-223. [\[Crossref\]](#)
17. Beaton DE, Bombardier C, Guillemin F, Ferraz MB. Guidelines for the process of cross-cultural adaptation of self-report measures. *Spine (Phila Pa 1976)*. 2000;25(24):3186-3191. [\[Crossref\]](#)
18. Arifin WN. A web-based sample size calculator for reliability studies. *Education in Medicine Journal*. 2018;10(3):67-76. [\[Crossref\]](#)
19. Jones PW, Quirk FH, Baveystock CM. The St George's respiratory questionnaire. *Respir Med*. 1991;85:25-31. [\[Crossref\]](#)
20. Ware J, Kosinski M, Keller SD. A 12-item Short-Form health survey: construction of scales and preliminary tests of reliability and validity. *Med Care*. 1996;34(3):220-233. [\[Crossref\]](#)
21. Soysal Gündüz Ö, Mutlu S, Aslan Baslı A, et al. Validation of the Turkish form of Short Form-12 health survey version 2 (SF-12v2). *Arch Rheumatol*. 2021;36(2):280-286. [\[Crossref\]](#)
22. Garrod R, Bestall JC, Paul EA, Wedzicha JA, Jones PW. Development and validation of a standardized measure of activity of daily living in patients with severe COPD: the London Chest Activity of Daily Living scale (LCADL). *Respir Med*. 2000;94(6):589-596. [\[Crossref\]](#)
23. Bestall JC, Paul EA, Garrod R, Garnham R, Jones PW, Wedzicha JA. Usefulness of the medical Research Council (MRC) dyspnoea scale as a measure of disability in patients with chronic obstructive pulmonary disease. *Thorax*. 1999;54(7):581-586. [\[Crossref\]](#)
24. Gur Kabul E, Demir P, Cagla Balkisli B, et al. The Validity and Reliability of the Turkish version of Modified Medical Research Council Dyspnea Scale in Systemic Sclerosis Patients with Interstitial Lung Disease. *Thorac Res Pract*. 2024;25(6):215-220. [\[Crossref\]](#)
25. Schober P, Boer C, Schwarte LA. Correlation coefficients: appropriate use and interpretation. *Anesthesia & Analgesia*. 2018;126(5):1763-1768. [\[Crossref\]](#)
26. Alpar R. Spor Sağlık ve Eğitim Bilimlerinden Örneklerle Uygulamalı İstatistik ve Geçerlik Güvenirlilik SPSS de Çözümleme Adımları ile Birlikte. 8th ed. İstanbul: Nobel Akademik Yayıncılık; 2025. p. 1-744. ISBN: 9786255532367. [\[Crossref\]](#)
27. Weir JP. Quantifying test-retest reliability using the intraclass correlation coefficient and the SEM. *J Strength Cond Res*. 2005;19(1):231-240. [\[Crossref\]](#)
28. Jastrzębski DT, Gumola A, Wojarski J, et al. A functional assessment of patients two years after lung transplantation in Poland. *Kardiochir Torakochirurgia Pol*. 2014;11(2):162-168. [\[Crossref\]](#)
29. Perez T, Roche N, Nunes H, et al. Dyspnea-induced limitation (DYSLIM), a new self-administered concise questionnaire to evaluate dyspnea-related activity limitation in chronic respiratory diseases. *Respir Med*. 2023;217:107309. [\[Crossref\]](#)
30. Seijo L, Gao Y, Betancourt L, Venado A, Hays SR, Kukreja J, et al. Improvements in patient-reported functioning after lung transplant is associated with improved quality of life and survival [Internet]. medRxiv; 2024. Accessed Jul 11, 2025. [\[Crossref\]](#)
31. Kristobak BM, Bezinover D, Geyer N, Cios TJ. Decline in Functional status while on the waiting list predicts worse survival after lung transplantation. *J Cardiothorac Vasc Anesth*. 2022;36(12):4370-4377. [\[Crossref\]](#)
32. Eisner MD, Iribarren C, Blanc PD, et al. Development of disability in chronic obstructive pulmonary disease: beyond lung function. *Thorax*. 2011;66(2):108-114. [\[Crossref\]](#)
33. Anthoine E, Moret L, Regnault A, Sébille V, Hardouin JB. Sample size used to validate a scale: a review of publications on newly-developed patient reported outcomes measures. *Health Qual Life Outcomes*. 2014;12:176. [\[Crossref\]](#)

Original Article

Compliance of Aerosol Therapy with Evidence-based Guideline and Cost Incurred in Adult Critically-ill Patients: A Prospective Observational Study

 Ayushi R. Verma¹,  Jignesh Shah²,  Sulochana Kumari³,  Asavari L. Raut¹,  Steffi Abraham¹,  Ritu Priya¹,  Kinjal K. Patil¹

¹Department of Pharmacy Practice, BVDU Poona College of Pharmacy, Pune, Maharashtra, India

²Department of Critical Care Medicine, Bharati Vidyapeeth (Deemed to be University) Medical College, Pune, Maharashtra, India

³Incharge Respiratory Therapist, Division of Respiratory Therapy, Bharati Hospital and Research Centre, Pune, Maharashtra, India

Cite this article as: Verma AR, Shah J, Kumari S, et al. Compliance of aerosol therapy with evidence-based guideline and cost incurred in adult critically-ill patients: a prospective observational study. *Thorac Res Pract.* 2026;27(3):155-164

ABSTRACT

OBJECTIVE: Aerosol therapy is widely used in intensive care units (ICUs) for managing respiratory conditions. However, non-adherence to evidence-based guidelines can compromise outcomes and increase healthcare costs. This study evaluated the compliance of aerosol therapy with the “Indian Guidelines on Nebulization Therapy” and the cost incurred in critically ill patients.

MATERIAL AND METHODS: A prospective observational study was conducted in 307 adult patients across the ICUs of a tertiary care hospital during a six-month study period. Analysis was performed using the chi-square test and the Wilcoxon rank-sum test in RStudio (version 4-4.3, 2024). Multivariate logistic regression identified independent predictors of compliance.

RESULTS: Of the 307 ICU patients analyzed, 64.5% were male, with an average age of 57±16 years. Jet nebulizers were used in 91.5% of cases. Bronchodilators (47.13%) and corticosteroids (35%) were widely used classes of drugs. Compliance of drug therapy with evidence-based guidelines varied significantly by duration of ICU stay ($P = 0.0062$) and by ICU category ($P = 0.0005$). Drug compliance was higher in critical care and neurology ICUs [odds ratio (OR): 6.500, $P = 0.0001$; OR: 4.574, $P = 0.005$]. Administration compliance was significantly associated with the diagnosis category ($P = 0.00186$) and was higher among patients with non-respiratory diagnoses (OR: 4.96, $P = 0.0068$). Adherence to guidelines for drug therapy significantly lowered costs ($P = 0.0103$).

CONCLUSION: Targeted interventions, protocol standardization, and staff training are needed to enhance compliance, optimize patient care, and control aerosol-related expenditures. Clinically, these findings highlight that adherence to evidence-based aerosol therapy not only enhances patient outcomes but also reduces ICU expenditure, thereby supporting integration into routine clinical practice.

KEYWORDS: Aerosol, critically ill patients, ICU, nebulizers, compliance, nebulization, cost

Received: 29.09.2025

Revision Requested: 13.11.2025

Last Revision Received: 20.11.2025

Accepted: 11.12.2025

Epub: 05.03.2026

Publication Date: 12.05.2026

INTRODUCTION

Aerosol therapy plays a crucial role in the management of respiratory conditions, particularly among critically ill patients who require immediate intervention. The prevalence of aerosol therapy use in India has been reported as 72.48%.¹

The administration of aerosolized medications enables direct delivery to the lungs, thereby ensuring rapid therapeutic response, increased bioavailability at the target site, minimized systemic side effects, and reduced risk of toxicity.^{2,3} It is routinely used for both mechanically ventilated and non-ventilated patients presenting with diseases such as asthma, chronic obstructive pulmonary disease (COPD), acute respiratory distress syndrome, pneumonia, and cystic fibrosis. Frequently administered medications, used as monotherapy or in combination, include bronchodilators, corticosteroids, mucolytics, and antibiotics.^{1,4,5}

Corresponding author: Asavari Raut, M. Pharm, PhD, e-mail: asavari.raut@gmail.com - asavari.raut@bharativedyapeeth.edu



The clinical efficacy of aerosol therapy depends on numerous factors, for example, characteristics of aerosolized particles, the patient's respiratory physiology, and management of the device.^{2,5,6} An extensive range of aerosol delivery devices is used in hospital settings, including jet, vibrating mesh, and ultrasonic nebulizers, each with its advantages and disadvantages.^{2,7}

Despite its therapeutic benefits, aerosol therapy is accompanied by several limitations, including variability in drug deposition due to device type, patient condition, and administration technique. Its effectiveness is further limited in the intensive care unit (ICU) environment due to increased risk of nosocomial infections due to device contamination,⁸ lack of standardized protocols, and inconsistency in clinical practice.^{9,10} Additionally, the limited availability of aerosol formulations and the high cost of advanced nebulization devices hinder their widespread use, particularly in resource-limited settings such as India.^{7,11,12}

Non-compliance with established guidelines further reduces the effectiveness of aerosol therapy. Issues such as reduced drug efficacy, increased incidence of adverse effects, variability in delivery techniques, inadequate training of healthcare personnel, and poor maintenance of devices are commonly observed in clinical practice.^{9,10,13} Financial barriers also play a significant role. In developing countries such as India, ICU-related expenses, including costs associated with aerosol therapy, ventilator use, and equipment maintenance, are often borne directly by patients and their families. This economic burden, compounded by inefficient drug delivery and deviations from recommended protocols, frequently results in premature discontinuation of therapy and suboptimal clinical outcomes.^{8,9,14}

Effective utilization of aerosol therapy in ICUs requires a structured evaluation of current practices, particularly regarding guideline adherence and cost-effectiveness. Inconsistent practices and financial constraints often undermine its potential benefits, particularly in resource-limited healthcare settings.^{11,12}

The "Indian Guidelines on Nebulization Therapy" provide a structured guide for the use of aerosol therapy in clinical settings, such as ICUs. However, compliance with this guideline and the associated costs incurred in Indian ICUs remain unclear.^{8,10} This study aims to determine the proportion of aerosol therapy sessions in adult ICU patients that complied with the "Indian Guidelines on Nebulization Therapy" with respect to (a) drug therapy (indication, drug selection, dose/frequency, incompatible combinations, and duration) and (b)

administration practices (device selection and placement, carrier gas, and device hygiene).

MATERIAL AND METHODS

Study Design and Ethics

A prospective, exploratory (descriptive) observational study was conducted among 307 patients in the ICU and high-dependency unit of Bharati Hospital and Research Centre, Pune, and was approved by the Bharati Vidyapeeth (Deemed to be University) Medical College Ethics Committee (approval ID: BVDUMC/IEC/91/24-25, date 28/09/2024). The study was conducted over a period of six months (October 2024-March 2025). This study was not registered with CTRI. The authors acknowledge that registration is recommended for observational studies in clinical practice and will register future audits of a similar nature and encourage readers to take this into consideration when interpreting the results. All procedures were conducted in accordance with the ethical standards of the institutional research committee and the principles outlined in the Declaration of Helsinki (2024 revision). A waiver of written informed consent for this observational study was approved by the Ethics Committee, as data collection used routine clinical records and did not require changes to patient care.

Sample Size

For the primary outcome, the sample size was calculated based on the proportion of aerosol therapy sessions expected to be compliant with guideline recommendations. Based on published estimates of aerosol therapy guideline adherence and utilization in India (expected compliance $\approx 72.48\%$ from⁽¹⁾) using a two-sided 95% confidence level ($Z = 1.96$) and a desired absolute precision of 5%, the required sample size was: $n = (Z^2 \times p \times (1-p)) / d^2 = (1.96^2 \times 0.7248 \times 0.2752) / 0.05^2 \approx 307$.

Study Criteria

The study included patients aged more than 18 years receiving aerosol therapy for ≥ 24 hours during their ICU stay. All patients older than 85 years and those receiving aerosol therapy for more than 2 months were excluded from the study. Additionally, patients using inhalation devices, such as dry powder inhalers and pressurized metered-dose inhalers, as well as those receiving nebulization therapy with normal saline alone were not included. A structured proforma was designed, consisting of three sections (information related to aerosol drug therapy, compliance and cost) and validated by four expert panelists, in adherence to the evidence-based guideline of the "Indian Guidelines on Nebulization Therapy".

Diagnostic Characterization

The study classified patients into three broad diagnostic categories: respiratory, respiratory with comorbidities, and non-respiratory because this structure reflects how cases are typically organized and managed in the ICU. Individual disease labels, such as COPD, pneumonia, myocardial infarction, or sepsis, had very small numbers of patients in several groups, which would not allow for statistically meaningful comparisons and would violate chi-square assumptions. Using the three broader categories ensured adequate sample distribution, maintained

Main Points

- Jet nebulizers were the most commonly used aerosol delivery devices in critically-ill patients.
- Compliance of drug therapy with evidence-based guidelines varied significantly across intensive care unit (ICU) categories and duration of ICU stay.
- Non-respiratory patients demonstrated higher administration compliance as compared with respiratory groups.
- Drug regimen adherence was associated with a significant reduction in mean cost incurred.

statistical validity, and allowed a more reliable evaluation of compliance patterns.

Operational Definitions and Timing

Aerosol Therapy Session: Any discrete episode of administration of an inhaled medication via a nebulizer or other inhalation device, documented in the patient’s chart.

Drug Therapy Compliance: A session was considered compliant with drug therapy if all of the following criteria were met: (a) the indication for therapy matched guideline indications; (b) the drug class selection was appropriate for the indication; (c) the dosing frequency was in accordance with guideline recommendations; (d) no guideline-listed incompatible drug combinations were present; and (e) the duration was appropriate for the indication (Supplementary Table 1).

Administration Compliance: A session was considered compliant if device selection, device placement (e.g., endotracheal tube or venturi mask), carrier gas (oxygen, air, or ventilator setting), and device hygiene (documented cleaning/disinfection) adhered to the components recommended in the “Indian Guidelines on Nebulization Therapy” Supplementary Table 2.

Time Points Assessed: Data were recorded systematically for each aerosol therapy session using information present in the patient’s drug chart and respiratory sheet during the patient’s ICU stay.

Statistical Analysis

All data were compiled and cleaned in Microsoft Excel. Analysis was performed using RStudio software (version 4-4.3, 2024). Average age was presented as mean ± standard

deviation. Categorical variables were presented as counts (n) and percentages (%). Associations between categorical variables (e.g., device placements) and compliance status (evaluated as per the guideline) were assessed using the chi-square test. To identify independent predictors of compliance, multivariate logistic regression models were used because they are well suited for binary outcomes. Covariates were selected based on clinical relevance and included ventilation type, age category, ICU categorization, length of ICU stay, and primary diagnosis. Results were expressed as odds ratios (ORs) with 95% confidence intervals (CIs).

Cost Incurred Assessment

The costs incurred in the study included direct medical costs attributable to aerosol therapy during the ICU stay, such as aerosol medication, device costs, respiratory therapist fees, nebulizer costs, and oxygen costs. Indirect (overhead) costs (e.g., ICU bed charges) were not included. The Wilcoxon rank-sum test was used to compare costs between compliant and non-compliant groups. A P value <0.05 was considered significant. In addition, a simple linear regression model was applied using ICU stay (in days) as the independent variable and total cost as the outcome, with model fit reported using R².

RESULTS

Patient Characteristics and Clinical Outcomes

A total of 307 patients admitted to the ICU between October 2024 and March 2025 were included in the study. The cohort had a male predominance, with 198 (64.5%) males and 109 (35.5%) females, and a mean age of 57±16 years. Of the total study population, 140 patients (45.6%) were discharged, 83 (27.03%) were transferred to the general ward, and 34 (11.07%) left against medical advice. The observed in-hospital mortality

Table 1. Demographic and clinical characteristics of the study population

| | All patients receiving aerosol therapy (n = 307) | Patients receiving invasive aerosol therapy (n = 99) | Patients receiving non-invasive aerosol therapy (n = 174) | Patients receiving both invasive and non-invasive aerosol therapy (n = 34) |
|---|--|--|---|--|
| Age (years) | 57±16 | | | |
| Male/female | 198 (64.5%)/109 (35.5%) | 66 (66.67%)/33 (33.33%) | 108 (62.1%)/66 (37.9%) | 24 (70.6%)/10 (29.4%) |
| Categorization of ICU | | | | |
| Critical care medicine | 143 (46.6%) | 61 (61.6%) | 61 (35.1%) | 21 (61.8%) |
| Neurological | 47 (15.3%) | 7 (7.1%) | 35 (20.1%) | 5 (14.7%) |
| Cardiovascular | 25 (8.14%) | 9 (9.1%) | 12 (6.8%) | 4 (11.8%) |
| Surgical | 17 (5.53%) | 6 (6.1%) | 10 (5.7%) | 1 (2.9%) |
| Non-speciality | 75 (24.43 %) | 16 (16.1%) | 56 (32.2%) | 3 (8.8%) |
| Classification of study population based on primary diagnosis | | | | |
| Respiratory | 41 (13.3%) | 5 (5.1%) | 32 (18.4%) | 4 (11.8%) |
| Respiratory with co-morbidities | 139 (45.3%) | 43 (43.4%) | 77 (44.3%) | 19 (55.8%) |
| Non-respiratory | 127 (41.4%) | 51 (51.5%) | 65 (37.3%) | 11 (32.4%) |

Values are presented as mean ± standard deviation or n (%), as appropriate
 ICU: intensive care unit

rate was 14%, whereas 2.3% of patients were transferred to deluxe care units for continued treatment. Regarding ventilation type, 99 (32.23%) received aerosol therapy via invasive ventilation, 174 (56.7%) via non-invasive ventilation (NIV), and 34 (11.07%) transitioned between these two modalities during their ICU stay. The details of ICU categorization and primary diagnoses are summarized in Table 1.

Drugs and Devices Used for Aerosol Therapy

Jet nebulizers were the most widely used devices, accounting for 91.5% of cases, whereas vibrating mesh nebulizers (VMNs) accounted for 8.5%. Ultrasonic nebulizers were not employed in this study.

Among the 575 aerosol therapy sessions analyzed, 543/575 (94.43%) involved single-agent therapy, and the remaining 32/575 (5.56%) were administered in combination. Among single-agent treatments, the majority [47.13% (271/575)] were bronchodilators, followed by corticosteroids [35% (201/575)]. In terms of regimen complexity, 36.2% of patients received monotherapy, 47.6% received dual-drug therapy, and 11.4% received a regimen consisting of three aerosolized medications. A small subset (4.8%) received more than four aerosolized medications. The distribution of medication classes is shown in Figure 1.

Indications for Aerosol Therapy

Aerosol therapy was most frequently prescribed for respiratory conditions, accounting for 58.63% (n = 180) of the cohort, with pneumonia and COPD being the leading indications. The remaining patients received aerosol therapy for neurological, cardiac, or post-surgical indications (see Table 1).

Device Placements for Aerosol Therapy

Device placement varied significantly across the types of ventilation used. For jet nebulizers, invasive ventilation predominantly used endotracheal tube placement, while

NIV was almost exclusively managed with Venturi masks. Patients who received both modalities commonly received a combination of a Venturi mask and an endotracheal tube. Similar patterns were observed in patients using VMNs. These findings, presented in Table 2, indicate a significant association between the type of ventilation and device placement for aerosol delivery.

Administration of Aerosol Therapy

Oxygen was the primary carrier medium, with the highest prevalence observed in the NIV group (77.32%). Flowmeter-based oxygen administration was used in 15.3% of cases, whereas ventilator-based delivery was limited to patients receiving invasive or combined ventilation. The diversity of administration methods highlighted the central role of oxygen in facilitating effective aerosol drug delivery. The distribution of administration methods is illustrated in Figure 2.

Compliance of Aerosol Therapy with Evidence-based Guideline

Compliance with evidence-based guidelines was assessed in two domains: drug therapy and administration (Tables 3 and 4).

The compliance with drug therapy was evaluated in terms of frequency, combination, and duration of treatment.

Drug therapy compliance varied significantly according to ICU categorization ($P = 0.0005$), suggesting that specific units of care may affect adherence. Furthermore, ICU stays affected drug compliance ($P = 0.0062$), indicating an influence on treatment adherence. Other variables, such as age group and diagnosis, were not associated with substantial differences in drug compliance. Drug administration compliance was largely uniform across all clinical subgroups, with no significant associations identified for most subgroups; however, a significant association was noted between diagnosis category and compliance ($P = 0.00186$).

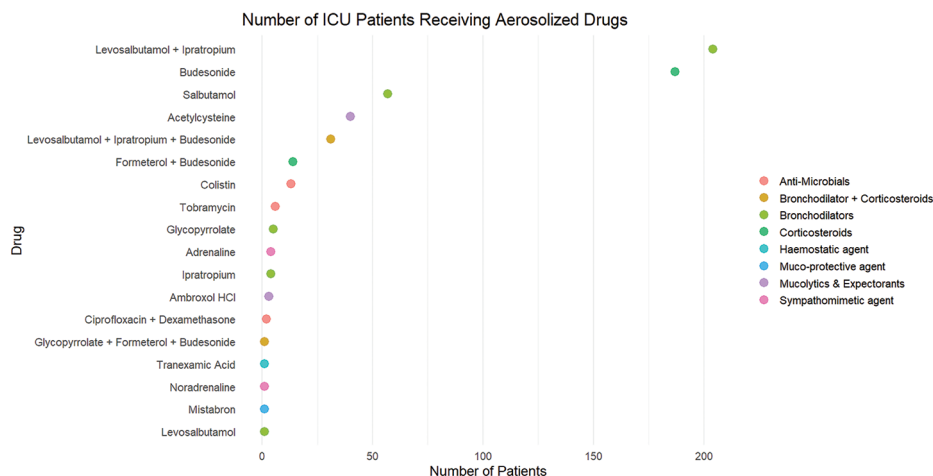


Figure 1. Drugs used as aerosol therapy in the study population. Dot plot depicting the number of ICU patients receiving aerosolized drugs, categorized by drug class. Each dot represents a drug; drug categories are color-coded. Frequencies are plotted on the x-axis

ICU: intensive care unit

Table 2. Device placements for aerosol therapy in the study population

| Type of aerosol delivery device | Device placements | Invasive | Non-invasive | Both | P value |
|---------------------------------|----------------------------------|----------------|-----------------|----------------|--------------------|
| Jet nebulizer | Endotracheal tube | 33/99 (33.33%) | 0/174 (0%) | 2/34 (5.9%) | P < 0.01 |
| | Nasal prongs | 4/99 (4.04%) | 0/174 (0%) | 1/34 (2.94%) | 0.14 |
| | Venturi mask | 22/99 (22.22%) | 173/174 (99.4%) | 5/34 (14.7%) | P < 0.01 |
| | Venturi mask + endotracheal tube | 20/99 (20.20%) | 0/174 (0%) | 20/34 (58.82%) | P < 0.01 |
| | Nasal prongs + venturi mask | 0/99 (0%) | 0/174 (0%) | 1/34 (2.94%) | 1.00 |
| Vibrating mesh nebulizer | Endotracheal tube | 13/99 (13.13%) | 0/174 (0%) | 1/34 (2.94%) | P < 0.01 |
| | Nasal prongs | 0/99 (0%) | 0/174 (0%) | 0/34 (0%) | - |
| | Venturi mask | 6/99 (6.06%) | 1/174 (0.6%) | 0/34 (0%) | 0.02 |
| | Venturi mask + endotracheal tube | 1/99 (1.01%) | 0/174 (0%) | 4/34 (11.76%) | 0.14 |
| | Nasal prongs + venturi mask | 0/99 (0%) | 0/174 (0%) | 0/34 (0%) | - |

Data are presented as the number of patients (percentage within group). P values were calculated using the chi-square test. P value of <0.05 was considered significant

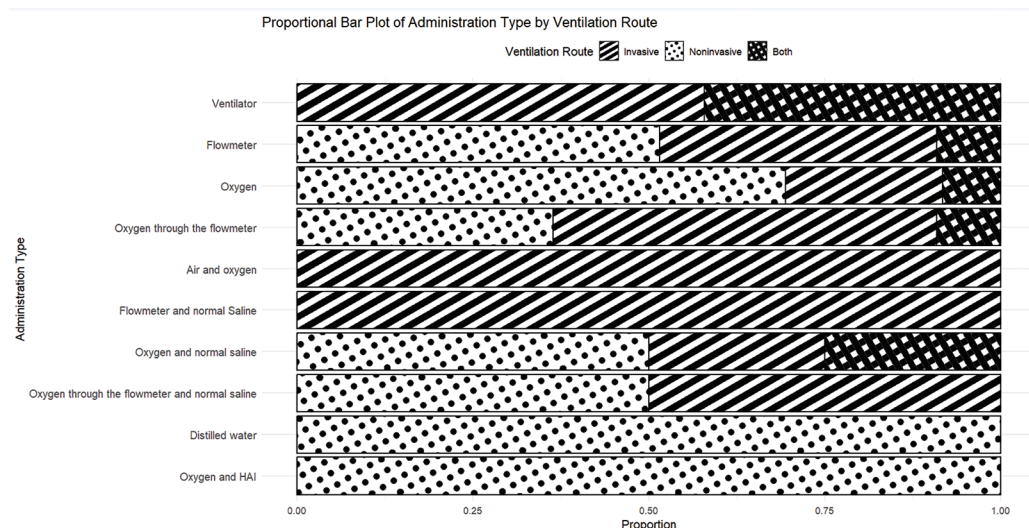


Figure 2. Patterned proportional bar chart representing types of aerosol therapy administration by ventilation route (invasive, non-invasive, both). Bars represent the proportion of each administration method used across invasive, non-invasive, and combined ventilation routes. Patterns differentiate the ventilation modes

HAI, hyperoxic anoxia

These findings highlight that, while drug administration practices were largely consistent, variations in medication adherence were influenced by incompatible drug combinations, prolonged therapy duration, and improper drug regimens.

Multivariate Analysis for Predictors of Compliance with Evidence-based Guideline

Multivariate logistic regression analysis identified several significant predictors of both drug and administration compliance, as illustrated in Figures 3a and 3b. For drug therapy, patients admitted to critical care medicine had higher odds of compliance than those in cardiology (OR: 6.50; 95% CI: 2.60–16.25; P = 0.0001), and patients in neurology ICUs also demonstrated increased compliance (OR: 4.57; 95% CI: 1.57–13.32; P = 0.005). In contrast, patients in cardiology ICUs had lower odds of compliance compared with both surgical (OR: 0.15; 95% CI: 0.03–0.83; P = 0.02) and non-speciality ICUs (OR: 0.13; 95% CI: 0.04–0.36; P = 0.0001). Shorter ICU

stays were associated with higher compliance (OR: 2.38; 95% CI: 0.97–5.85, P = 0.05).

With respect to administration compliance, most comparisons did not reveal notable relationships. However, a significant association between diagnosis and compliance was observed: patients with non-respiratory conditions had significantly higher odds of compliance with the evidence-based guideline compared with those with respiratory illness and co-morbidities (OR: 4.959; 95% CI: 1.399–17.57; P = 0.007).

Cost Incurred Due to Aerosol Therapy

Among patients compliant with drug therapy protocols, the mean cost incurred was significantly lower (P = 0.01). Linear regression showed that ICU stay duration explained a moderate proportion of cost variation (R² = 0.56), with an estimated increase of ₹3495.5 per additional ICU day. These findings underscore the economic burden of prolonged hospitalization

Table 3. Drug compliance in terms of frequency, combination and duration of therapy with evidence-based guideline among different clinical variables in the study population

| Compliance category | Clinical variable | Sub group | Compliant (n) | Non-compliant (n) | P value |
|---|-----------------------|----------------------------------|-----------------|-------------------|-----------------|
| Drug compliance | Invasive/non-invasive | Invasive (n = 99) | 79/99 (79.8%) | 20/99 (20.2%) | 0.78 |
| | | Non-invasive (n = 174) | 148/174 (85.1%) | 26/174 (14.9%) | |
| | | Both (n = 34) | 27/34 (79.4%) | 7/34 (20.6%) | |
| | ICU categorization | Critical care medicine (n = 143) | 123/143 (86%) | 20/143 (14%) | P = 0.01 |
| | | Neurological (n = 47) | 38/47 (80.9%) | 9/47 (19.1%) | |
| | | Cardiology (n = 25) | 12/25 (48%) | 13/25 (52%) | |
| | | Surgery (n = 17) | 15/17 (88.2%) | 2/17 (11.8%) | |
| | | Non-speciality (n = 75) | 66/75 (88%) | 9/75 (12%) | |
| | Days in ICU | <5 days (n = 65) | 57/65 (87.7%) | 8/65 (12.3%) | P = 0.01 |
| | | 6–10 days (n = 129) | 106/129 (82.2%) | 23/129 (17.8%) | |
| | | >10 days (n = 113) | 91/113 (80.5%) | 22/113 (19.5%) | |
| | Age | <30 (n = 16) | 13/16 (81.3%) | 3/16 (18.7%) | 0.36 |
| | | 30–44 (n = 46) | 37/46 (80.4%) | 9/46 (19.6%) | |
| | | 45–59 (n = 82) | 67/82 (81.7%) | 15/82 (18.3%) | |
| | | 60–74 (n = 101) | 89/101 (88.1%) | 12/101 (11.9%) | |
| | | >75 (n = 62) | 48/62 (77.4%) | 14/62 (22.6%) | |
| | Diagnosis | Respiratory (n = 41) | 35/41 (85.4%) | 6/41 (14.6%) | 0.42 |
| | | Non-respiratory (n = 127) | 101/127 (79.5%) | 26/127 (20.5%) | |
| Respiratory with co-morbidities (n = 139) | | 118/139 (84.9%) | 21/139 (15.1%) | | |

Compliance patterns for aerosol therapy in ICU patients are represented for drug therapy. The table presents the number of patients categorized as compliant or non-compliant for drug use. Comparisons are made across ventilation type, ICU categorization, ICU stay duration, aerosol mode, age and diagnosis. Statistically significant results are highlighted with corresponding P values
 ICU: intensive care unit

and highlight the potential financial benefits of improving compliance. A detailed summary of cost data is presented as a grouped box plot in Figure 4.

DISCUSSION

This study provides a detailed evaluation of aerosol therapy utilization, compliance, and associated costs in critically ill patients admitted during the study period. The findings underscore the complexity of delivering standardized aerosol treatment in high-acuity settings and reveal important gaps in adherence despite well-established recommendations.

Among the 307 patients studied, demographic patterns and clinical outcomes were comparable to national data, reflecting the typical profile of critically ill patients in Indian ICUs. These consistencies reaffirm that the study cohort represents real-world practice and aligns with previously published literature on ICU severity and outcomes.^{1,7,9}

Bronchodilators emerged as the most frequently administered drug class (47.13%), consistent with previous findings emphasizing their essential role in managing obstructive airway diseases.^{8,11} Respiratory illnesses constituted the majority of indications for aerosol therapy. These findings mirror those reported in multiple Indian and international studies that identify respiratory infections and airway obstruction as the

predominant drivers of nebulization in ICU settings.^{1,3} This study supports the notion that aerosol therapy is primarily reserved for such conditions, while highlighting the importance of ongoing evaluation of compliance, cost-effectiveness, and staff training.^{11,12}

The research also assessed adherence to the “Indian Guidelines on Nebulization Therapy”,¹⁵ which are divided into two key areas: medication regimen (drug frequency, incompatible combinations & duration of therapy) and administration procedures. While some elements of the treatment were consistent with the guidelines, there were notable discrepancies in several areas, highlighting a disconnect between theoretical recommendations and practical implementation.

The study highlighted issues with drug regimens, including extended treatment periods and the use of incompatible agents. These practices are frequently influenced by the prescriber’s preferences and by a lack of awareness of guidelines.¹ Such deviations can result in reduced therapeutic effectiveness, increased adverse drug reactions, and prolonged ICU stays. To improve the rational use of aerosol therapy, it is essential to systematically incorporate guidelines into clinical practice.

Irregularities in dosing frequency were observed: some patients received excessive aerosol treatment, thereby increasing their risk of adverse events; others were undertreated,

Table 4. Administration compliance in terms of delivery of aerosol drugs (oxygen or air-driven)with evidence-based guideline among different clinical variables in the study population

| Compliance category | Clinical variable | Sub group | Compliance (n) | Non-compliance (n) | P value | |
|---|-----------------------|------------------------|----------------------------------|--------------------|---------------|-----------------|
| Administration compliance | Invasive/non-invasive | Invasive (n = 99) | 95/99 (96%) | 4/99 (4%) | 0.71 | |
| | | Non-invasive (n = 174) | 158/174 (90.8%) | 16/174 (9.2%) | | |
| | | Both (n = 34) | 31/34 (91.2%) | 3/34 (8.8%) | | |
| | ICU categorization | | Critical care medicine (n = 143) | 136/143 (95.1%) | 7/143 (4.9%) | 0.20 |
| | | | Neurological (n = 47) | 42/47 (89.4%) | 5/47 (10.6%) | |
| | | | Cardiology (n = 25) | 25/25 (100%) | 0/25 (0%) | |
| | | | Surgery (n = 17) | 14/17 (82.4%) | 3/17 (17.6%) | |
| | | | Non-speciality (n = 75) | 67/75 (89.3%) | 8/75 (10.7%) | |
| | Days in ICU | | <5 days (n = 65) | 62/65 (95.4%) | 3/65 (4.6%) | 0.71 |
| | | | 6–10 days (n = 129) | 118/129 (91.5%) | 11/129 (8.5%) | |
| | | | >10 days (n = 113) | 104/113 (92%) | 9/113 (8%) | |
| | Age | | <30 (n = 16) | 15/16 (93.8%) | 1/16 (6.2%) | 0.61 |
| | | | 30–44 (n = 46) | 44/46 (95.7%) | 2/46 (4.3%) | |
| | | | 45–59 (n = 82) | 76/82 (92.7%) | 6/82 (7.3%) | |
| | | | 60–74 (n = 101) | 92/101 (91.1%) | 9/101 (8.9%) | |
| | | | >75 (n = 62) | 57/62 (91.9%) | 5/62 (8.1%) | |
| | Diagnosis | | Respiratory (n = 41) | 38/41 (92.7%) | 3/41 (7.3%) | P = 0.02 |
| | | | Non-respiratory (n = 127) | 122/127 (96.1%) | 5/127 (3.9%) | |
| Respiratory with co-morbidities (n = 139) | | | 124/139 (89.2%) | 15/139 (10.8%) | | |

Compliance patterns for aerosol therapy in ICU patients are represented for administration. The table presents the number of patients categorized as compliant or non-compliant for administration. Comparisons are made across ventilation type, ICU categorization, ICU stay duration, aerosol mode, age and diagnosis. Statistically significant results are highlighted with corresponding P values
 ICU: intensive care unit

raising concerns about therapeutic insufficiency and clinical deterioration.^{7,14} These patterns emphasized the need for standardized scheduling and electronic administration records to minimize human errors and optimize clinical decisions.

Regarding device selection, the study confirmed that jet nebulizers predominated, reflecting their affordability and widespread availability. VMNs, though used less frequently, demonstrate superior drug delivery efficiency and reduced medication loss, consistent with published evidence from Western settings.^{6,16}

An important clinical observation was that non-respiratory patients demonstrated higher compliance with administration. This may be due to simpler therapeutic protocols, fewer aerosol sessions, and reduced disease complexity, which allow guideline-recommended administration to be implemented more consistently than in patients with respiratory illnesses.

Maintenance and hygiene practices showed positive trends, with high adherence to cleaning protocols and disinfection standards outlined by national guidelines. This contrasted with earlier reports documenting poor compliance with device hygiene and elevated risks of nosocomial infections.¹⁷ Effective sterilization and maintenance practices contribute to improved clinical outcomes and patient safety.

The cost assessment of aerosol therapy revealed that multiple factors contributed to the overall expense in the ICU. Non-

compliance with treatment protocols, particularly with respect to device selection, dosing, and the use of incompatible combinations, was associated with higher therapy costs.^{11,18} Inappropriate device choices, especially frequent reliance on jet nebulizers, led to inefficient drug utilization and higher cumulative costs despite their initially lower unit price.^{6,16} Adoption of VMNs in Indian ICUs, while limited due to cost, could offer savings in the long-term and improved therapeutic outcomes.

Frequent bronchodilator use, although clinically justified, contributed to increased pharmaceutical costs and indicated potential overuse or inappropriate dosing.⁹ Studies suggest that implementing a national-level standardized aerosol protocol could reduce ICU expenditure by as much as 25–40%.^{9,12}

This study adds a meaningful real-world perspective by demonstrating that following guideline-based aerosol therapy in critically ill patients can help maintain therapeutic effectiveness while reducing unnecessary costs. Optimized drug regimen (frequency and duration of therapy) and appropriate device selection, both of which can enhance drug delivery efficiency and minimize wastage, are likely to contribute to these benefits. However, the findings acknowledge that strict adherence may not always be feasible in resource-limited ICUs, where variations in practice may justify deviations from guidelines. This highlights the importance of balancing protocol adherence with individualized treatment.

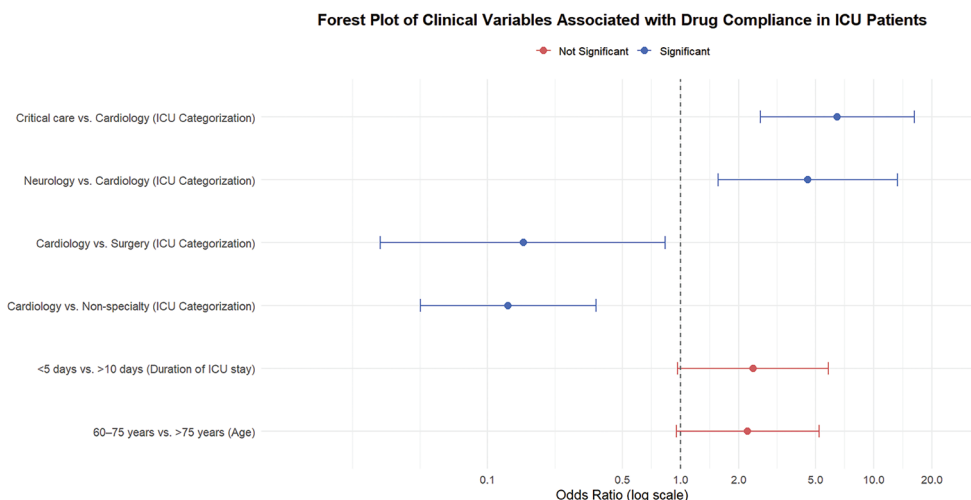


Figure 3a. Forest plot of clinical predictors of drug therapy compliance to aerosol therapy in ICU patients. It depicts the forest plot of odds ratios for drug therapy across various clinical comparisons. Statistically significant comparisons are shown in blue, with 95% confidence intervals represented by horizontal lines

ICU: intensive care unit

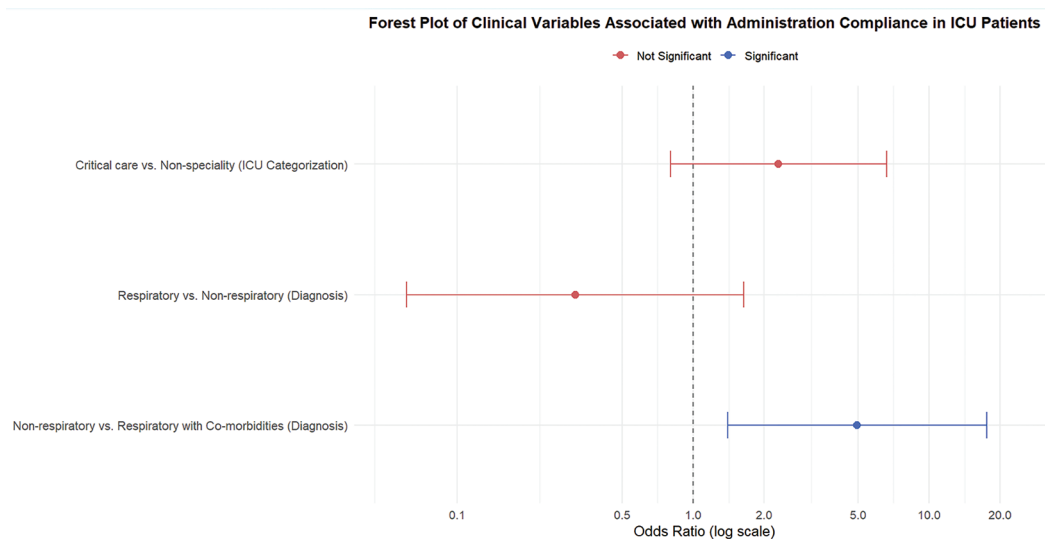


Figure 3b. Forest plot of clinical predictors of administration compliance to aerosol therapy in ICU patients. It depicts the forest plot of odds ratios for administration across various clinical comparisons. Statistically significant comparisons are shown in blue, with 95% confidence intervals represented by horizontal lines

ICU: intensive care unit

Future research should include multicentre studies conducted across diverse settings and regions to ensure external validity. Also, incorporating physician perspectives through qualitative or mixed-methods research could provide valuable insights into decision-making practices and challenges in guideline adherence.

Clinical Significance

Ensuring compliance with evidence-based guidelines for aerosol therapy in the ICU setting promotes uniformity in prescribing, administration, and overall patient care. This not only enhances therapeutic effectiveness and patient safety, but also minimizes unnecessary expenditure. Regular monitoring, periodic staff training, and cost-awareness strategies should

be integrated into the hospital’s ICU protocols to increase compliance and cost efficiency.

Study Limitations

The study has several limitations which must be acknowledged. Although data collection was prospective, the study was conducted in a single tertiary care teaching hospital, which limits the generalizability of its results to other healthcare settings with different infrastructure and resource availability. The relatively short duration of the study, i.e., 6 months, limited the ability to assess long-term trends in compliance and cost-effectiveness; a longer follow-up period could provide more insight into sustained adherence to guidelines. Validated severity scores (e.g., APACHE II/SOFA)

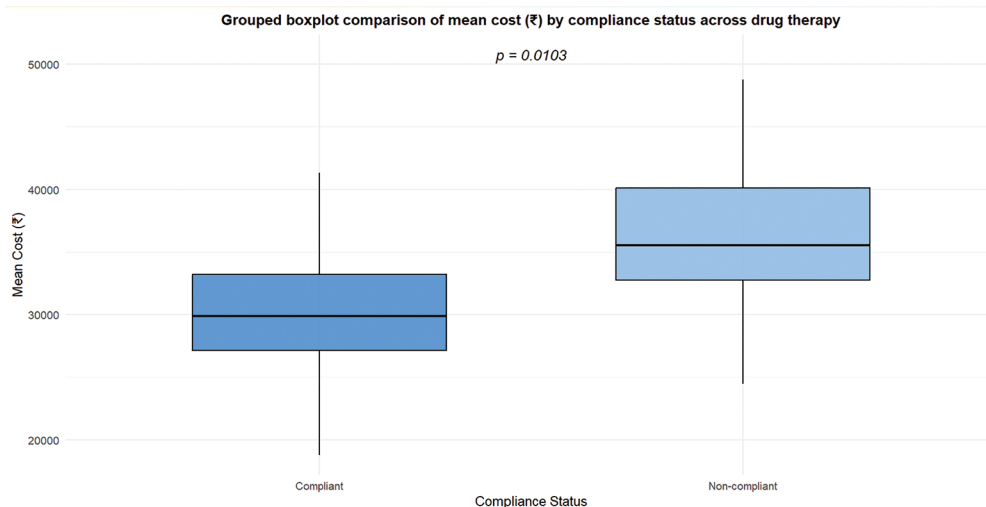


Figure 4. Grouped boxplot comparison of mean cost (₹) by compliance status across drug therapy. It shows a boxplot comparison of mean aerosol therapy costs between compliant and non-compliant cases across the drug therapy. Costs (₹) are represented for compliant and non-compliant groups

were not available for all patients, and adjustment for illness severity could not be undertaken because these scores are not routinely recorded in the hospital's workflow. This limits the study's ability to adjust for baseline severity, and the absence of a standardized severity assessment may have influenced the observed associations among compliance, duration of ICU stay, and overall cost. The study of costs incurred only included direct medical costs and excluded broader system or societal costs; integrating a formal health-economic evaluation would strengthen the study's conclusion. The study did not take into account the variability of clinical decision-making because physician preferences, experience level, awareness, workload, and institutional constraints were not assessed. These factors can act as barriers and affect the compliance pattern to it. Lastly, the study was not registered in CTRI, which is considered a methodological limitation with respect to clinical research transparency.

CONCLUSION

This single-centre study identified significant non-adherence to the "Indian Guidelines on Nebulization Therapy" among critically ill patients, particularly in the choice of drug regimen and its duration; this non-adherence was associated with increased healthcare expenditure and poorer therapeutic outcomes. Compliance with drug therapy was associated with lower direct costs of aerosol therapy. Non-compliance resulted in increased medication wastage, prolonged therapy, and extended ICU stays, which, in total, increased expenditures. The findings of this study underscore the imperative need for standardized protocols, comprehensive training, enforced compliance audits, and an enhanced focus on adherence. Reinforcing hospital policies and fostering interdisciplinary synergy among healthcare providers, including pharmacists and respiratory therapists can enhance the quality and cost-effectiveness of aerosol therapy in ICUs, ensuring judicious resource allocation and superior patient outcomes.

Ethics

Ethics Committee Approval: The Bharati Vidyapeeth (Deemed to be University) Medical College Ethics Committee (approval ID: BVDUMC/IEC/91/24-25, date 28/09/2024).

Informed Consent: A waiver of written informed consent for this observational study was approved by the Ethics Committee, as data collection used routine clinical records and did not require changes to patient care.

Footnotes

Authorship Contributions

Surgical and Medical Practices: A.L.R., J.S., S.K., A.R.V., S.A., R.P., K.K.P., Concept: A.L.R., J.S., S.K., Design: A.L.R., J.S., Data Collection or Processing: A.L.R., A.R.V., S.A., R.P., K.K.P., Analysis or Interpretation: A.L.R., A.R.V., S.A., R.P., Literature Search: A.L.R., A.R.V., S.A., R.P., K.K.P., Writing: A.L.R., J.S., S.K., A.R.V., S.A., R.P., K.K.P.,

Conflict of Interest: No conflict of interest was declared by the authors.

Financial Disclosure: The authors declared that this study received no financial support.

Supplementary Table Link: <https://d2v96fxpocvxx.cloudfront.net/beb8919b-f013-4ea1-b1c8-40332e840fe1/content-images/d2fb09dd-e543-438d-b162-bad2450eaf75.pdf>






REFERENCES

1. Singhal S, Gurjar M, Sahoo JN, et al. Aerosol drug therapy in critically ill patients (Aero-in-ICU study): a multicentre prospective observational cohort study. *Lung India*. 2024;41(3):200-208. [Crossref]
2. Dhanani J, Fraser JF, Chan HK, Rello J, Cohen J, Roberts JA. Fundamentals of aerosol therapy in critical care. *Crit Care*. 2016;20(1):269. [Crossref]

3. Ehrmann S, Roche-Campo F, Bodet-Contentin L, et al. Aerosol therapy in intensive and intermediate care units: prospective observation of 2808 critically ill patients. *Intensive Care Med.* 2016;42(2):192-201. [\[Crossref\]](#)
4. Dhanani J, Taniguchi LU, Ranzani OT. Optimising aerosolized therapies in critically ill patients. *Intensive Care Med.* 2022;48(10):1418-1421. [\[Crossref\]](#)
5. Li J, Liu K, Lyu S, et al. Aerosol therapy in adult critically ill patients: a consensus statement regarding aerosol administration strategies during various modes of respiratory support. *Ann Intensive Care.* 2023;13(1):63. [\[Crossref\]](#)
6. Arnott A, Watson M, Sim M. Nebuliser therapy in critical care: the past, present and future. *J Intensive Care Soc.* 2024;25(1):78-88. [\[Crossref\]](#)
7. Singla SK. A survey on method of aerosol therapy in patients on invasive mechanical ventilation in intensive care unit and its impact on drug delivery. *Int J Nurs Didact.* 2020;10(2):68. [\[Crossref\]](#)
8. Naughton PJ, Joyce M, Mac Giolla Eain M, O'Sullivan A, MacLoughlin R. Evaluation of aerosol drug delivery options during adult mechanical ventilation in the COVID-19 era. *Pharmaceutics.* 2021;13(10):1574. [\[Crossref\]](#)
9. Lyu S, Li J, Yang L, et al. The utilization of aerosol therapy in mechanical ventilation patients: a prospective multicenter observational cohort study and a review of the current evidence. *Ann Transl Med.* 2020;8(17):1071. [\[Crossref\]](#)
10. Santambrogio M, Lazzeri M, Bonitta G, et al. Hospital staff practical skills and theoretical knowledge in inhaled aerosol therapy: a single centre cross-sectional observational study. *Monaldi Arch Chest Dis.* 2021;91(1). [\[Crossref\]](#)
11. Jayaram R, Ramakrishnan N. Cost of intensive care in India. *Indian J Crit Care Med.* 2008;12(2):55-61. [\[Crossref\]](#)
12. Shweta K, Kumar S, Gupta AK, Jindal SK, Kumar A. Economic analysis of costs associated with a respiratory intensive care unit in a tertiary care teaching hospital in Northern India. *Indian J Crit Care Med.* 2013;17(2):76-81. [\[Crossref\]](#)
13. Reddy PNK, Reddy PS. Aerosol therapy compliance in patients with bronchial asthma – a real-world study. *Indian J Appl Res.* 2020. [\[Crossref\]](#)
14. Sun Q, Chang W, Liu X, et al. Aerosol therapy during mechanical ventilation in intensive care units: a questionnaire-based survey of 2203 ICU medical staff in China. *J Intensive Med.* 2022;2(3):189-194. [\[Crossref\]](#)
15. Katiyar SK, Gaur SN, Solanki RN, et al. Indian Guidelines on Nebulization Therapy. *Indian J Tuberc.* 2022;69 Suppl 1:S1-S191. [\[Crossref\]](#)
16. Myers TR. The science guiding selection of an aerosol delivery device. *Respir Care.* 2013;58(11):1963-1973. [\[Crossref\]](#)
17. Solé-Lleonart C, Roberts JA, Chastre J, et al. Global survey on nebulization of antimicrobial agents in mechanically ventilated patients: a call for international guidelines. *Clin Microbiol Infect.* 2016;22(4):359-364. [\[Crossref\]](#)
18. Dasta JF, McLaughlin TP, Mody SH, Piech CT. Daily cost of an intensive care unit day: the contribution of mechanical ventilation. *Crit Care Med.* 2005;33(6):1266-1271. [\[Crossref\]](#)

Original Article

Cost Analysis of Tuberculosis Disease in the Case of Tuberculosis Control Dispensary

 Dolunay Özlem Zeybek¹,  Mustafa Zeybek²,  İskender Çetintürk³,  Yasemin Aslan¹,
 Filiz Özyiğit⁴

¹Department of Health Management, Bandırma Onyedi Eylül University Faculty of Health Sciences, Balıkesir, Türkiye

²Department of Medical Documentation and Secretariat, Bilecik Şeyh Edebali University, Vocational School of Health Services, Bilecik, Türkiye

³Independent Researcher, Isparta, Türkiye

⁴Department of Medical Pharmacology, Bandırma Onyedi Eylül University Faculty of Health Sciences, Balıkesir, Türkiye

Cite this article as: Zeybek DÖ, Zeybek M, Çetintürk İ, Aslan Y, Özyiğit F. Cost analysis of tuberculosis disease in the case of tuberculosis control dispensary. *Thorac Res Pract.* 2026;27(3):165-172

ABSTRACT

OBJECTIVE: To estimate the direct and indirect costs associated with tuberculosis (TB) prevention, control, and treatment activities conducted at a TB control dispensary in Türkiye and to assess the economic burden of TB at the patient level.

MATERIAL AND METHODS: Patient-level cost data for individuals treated in 2023 with International Classification of Diseases, 10th Revision diagnostic codes A15–A19 were analyzed from the perspective of the healthcare provider. Direct medical costs were calculated based on healthcare service utilization using reimbursement prices specified in the Turkish Social Security Institution's Health Implementation Communiqué. Indirect costs were estimated using patient-reported data and included productivity loss, time spent accessing healthcare services, transportation expenses, and other out-of-pocket expenditures. All costs were calculated as the average annual cost per patient.

RESULTS: The average annual direct cost per patient was \$346.39 (9,271.59₺), with prescribed medications constituting the largest component of direct costs. The average annual indirect cost per patient amounted to \$1,087.80 (32,013.50₺), mainly driven by productivity losses and time spent in healthcare facilities. Overall, the average annual cost per TB patient was estimated at \$1,434.22 (41,285.09₺), with indirect costs accounting for nearly three-quarters of the total economic burden.

CONCLUSION: The findings demonstrate that TB imposes a substantial economic burden on patients, primarily through indirect costs, even when TB-related healthcare services are covered by the social security system. These results underscore the need for TB control strategies that extend beyond medical care and incorporate social protection and economic support mechanisms to reduce productivity losses and financial vulnerability among patients.

KEYWORDS: Tuberculosis, health care cost, cost of illness, tuberculosis control, health expenditures

Received: 17.10.2025

Revision Requested: 01.12.2025

Last Revision Received: 31.12.2025

Accepted: 16.01.2026

Epub: 24.03.2026

Publication Date: 12.05.2026

INTRODUCTION

Tuberculosis (TB) is a respiratory disease caused by the bacillus *Mycobacterium tuberculosis*, typically affecting the lungs.¹ It has been stated that approximately 85% of patients can be treated with the treatment regimens recommended by the World Health Organization (WHO), but in cases where access to treatment is not possible, the mortality rate can be up to 70%.¹⁻³ For this reason, on a global scale, one of the United Nations Sustainable Development Goals (2016-2030) is to reduce deaths from TB by 90 per cent by 2030.⁴

WHO has stated that TB was the second leading cause of death from a single infectious agent worldwide in 2022, despite being a preventable and treatable disease. More than 10 million people are newly diagnosed with TB every year, and approximately 1.3 million individuals worldwide died due to TB in 2022.¹ The global incidence of TB in 2022 was

Corresponding author: Mustafa Zeybek, MD, e-mail: mustafa.zeybek@bilecik.edu.tr



133 per 100,000, and the estimated mortality rate was 19.7 per 100,000. According to the data for 2021, the incidence rate of TB in Türkiye is 15 per 100,000 and the estimated mortality rate is 0.55 per 100,000.^{1,3} TB dispensaries play an important role in the outpatient follow-up and treatment of patients diagnosed with TB in Türkiye.

TB control activities in Türkiye date back to 1918, with the establishment of the Tuberculosis Control Society by Besim Ömer Akalın and the opening of the first TB dispensary in İstanbul in the early 1920s.⁵ Today, tuberculosis control dispensaries (TCD) operate under the Ministry of Health at the provincial level, providing comprehensive services including diagnosis, contact tracing, directly observed treatment, and preventive care. As of the end of 2021, a total of 173 TCDs were actively providing services across the country.^{3,6} In accordance with national regulations, anti-TB medications are financed by the Social Security Institution for patients with social security coverage and by the government for patients without social security coverage.

While the number of patients entering the records of TCDs in Türkiye in 2019 was 11,401, this number decreased to 8,925 in 2020. The TB case rate in 2020 was 10.7 per 100,000 for Türkiye overall and 13.9 per 100,000 for Balıkesir province. When the distribution of cases by gender was analyzed, it was found that males were more common in Türkiye and Balıkesir province (57.2% and 64.5%, respectively). When the distribution of cases by site of involvement was analyzed, the lungs were the most common site; the lung involvement rate was 58.4% for Türkiye overall and 66.9% for Balıkesir province. In addition, most cases occurred in individuals aged 65 years and over. The treatment success rate among patients treated at TCDs was 82.6% for new cases, 71.9% for previously treated cases, and 81.9% for total cases. One of the factors contributing to this success is the strategy of directly supervised treatment. The National Tuberculosis System was launched in 2018 to effectively collect data on TB in Türkiye.³ TB imposes direct and indirect costs on individuals, society, and the health system.

Studies show that the economic burden of TB on the national economy is high.^{1,7-9} In addition, TB treatment can be lengthy,

ranging from 4–6 months to 1 year, and in Türkiye typically lasts between 6 months and 1 year.⁶ As patients may be unable to work during treatment, they may require cash support. In order to benefit from these cash social aids in Türkiye, patients must be a Turkish citizen, be physically followed up at a TCD and receive TB treatment, be registered in the national TB system, adhere to TB treatment, undertake to comply with the treatment and take their medication every day under the supervision of health personnel, and be approved by the responsible physician of the TCD to receive this aid.¹⁰

In addition to the high cost of TB treatment, indirect costs impose a substantial economic burden on families and can lead to catastrophic expenditures. In particular, loss of income and the costs of food and nutritional supplements beyond patients' regular diets are the main causes of catastrophic costs. These catastrophic expenditures have been found to impose a large economic burden on patients.^{11,12} A systematic review and meta-analysis of the financial burden of TB diagnosis and treatment among patients with TB in Ethiopia found that 51% of patients faced catastrophic costs. Drug-resistant TB, TB-human immunodeficiency virus (HIV) co-infection and hospitalisation have been found to be associated with catastrophic costs.⁷ Based on studies in the literature, it is important to determine the direct and indirect costs of treating TB patients at TB dispensaries. It was stated that the treatment and management costs of TB disease are among the basic inputs for economic evaluations to assess the cost-effectiveness of public health interventions and are important for determining health policies and making public health planning.¹³ This study aimed to calculate the direct and indirect disease-related costs of patients who received outpatient treatment at the TCD in Bandırma district of Balıkesir province from 1 January to 31 December 2023. The aim was to calculate the costs of TB for primary health care services and patients, and to propose future TB prevention, control, and treatment policies.

MATERIAL AND METHODS

This cost-of-illness study was conducted at a TCD in Türkiye. In this study, annual follow-up data for TB patients with International Classification of Diseases, 10th Revision diagnosis codes A15–A19 in 2023 were used. All patients who received treatment at the TCD in 2023 were initially considered for inclusion. However, 12 patients were excluded based on predefined exclusion criteria, including (i) irregular adherence to treatment or follow-up schedules, (ii) discontinuation of treatment for any reason, (iii) incomplete service records that did not allow reliable estimation of direct and/or indirect costs, and (iv) failure to complete the follow-up period within the study timeframe. Accordingly, service data from 70 patients aged 18 years or older were analyzed. The study was conducted from a service provider perspective. Ethical approval for the study was obtained from the Bandırma Onyedü Eylül University Non-Interventional Research Ethics Committee on June 21, 2023, with the decision number 2023-98.

Retrospectively obtained data were used in this study. As this was a retrospective analysis based on routinely collected data, informed consent was not required. Cost data were derived from two primary sources and classified as direct and

Main Points

- The annual total cost per tuberculosis patient was calculated as \$1,434.22, with 76% of this amount attributed to indirect costs.
- 38.6% of patients were identified as low-income, which significantly increases the disease's economic impact.
- Among direct cost components, prescribed medications represented the highest expense, at \$240.47; Streptomycin, pyrazinamide, and rifampicin were the most costly medications.
- Acid-fast bacilli microscopy and culture tests were performed 24 times per year, constituting the largest laboratory expense.
- 61.4% of the patients had additional chronic illnesses, indicating a high risk of developing complications during the treatment process.

indirect costs. Clinical characteristics of the patients were also reviewed; no cases of drug-resistant TB or HIV positivity were identified during the study period. All patients included in the study ($n = 70$, 100%) received directly observed therapy (DOT) in accordance with the national TB control program. Direct medical costs were obtained from patient service records maintained by the TCD and included physician examinations, laboratory tests, imaging procedures, and prescribed medications. These procedures were costed in accordance with the reimbursement prices specified in the Republic of Türkiye Healthcare Implementation Communiqué.¹⁴ Indirect costs, derived from patient-reported data collected through a structured questionnaire administered voluntarily after completion of treatment, included productivity loss, transportation expenses, and other out-of-pocket expenditures related to TB care.

Average direct medical costs per patient were determined according to the level of utilisation of physician examinations, laboratory tests, imaging procedures, and prescribed medicines. Indirect costs were defined as productivity loss due to illness, productivity loss associated with time spent in healthcare facilities, transportation costs, and other out-of-pocket expenditures incurred during the treatment process, in line with standard cost-of-illness methodology.^{15,16}

In determining the average costs of medicines prescribed during patient follow-up, the number of tablets or capsules and the retail prices per mg/mcg of the active ingredients were used as the basis. Cost calculations were performed using the formula $\text{Cost} = \sum (\text{number of procedures}) \times (\text{unit price}) \times (\text{patient rate } \%)$, and pharmaceutical costs were valued based on retail prices in accordance with national reimbursement tariffs.

Indirect cost data were obtained using a structured questionnaire voluntarily administered to patients after completion of treatment. The questionnaire collected information on transportation expenses incurred due to healthcare visits, productivity loss associated with time spent within the healthcare system, and other out-of-pocket expenditures related to TB care.

Transportation costs were calculated based on the total number of healthcare visits for diagnostic, treatment, and follow-up purposes and the average round-trip transportation cost reported per visit and expressed as average annual transportation costs per patient. Productivity loss related to time spent in the healthcare system was estimated by determining the total number of days that patients spent attending medical examinations, diagnostic tests, treatment sessions, and follow-up visits, and multiplying this duration by a daily reference income. The national minimum wage for 2023 was used as the reference income, corresponding to 11,402₺ per month (\$425.8) and 447.15₺ per day (\$16.7), as determined by the Minimum Wage Determination Commission of the Ministry of Labour and Social Security of the Republic of Türkiye.¹⁷ The use of the national minimum wage as a reference income represents a conservative and standardized approach commonly applied in cost-of-illness studies where income levels are heterogeneously defined.^{15,18}

All indirect costs were calculated and reported as average annual costs per patient. Costs were converted to US dollars using the

exchange rate of the Central Bank of the Republic of Türkiye effective on 1 September 2023 ($\$1 = 26.766₺$), consistent with the effective date of the Healthcare Implementation Communiqué tariff applied.¹⁹

RESULTS

Sociodemographic Profile

Of the TB patients included in the study, 68.6% were male and 31.4% were female. Regarding income status, 38.6% of patients reported monthly incomes of 5,001–10,000₺, 31.4% reported 10,001–30,000₺, and 30.0% reported 0–5,000₺, indicating that most patients belonged to low- and middle-income groups. More than half of the patients (61.4%) reported having at least one comorbid chronic condition in addition to TB, and a substantial proportion (72.9%) did not have social security coverage.

With respect to disease status, 80.0% of patients were newly diagnosed cases of TB, while 20.0% were relapse cases. Most patients (85.7%) received treatment and follow-up services within the same city, whereas 14.3% accessed care from another city. Pulmonary TB was observed in 65.7% of patients, while 34.3% had extrapulmonary involvement. Body mass index (BMI) assessment showed that 52.9% of patients had a BMI in the 21–29 kg/m² range, 25.7% were classified as obese (30–42 kg/m²), and 21.4% had a BMI in the 8–20 kg/m² range. These sociodemographic and clinical characteristics are summarized in Table 1.

Cost Findings

Examinations, tests, radiological imaging, and prescribed medications for patients with TB constitute the direct costs of the disease. Indirect costs include loss of labor due to disease or medical leave, time spent in healthcare institutions, and transportation costs.

Direct Costs

During TB treatment, patients attend examinations 14 times per year (on average every 25 days). Within the framework of the Ministry of Health HIC in Türkiye, the average annual physician examination cost for TB dispensaries—primary health care institutions under the Ministry of Health Healthcare Implementation Communiqué—was determined to be \$33.96 (908.88₺), including normal and control examinations.

Various biochemical laboratory are performed during patients' annual follow-up. Among these tests: C-reactive protein test was performed 6 times with a total annual cost of \$1.47 (39.30₺); complete blood count (haemogram) test was performed 6 times with a total cost of \$1.51 (40.37₺); lactate dehydrogenase test was also performed 6 times; the adenosine deaminase activity test was performed once a year with a total cost of \$0.50 (13.45₺); the procalcitonin test was performed 2 times with a total cost of \$1.14 (30.51₺); and the procalcitonin test was performed 2 times with a total cost of \$2.14 (57.24₺). Accordingly, the total annual cost for biochemistry laboratory tests was \$6.76 (180.87₺) (Table 2).

As part of microbiological examinations and culture tests, mycobacterial culture was performed nine times per year, at

Table 1. Sociodemographic and clinical characteristics of the patients

| Characteristics | Variable | Number [percentage (%)] |
|---|-------------------------|-------------------------|
| Gender | Woman | 22 (31.4) |
| | Man | 48 (68.6) |
| Income status | 0–5000₺ | 21 (30.0) |
| | 5001–10000₺ | 27 (38.6) |
| | 10001–30000₺ | 22 (31.4) |
| Do you have any other chronic illnesses? | Yes | 43 (61.4) |
| | No | 27 (38.6) |
| Do you have social security? | Yes | 19 (27.1) |
| | No | 51 (72.9) |
| Case status | New | 56 (80.0) |
| | Relapse | 14 (20.0) |
| Do you provide transport for treatment/follow-up from another city? | Yes | 10 (14.3) |
| | No | 60 (85.7) |
| Site of disease | Pulmonary | 46 (65.7) |
| | Non-pulmonary | 24 (34.3) |
| Body mass index (kg/m ²) | 8–20 kg/m ² | 15 (21.4) |
| | 21–29 kg/m ² | 37 (52.9) |
| | 30–42 kg/m ² | 18 (25.7) |

The information in Table 1 includes information on the sociodemographic and clinical characteristics of the patients included in the study

a total cost of \$25.16 (673.32₺). Direct microscopy for acid-fast bacilli was also performed nine times, incurring a total cost of \$8.80 (235.42₺). In addition, sputum culture testing was performed six times, with a total cost of \$4.69 (125.40₺). The total annual cost of microbiological examinations and culture tests was calculated to be \$38.65 (1034.14₺) (Table 2).

Within the scope of functional assessment tests, pulmonary function tests were performed once a year at a cost of \$2.88 (77.21₺), and bronchoalveolar lavage test was performed twice a year at a total cost of \$17.89 (478.80₺). The total annual cost of functional assessment was \$20.77 (556.01₺) (Table 2).

Within the scope of radiological imaging procedures, chest X-rays were performed 4 times a year at a total cost of \$3.42 (91.54₺). High-resolution chest computed tomography (CT) and non-contrast thorax CT tests were also performed, with total costs of \$0.08 (2.06₺) and \$2.31 (61.73₺), respectively. The total annual cost of radiological imaging procedures was \$5.81 (155.33₺) (Table 2).

Among the prescribed drugs, streptomycin (\$86.63), pyrazinamide (\$65.21), and rifampicin (\$54.02) had the highest costs. Isoniazid (\$31.17) and ethambutol (\$3.44) were also among the important cost items. The total annual cost of prescribed drugs was \$240.47 (6436.37₺). In this context, total direct patient costs were determined to be \$346.39 (9271.59₺). Most of these costs are due to prescription drugs, microbiological tests, and laboratory tests. It is noteworthy that drug costs constitute the largest component of direct treatment expenditures.

Indirect Costs

This section presents patient-level findings on average annual indirect costs related to TB. Indirect costs consisted of productivity loss due to illness, loss of labour resulting from medical leave and from time spent in healthcare facilities, transportation expenses, and other out-of-pocket expenditures. These costs were estimated based on patient-reported data collected through a structured questionnaire administered after completion of treatment. Patients were reported to be on medical leave for an average of 40 days and to have spent 25 days in healthcare institutions during the annual treatment period. Accordingly, the average annual productivity loss due to illness was calculated at \$607.75 (17,886₺) per patient, while the labour loss associated with medical leave and time spent in healthcare facilities was estimated at \$379.85 (11,178.75₺) per patient. Regarding transportation costs, 85% of patients reported attending healthcare facilities alone, whereas the remaining patients were accompanied. Transportation costs were calculated based on the number of healthcare visits and the average round-trip cost reported by patients, resulting in an average annual transportation cost of \$100.20 (2,948.75₺) per patient. Overall, the average annual indirect cost per patient was \$1,087.80 (32,013.50₺). Indirect patient follow-up costs for TB in TCDs are presented in Table 3.

Cost of Illness (Direct and Indirect Costs)

In this section of the study, the direct and indirect costs associated with the treatment of patients with TB were analyzed. The total annual cost of routine physician examinations was USD 33.96 (TRY 908.88), while the total annual cost of biochemistry laboratory tests, microbiological examinations,

Table 2. Direct costs

| HIC code | Transactions | Unit price (£) | Utilisation percentage (%) | Number of uses (n) | Total amount (£) | Total amount (\$) |
|---|---|----------------|----------------------------|--------------------|------------------|-------------------|
| Examination | | | | | | |
| 520030 | Normal physician examination | 64.92 | 1 | 14 | 908.88 | 33.96 |
| Biochemistry laboratory tests | | | | | | |
| L101850 | C-reactive protein | 9.36 | 0.7 | 6 | 39.30 | 1.47 |
| L107020 | Complete blood count (haemogram) | 11.21 | 0.6 | 6 | 40.37 | 1.51 |
| L104920 | Lactate dehydrogenase | 3.74 | 0.6 | 6 | 13.45 | 0.50 |
| L100230 | Adenosine deaminase activity | 38.14 | 0.8 | 1 | 30.51 | 1.14 |
| L106240 | Procalcitonin (serum/plasma) | 95.41 | 0.3 | 2 | 57.24 | 2.14 |
| Microbiological investigations and culture tests | | | | | | |
| 906160 | Mycobacteria culture | 74.81 | 1 | 9 | 673.32 | 25.16 |
| 906141 | Mycobacteria search (ARB) direct microscopy | 26.16 | 1 | 9 | 235.42 | 8.80 |
| 905671 | Urine culture | 20,90 | 1 | 9 | 188.10 | 7.03 |
| 905675 | Sputum culture | 20.90 | 1 | 6 | 125.40 | 4.69 |
| Functional assessment | | | | | | |
| 701220 | Pulmonary function tests | 77.21 | 1 | 1 | 77.21 | 2.88 |
| 701080 | Bronchoalveolar lavage | 239.40 | 1 | 2 | 478.80 | 17.89 |
| Radiological imaging | | | | | | |
| 801720 | Lung X-ray | 25.43 | 0.9 | 4 | 91.54 | 3.42 |
| R100030 | CT, lung, high resolution | 205.77 | 0.01 | 1 | 2.06 | 0.08 |
| R100450 | CT, thorax, without contrast | 205.77 | 0.3 | 1 | 61.73 | 2.31 |
| Active ingredient of prescribed drugs | | | | | | |
| | Isoniazid | | | | 834.25 | 31.17 |
| | Rifampisin | | | | 1445.86 | 54.02 |
| | Etambutol | | | | 92.19 | 3.44 |
| | Pirazinamid | | | | 1745.30 | 65.21 |
| | Streptomisin | | | | 2318.77 | 86.63 |
| | Total | | | | 9271.59£ | \$346.39 |

The information in Table 2 includes the direct costs of tuberculosis
ARB: acid-fast bacilli, CT: computed tomography

Table 3. Annual indirect costs

| Cost items | Total cost (£) | Total cost (\$) |
|---|-----------------|-----------------|
| Lost productivity due to illness | 17886£ | \$607.75 |
| Lost productivity due to time spent in the health institution and health report | 11178.75£ | \$379.85 |
| Transport costs | 2948.75£ | \$100.2 |
| Total | 32013.5£ | \$1087.8 |

The information in Table 3 includes the indirect costs of tuberculosis

functional assessments, and radiological imaging was USD 71.99 (TRY 1,926.35). Prescribed medications-particularly streptomycin, pyrazinamide, and rifampicin-constituted the highest cost components incurred by patients, with a total cost of USD 240.47 (TRY 6,436.37). Accordingly, total direct costs per patient amounted to USD 346.39 (TRY 9,271.59). The total indirect costs were calculated as USD 1,087.80 (TRY 32,013.50).

Consequently, the overall direct and indirect costs incurred by TB patients throughout the treatment period were estimated at USD 1,434.22 (TRY 41,285.09). These findings indicate that patients experience a substantial economic burden during the treatment process, driven not only by healthcare-related expenditures but also by indirect costs.

The catastrophic cost burden among TB patients was evaluated in accordance with the WHO definition, whereby catastrophic costs are defined as TB-related expenditures exceeding 20% of annual household income. Based on this criterion and using the midpoint of reported household income categories to estimate annual income, 68.6% of patients (48 out of 70) were identified as experiencing catastrophic total costs during the treatment period. Catastrophic costs were predominantly observed among patients in lower-income groups, indicating that despite the coverage of TB-related health services, the combined effect of direct and indirect costs imposes a substantial financial burden on households.

DISCUSSION

Primary healthcare services play a critical role in the prevention and control of TB.²⁰ The prolonged treatment duration, complexity of diagnostic procedures, and the use of multiple medications contribute to a significant economic burden associated with TB.^{7,9} The study by Capeding et al.²¹ revealed that, except for resistant cases and pediatric patients, the costs of TB follow-up care in hospitals are generally higher compared to primary healthcare facilities.

In this study, the annual direct cost for TB patients followed up as outpatients at a district TCD was, on average, \$346.39 (9,271.59₺). Medication costs accounted for the largest proportion of direct expenses, with an average cost of \$240.47 (6,436.37₺). A study conducted in the United States reported that the total per-person cost for drug-susceptible TB treatment over 4- or 6-month regimens was \$23,000 and \$34,600, respectively.^{9,13} The same study indicated that outpatient visits cost approximately \$400 per person, while resistant cases could incur costs up to \$1,200. The average cost of laboratory and imaging tests was estimated at \$1,500, rising to \$4,200 in resistant cases. The cost of anti-TB medications was estimated to be \$800 on average, but this increased to \$30,400 for resistant cases. A study in South Africa found that the average cost of treating drug-susceptible TB in primary healthcare facilities was \$141.29, with 44% of costs attributed to fixed expenditures, 30.7% to outpatient visits, 19.3% to medication, and 6% to laboratory tests.²² In another study conducted in Malawi, the indirect costs of TB follow-up over 56 days were estimated at \$8.47 per patient, with 5% of these expenses leading to catastrophic costs.²³

In this study, the annual indirect costs incurred by patients followed up at the TCD were calculated as \$1,087.8 (32,013.5₺) per person. The largest component of these indirect costs was productivity loss due to illness, amounting to \$607.75 (17,886₺). The findings show that indirect costs are higher than direct costs. Similar results have been reported in the literature.²⁴⁻²⁹ Studies conducted in low- and middle-income countries suggest that indirect costs for TB are generally high, reaching an average of \$530 per patient.²⁵ A study in Ethiopia found that 70.6% of the total costs incurred by TB patients were indirect costs.³⁰ In rural India, the average indirect costs for TB patients treated in primary healthcare settings were \$526.87.²⁷

In this study, the total direct and indirect costs for TB treatment amounted to \$1,434.22 (41,285.09₺) per patient. John et al.²⁷

reported that the average total cost for TB treatment in primary healthcare settings was \$562.66 per patient. Notably, these findings emerge in a setting with a long-established, well-functioning DOT short-course infrastructure, where diagnosis and treatment are widely accessible. Despite this strong healthcare delivery system, TB patients continue to experience a considerable economic burden, driven predominantly by indirect costs.

This contrast highlights that the financial impact of TB extends beyond medical expenditures and underscores the importance of early diagnosis and timely initiation of treatment to reduce productivity losses and hospitalization-related costs.^{31,32} Given the high hospitalization costs observed, strengthening TB control within primary healthcare services through early detection and outpatient-based management may contribute to cost containment.^{9,27,32-34}

Study Limitations

From a broader health policy perspective, these findings are closely aligned with the WHO's End TB Strategy, which emphasizes the elimination of catastrophic costs for TB-affected households.⁴ The persistence of high indirect costs in a context of universal access to TB services suggests that achieving this goal will require not only effective clinical care but also strengthened social protection and economic support mechanisms.

This study has several limitations. First, catastrophic costs were estimated using the midpoint values of reported household income categories rather than exact household income data. This approach may have introduced some degree of estimation bias. Second, individual productivity losses were estimated based on the minimum wage rather than patients' self-reported income. This assumption was considered a limitation, as it may have led to an overestimation or underestimation of the actual costs.

CONCLUSION

This study demonstrates that TB imposes a substantial economic burden on patients, with indirect costs constituting the dominant component of total costs. The average direct medical cost per patient was calculated to be \$346.39 (9,271.59₺) and included physician examinations, laboratory tests, radiological imaging, and prescribed medications. In contrast, indirect costs amounted to \$1,087.80 (32,013.50₺) per patient, representing approximately 76% of the total cost burden.

Despite coverage of TB-related healthcare services by the social security system, patients continue to incur significant out-of-pocket expenditures and loss of income during treatment. The average annual cost per patient was estimated at \$1,434.22 (41,285.09₺), indicating that the financial burden of TB extends well beyond direct medical expenditures. Consistent with this finding, a substantial proportion of patients in this study experienced catastrophic total costs, defined as TB-related expenditures exceeding 20% of annual household income, highlighting the pronounced financial vulnerability of affected households.

The predominance of indirect costs and the high prevalence of catastrophic cost burden underscore the socioeconomic impact of TB, particularly among lower-income groups. These findings suggest that TB control strategies should not be limited to the provision of medical care alone but should also incorporate social and economic support mechanisms aimed at reducing indirect costs. Policies that promote early timely treatment initiation, improve access to healthcare services, and strengthen social protection programs for TB patients may play a critical role in mitigating the overall economic burden of the disease. Addressing both the medical and socioeconomic dimensions of TB is essential for achieving sustainable disease control and enhancing the efficiency and equity of healthcare systems.

Ethics

Ethics Committee Approval: Ethical approval for the study was obtained from the Bandırma Onyedi Eylül University Non-Interventional Research Ethics Committee on June 21, 2023, with the decision number 2023-98.

Informed Consent: As this was a retrospective analysis based on routinely collected data, informed consent was not required.

Footnotes

Authorship Contributions

Concept: D.Ö.Z., F.Ö., Design: D.Ö.Z., M.Z., F.Ö., Data Collection or Processing: D.Ö.Z., M.Z., Y.A., Analysis or Interpretation: İ.Ç., Literature Search: D.Ö.Z., M.Z., İ.Ç., Writing: D.Ö.Z., M.Z., İ.Ç., Y.A.

Conflict of Interest: No conflict of interest was declared by the authors.

Financial Disclosure: The authors declared that this study received no financial support.











REFERENCES

- World Health Organization. Global Tuberculosis Report 2023. Accessed February 26, 2026. [\[Crossref\]](#)
- Tiemersma EW, van der Werf MJ, Borgdorff MW, Williams BG, Nagelkerke NJ. Natural history of tuberculosis: duration and fatality of untreated pulmonary tuberculosis in HIV negative patients: a systematic review. *PLoS One*. 2011;6(4):17601. [\[Crossref\]](#)
- T.C. Sağlık Bakanlığı, Halk Sağlığı Genel Müdürlüğü. Türkiye’de Verem Savaşı 2021 Raporu (Türkiye Tuberculosis Control Report 2021) [Internet]. Ankara: T.C. Sağlık Bakanlığı; 2023. Accessed February 26, 2026. [\[Crossref\]](#)
- World Health Organization (WHO). The end TB strategy: global strategy and targets for tuberculosis prevention, care and control after 2015. Geneva: WHO; 2014. [\[Crossref\]](#)
- Türkiye Ulusal Verem Savaş Dernekleri Federasyonu. Ülkemizde veremle savaş çalışmaları 1918 yılında Prof. Dr. Besim Ömer (Akalın) Paşa’nın “Veremle Mücadele Osmanlı Cemiyeti”ni kurmasıyla başlamıştır (The tuberculosis control activities in Turkey started in 1918 with the establishment of the “Ottoman Society for Combating Tuberculosis” by Prof. Dr. Besim Ömer (Akalın) Pasha) [Internet]. Accessed February 26, 2026. [\[Crossref\]](#)
- T.C. Sağlık Bakanlığı, Halk Sağlığı Genel Müdürlüğü. Tüberküloz Tanı ve Tedavi Rehberi (Tuberculosis Diagnosis and Treatment Guideline) [Internet]. Ankara: T.C. Sağlık Bakanlığı; 2019. Accessed February 26, 2026. [\[Crossref\]](#)
- Assefa DG, Dememew ZG, Zeleke ED, et al. Financial burden of tuberculosis diagnosis and treatment for patients in Ethiopia: a systematic review and meta-analysis. *BMC Public Health*. 2024;24(1):260. [\[Crossref\]](#)
- Burki TK. The global cost of tuberculosis. *Lancet Respir Med*. 2018;6(1):13. [\[Crossref\]](#)
- Winston CA, Marks SM, Carr W. Estimated costs of 4-month pulmonary tuberculosis treatment regimen, United States. *Emerg Infect Dis*. 2023;29(10):2102-2104. [\[Crossref\]](#)
- T.C. Sağlık Bakanlığı, Halk Sağlığı Genel Müdürlüğü. Ek Tüberküloz Hastalarına Yönelik Şartlı ve Düzenli Nakdi Sosyal Yardım Kılavuzu (Supplement: Conditional and Regular Cash Social Assistance Guide for Tuberculosis Patients) [Internet]. Ankara: T.C. Sağlık Bakanlığı; 2023. Accessed February 26, 2026. [\[Crossref\]](#)
- Ghazy RM, El Saeh HM, Abdulaziz S, et al. A systematic review and meta-analysis of the catastrophic costs incurred by tuberculosis patients. *Sci Rep*. 2022;12(1):558. [\[Crossref\]](#)
- Prasanna T, Jeyashree K, Chinnakali P, Bahurupi Y, Vasudevan K, Das M. Catastrophic costs of tuberculosis care: a mixed methods study from Puducherry, India. *Glob Health Action*. 2018;11(1):1477493. [\[Crossref\]](#)
- Oh P, Pascopella L, Barry PM, Flood JM. A systematic synthesis of direct costs to treat and manage tuberculosis disease applied to California, 2015. *BMC Res Notes*. 2017;10(1):434. [\[Crossref\]](#)
- Sosyal Güvenlik Kurumu (SGK). 19/10/2023 SUT Değişiklik Tebliği İşlenmiş Güncel 2013 SUT [Health Implementation Communiqué Amendment Notice]. Ankara: SGK; 2023. Accessed March 03, 2026. [\[Crossref\]](#)
- Drummond MF, Sculpher MJ, Claxton K, Stoddart GL, Torrance GW. (2015). *Methods for the Economic Evaluation of Health Care Programmes* (4th ed.). Oxford: Oxford University Press. [\[Crossref\]](#)
- Rice DP. Cost of illness studies: what is good about them? *Inj Prev*. 2000;6(3):177-179. [\[Crossref\]](#)
- T.C. Resmî Gazete (Official Gazette of the Republic of Türkiye). 30.12.2023 tarihli sayı. Accessed March 03, 2026. [\[Crossref\]](#)
- World Health Organization. Global Tuberculosis Report 2022. Geneva: World Health Organization; 2022. Accessed March 03, 2026. [\[Crossref\]](#)
- Türkiye Cumhuriyet Merkez Bankası (Central Bank of the Republic of Turkey, CBRT). Daily exchange rates dated 01 September 2023. Accessed March 03, 2026. [\[Crossref\]](#)
- Jesus GS, Pescarini JM, Silva AF, et al. The effect of primary health care on tuberculosis in a nationwide cohort of 7.3 million Brazilian people: a quasi-experimental study. *Lancet Glob Health*. 2022;10(3):390-397. [\[Crossref\]](#)
- Capeding TPJ, Rosa JD, Lam H, et al. Cost of TB prevention and treatment in the Philippines in 2017. *Int J Tuberc Lung Dis*. 2022;26(5):392-398. [\[Crossref\]](#)
- Budgell EP, Evans D, Leuner R, Long L, Rosen S. The costs and outcomes of paediatric tuberculosis treatment at primary healthcare clinics in Johannesburg, South Africa. *S Afr Med J*. 2018;108(5):423-431. [\[Crossref\]](#)
- Kamchedzera W, Maheswaran H, Squire SB, et al. Economic costs of accessing tuberculosis (TB) diagnostic services in Malawi: an analysis of patient costs from a randomised controlled trial of

- computer-aided chest X-ray interpretation. *Wellcome Open Res.* 2021;6:153. [\[Crossref\]](#)
24. Chandra A, Kumar R, Kant S, Parthasarathy R, Krishnan A. Direct and indirect patient costs of tuberculosis care in India. *Trop Med Int Health.* 2020;25(7):803-812. [\[Crossref\]](#)
 25. Portnoy A, Yamanaka T, Nguhiu P, et al. Costs incurred by people receiving tuberculosis treatment in low-income and middle-income countries: a meta-regression analysis. *Lancet Glob Health.* 2023;11:1640-1647. [\[Crossref\]](#)
 26. Tanimura T, Jaramillo E, Weil D, Raviglione M, Lönnroth K. Financial burden for tuberculosis patients in low- and middle-income countries: a systematic review. *Eur Respir J.* 2014;43(6):1675-1763. [\[Crossref\]](#)
 27. John KR, Daley P, Kincler N, Oxlade O, Menzies D. Costs incurred by patients with pulmonary tuberculosis in rural India. *Int J Tuberc Lung Dis.* 2009;13(10):1281-1287. [\[Crossref\]](#)
 28. Razzaq S, Zahidie A, Fatmi Z. Estimating the pre- and post-diagnosis costs of tuberculosis for adults in Pakistan: household economic impact and costs mitigating strategies. *Glob Health Res Policy.* 2022;7(1):22. [\[Crossref\]](#)
 29. Xia L, Gao L, Zhong Y, et al. Assessing the influencing factors of out-of-pocket costs on tuberculosis in Sichuan Province: a cross-sectional study. *BMC Public Health.* 2023;23:1391. [\[Crossref\]](#)
 30. Asres A, Jerene D, Deressa W. Pre- and post-diagnosis costs of tuberculosis to patients on directly observed treatment short course in districts of southwestern Ethiopia: a longitudinal study. *J Health Popul Nutr.* 2018;37(1):15. [\[Crossref\]](#)
 31. Pichenda K, Nakamura K, Morita A, Kizuki M, Seino K, Takano T. Non-hospital DOT and early diagnosis of tuberculosis reduce costs while achieving treatment success. *Int J Tuberc Lung Dis.* 2012;16(6):828-834. [\[Crossref\]](#)
 32. Mauch V, Melgen R, Marcelino B, Acosta I, Klinkenberg E, Suarez P. Tuberculosis patients in the Dominican Republic face severe direct and indirect costs and need social protection. *Rev Panam Salud Publica.* 2013;33(5):332-339. [\[Crossref\]](#)
 33. Floyd K, Skeva J, Nyirenda T, Gausi F, Salaniponi F. Cost and cost-effectiveness of increased community and primary care facility involvement in tuberculosis care in Lilongwe District, Malawi. *Int J Tuberc Lung Dis.* 2003;7(Suppl 1):29-37. [\[Crossref\]](#)
 34. Gullón JA, García-García JM, Villanueva MÁ, et al. Tuberculosis costs in Spain and related factors. *Arch Bronconeumol.* 2016;52(12):583-589. [\[Crossref\]](#)

Original Article

Clinical Characteristics of Moderate-to-Severe Obstructive Sleep Apnea: A Cross-sectional Analysis of 12,715 Adults from the TURKAPNE Cohort

 Baran Balcan¹,  Aylin Pıhtılı²,  Esen Kıyan²,  Mehmet Sezai Taşbakan³,  Özen K. Başoğlu³,  Şenay Aydın⁴,  Aykut Çilli⁵,  Neşe Dursunoğlu⁶,  Nur Aleyna Yetkin⁷,  Yüksel Peker^{1,8,9,10,11}, TURKAPNE Study Group*

¹Department of Pulmonary Medicine, Koç University Faculty of Medicine, İstanbul, Türkiye

²Department of Pulmonary Medicine, İstanbul University, İstanbul Faculty of Medicine, İstanbul, Türkiye

³Department of Pulmonary Medicine, Ege University Faculty of Medicine, İzmir, Türkiye

⁴Clinic of Neurology, University of Health Sciences Türkiye, Yedikule Chest Diseases and Thoracic Surgery Training and Research Hospital, İstanbul, Türkiye

⁵Department of Pulmonary Medicine, Akdeniz University Faculty of Medicine, Antalya, Türkiye

⁶Department of Pulmonary Medicine, Pamukkale University Faculty of Medicine, Denizli, Türkiye

⁷Department of Pulmonary Medicine, Erciyes University Faculty of Medicine, Kayseri, Türkiye

⁸Koç University Research Center for Translational Medicine (KUTTAM), İstanbul, Türkiye

⁹Department of Molecular and Clinical Medicine, Institute of Medicine, University of Gothenburg, Sahlgrenska Academy, Gothenburg, Sweden

¹⁰Department of Clinical Sciences, Respiratory Medicine and Allergology, Lund University School of Medicine, Lund, Sweden

¹¹Division of Pulmonary, Allergy, and Critical Care Medicine, University of Pittsburgh School of Medicine, Pittsburgh, PA, USA

Cite this article as: Balcan B, Pıhtılı A, Kıyan E, et al. Clinical characteristics of moderate-to-severe obstructive sleep apnea: a cross-sectional analysis of 12,715 adults from the TURKAPNE cohort. *Thorac Res Pract.* 2026;27(3):173-181

ABSTRACT

OBJECTIVE: Obstructive sleep apnea (OSA) is a common sleep-related breathing disorder associated with cardiometabolic morbidity. However, its clinical presentation is heterogeneous, and subjective sleepiness does not consistently reflect disease severity. We aimed to describe the clinical and polysomnographic characteristics of moderate-to-severe OSA and to identify factors independently associated with disease severity in a large nationwide sleep clinic cohort.

MATERIAL AND METHODS: This cross-sectional study was conducted within the Turkish Sleep Apnea Database cohort and included 12,715 adults with complete baseline clinical and polysomnographic data from 34 sleep centers. Moderate-to-severe OSA was defined as an apnea–hypopnea index (AHI) ≥ 15 events/h. Demographic and anthropometric variables, sleep-related symptoms, Epworth Sleepiness Scale (ESS) scores, polysomnographic parameters, and comorbidities were analyzed. Independent factors associated with moderate-to-severe OSA were identified using multivariable logistic regression.

RESULTS: Overall, 8,393 patients (66.0%) had moderate-to-severe OSA and 4,322 (34.0%) had no or mild OSA (AHI < 15 events/h). Patients with moderate-to-severe OSA were older, more frequently male, and had a higher body mass index (BMI) (all $P < 0.001$). Although excessive daytime sleepiness (ESS ≥ 11) was more common (25.8% vs. 17.7%, $P < 0.001$), ESS score was not independently associated with disease severity. Increasing age, male sex, higher BMI, snoring, witnessed apneas, and nocturnal dyspnea remained independent associates of moderate-to-severe OSA.

CONCLUSION: In this large nationwide sleep clinic cohort, objective risk factors and classic nocturnal symptoms were more informative than subjective sleepiness in identifying clinically significant OSA and support a risk-based approach in routine pulmonary practice.

KEYWORDS: Insomnia, sleep apnea, comorbidity, polysomnography

Received: 12.01.2026

Revision Requested: 02.03.2026

Last Revision Received: 02.03.2026

Accepted: 05.03.2026

Epub: 22.04.2026

Publication Date: 12.05.2026

Corresponding author: Baran Balcan, MD, e-mail: drbaranbalcan@gmail.com



INTRODUCTION

Obstructive sleep apnea (OSA) is a common chronic sleep-related breathing disorder characterized by recurrent upper airway obstruction during sleep, leading to intermittent hypoxemia and sleep fragmentation. Global prevalence estimates indicate that nearly one billion adults have OSA, with approximately 400–450 million affected by moderate-to-severe disease [apnea–hypopnea index (AHI) ≥ 15 events/h], underscoring its major public health impact.^{1–3}

Moderate-to-severe OSA is strongly associated with adverse cardiometabolic outcomes. Large observational and longitudinal studies have demonstrated robust associations between OSA and hypertension (HT), coronary artery disease (CAD), heart failure (HF), diabetes mellitus (DM), and increased cardiovascular morbidity and mortality.^{4–7} These associations are thought to be mediated by sympathetic nervous system activation, oxidative stress, endothelial dysfunction, metabolic dysregulation, and systemic inflammation driven by intermittent hypoxia and sleep disruption.^{8,9} In addition, OSA is linked to impaired daytime functioning, neurocognitive complaints, reduced quality of life, and increased risk of motor vehicle and occupational accidents.^{10–12}

Despite these well-established consequences, the clinical presentation of OSA is heterogeneous. While loud snoring, witnessed apneas, and excessive daytime sleepiness (EDS) are considered classic features, symptom burden does not consistently parallel objective disease severity.¹⁰ EDS is commonly assessed using the Epworth Sleepiness Scale (ESS), a validated and widely used questionnaire.¹³ However, a substantial proportion of patients with moderate-to-severe OSA report minimal subjective sleepiness, whereas some individuals with lower AHI values experience marked daytime impairment.^{10,14}

Demographic and anthropometric factors remain among the most consistent clinical correlates of OSA severity. Increasing age, male sex, obesity, and central adiposity—often reflected by body mass index (BMI) and neck circumference—are

strongly associated with moderate-to-severe OSA across populations.^{2,3,15,16} Nevertheless, the relative contribution of symptoms, anthropometrics, and comorbidities may vary by population and referral setting.

Using data from a nationwide sleep clinic cohort, the present study aimed to characterize demographic, anthropometric, polysomnographic, symptomatic, and comorbidity profiles associated with moderate-to-severe OSA and to identify clinical factors independently associated with this disease severity.

MATERIAL AND METHODS

Study Design and Data Source

The present study was conducted as a cross-sectional analysis within the framework of the Turkish Sleep Apnea Database (TURKAPNE), a nationwide, multicenter cohort established to investigate the clinical and polysomnographic characteristics of patients evaluated for OSA in routine clinical practice.¹⁷ Since October 2017, adults referred to participating sleep centers for suspected OSA have been prospectively enrolled.

For the current analysis, records obtained from 34 accredited sleep centers were screened. Only patients with complete demographic information, anthropometric measurements, clinical characteristics, questionnaire data, and full-night polysomnography were included (Figure 1). Individuals with advanced systemic illnesses limiting life expectancy, active or uncontrolled malignancy, alcohol dependence, or prior treatment with positive airway pressure devices or mandibular advancement devices were excluded to avoid confounding.

Ethical Approval and Patient Consent

All procedures were performed in accordance with internationally accepted ethical standards. The study protocol received approval from the Ethics Committee of the Medical Faculty of Marmara University, İstanbul (approval no: 09.2016.311, date: 05.09.2016). Written informed consent was obtained from all participants prior to data collection. The TURKAPNE registry is listed on ClinicalTrials.gov (identifier: NCT02784977).

Registry Structure and Data Management

Clinical data were entered into a dedicated, password-protected electronic registry designed specifically for the TURKAPNE project. Each participating center accessed the system using individualized credentials and entered patient data through standardized electronic case report forms. Data were stored on a secure central server, while personally identifiable information remained locally archived at each center. To ensure data reliability, periodic random audits were conducted by an independent monitoring committee with unrestricted access to the database.

Clinical, Demographic, and Anthropometric Assessments

Baseline demographic characteristics included age and sex. Elderly status was defined as age ≥ 65 years. Anthropometric assessments comprised BMI, calculated as weight divided by height squared (kg/m^2), obesity was defined as a BMI ≥ 30 kg/m^2 .

Main Points

- In a large nationwide cohort of over 12,000 sleep clinic patients, two-thirds were diagnosed with moderate-to-severe obstructive sleep apnea (OSA), highlighting the substantial burden of clinically significant disease in routine practice.
- Objective risk factors—including increasing age, male sex, higher body mass index, and classic nocturnal symptoms (snoring, witnessed apneas, nocturnal dyspnea)—were independently associated with OSA severity.
- Although excessive daytime sleepiness was more prevalent in patients with moderate-to-severe OSA, subjective sleepiness (Epworth Sleepiness Scale score) was not an independent predictor of disease severity.
- These findings support a risk-based, symptom-informed diagnostic approach, emphasizing objective clinical characteristics over subjective sleepiness in the identification of clinically relevant OSA.

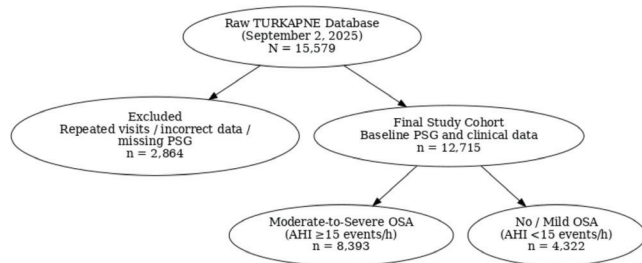


Figure 1. Flow chart of the participants

OSA: obstructive sleep apnea, PSG: polysomnography, AHI: apnea-hypopnea index

Clinical symptom variables were derived from standardized patient-reported items recorded in the registry and included sleep-related complaints (difficulty initiating sleep, difficulty maintaining sleep, subjective sleep latency ≥ 30 minutes, total sleep time < 6 hours, and reduced sleep efficiency), nocturnal symptoms (snoring, witnessed apneas, nocturnal dyspnea, nocturia, night sweats, and morning headache), and daytime outcomes (daytime sleepiness, daytime tiredness, fatigue, impaired concentration, and history of sleep-related accidents).

Comorbid conditions were identified based on physician-reported diagnoses and/or ongoing medical treatment, and categorized as cardiometabolic (HT or antihypertensive medication use, DM, hyperlipidemia, CAD, and HF); respiratory (chronic obstructive pulmonary disease and asthma); neuropsychiatric (depression, restless legs syndrome, epilepsy, and other psychiatric disorders); endocrine (hypothyroidism); cerebrovascular disease (prior stroke or transient ischemic attack); and malignancy. Concomitant medication use, including antihypertensive, antidiabetic, lipid-lowering, antiepileptic, and immunosuppressive therapies, was also recorded and considered in the analyses.

Assessment of Sleep-related Symptoms and Daytime Function

Sleep-related symptoms were evaluated using standardized patient-reported items embedded in the TURKAPNE registry. These included habitual snoring, witnessed apneas, nocturnal dyspnea, nocturia, night sweats, morning headache, difficulties with sleep initiation or maintenance, prolonged subjective sleep latency (≥ 30 minutes), short sleep duration (< 6 hours), impaired concentration, and history of sleep-related accidents.

Daytime sleepiness was quantified using the validated Turkish version of the ESS. The ESS yields a total score between 0 and 24, with higher scores indicating greater daytime sleep propensity. EDS was defined as an ESS score of 11 or higher.¹³

Polysomnographic Evaluation and Obstructive Sleep Apnea Classification

All participants underwent attended overnight polysomnography with a minimum recording duration of seven hours. Subjects were instructed to refrain from alcohol, caffeine, and sedative agents on the day of the study. Standard recordings included electroencephalography, electrooculography,

electromyography, electrocardiography, airflow measurements, respiratory effort, oxygen saturation, snoring, and body position.

Sleep staging and respiratory event scoring were performed according to contemporary international criteria.¹⁸ Apnea was defined as a reduction in airflow of at least 90% lasting 10 seconds or longer, while hypopnea was defined as a reduction in airflow of at least 30% lasting 10 seconds or longer, accompanied by either oxygen desaturation of $\geq 3\%$ or an arousal.

The AHI was calculated as the number of respiratory events per hour of sleep. OSA was defined as an AHI ≥ 5 events/h. For the purposes of this study, patients were categorized as having moderate-to-severe OSA if AHI was ≥ 15 events/h. Severe OSA was defined as an AHI ≥ 30 events/h. Additional polysomnographic parameters included sleep architecture, arousal index, oxygen desaturation index, minimum and mean oxygen saturation, time spent with oxygen saturation below 90%, rapid eye movement (REM)-related AHI, and supine AHI.

Statistical Analysis

Continuous variables were summarized as mean \pm standard deviation, while categorical variables were presented as counts and percentages. The normality of continuous variables was assessed visually and statistically. Between-group comparisons by OSA severity (moderate-severe vs. non-moderate-severe OSA) were performed using the independent-samples t-test for continuous variables and the chi-square test for categorical variables. Polysomnographic parameters, sleep architecture variables, sleep-related symptoms, daytime outcomes, and comorbid conditions were compared between groups using the same approach. A two-sided *P* value was considered statistically significant. To identify independent predictors of moderate-to-severe OSA, univariable logistic regression analyses were first performed on demographic, anthropometric, sleep-related, and clinical variables. Subsequently, multivariable logistic regression models were constructed using a hierarchical modeling strategy. Results of logistic regression analyses were reported as odds ratios with 95% confidence intervals. All analyses were conducted using a standard statistical software package, and statistical significance was defined as a two-tailed *P* value < 0.05 .

RESULTS

Study Population

As shown in Figure 1, 15,579 individuals were screened from the TURKAPNE database. After exclusion of repeated visits, incorrectly entered records, and missing polysomnographic data ($n = 2,864$), the final study cohort comprised 12,715 adults with complete baseline clinical and polysomnographic information. Of these, 8,393 patients (66.0%) had moderate-to-severe OSA (AHI ≥ 15 events/h), while 4,322 (34.0%) had no or mild OSA.

Demographic and Anthropometric Characteristics

Patients with moderate-to-severe OSA were older, more likely to be male, and had a higher prevalence of obesity and greater central and peripheral adiposity compared with those without moderate-to-severe OSA (all $P < 0.001$; Table 1).

Polysomnographic Characteristics and Sleep-related Symptoms

Moderate-to-severe OSA was associated with a substantially higher respiratory event burden, more pronounced nocturnal hypoxemia, a higher arousal index, and altered sleep architecture,

characterized by a higher proportion of N1 sleep and lower proportions of N3 and REM sleep (all $P < 0.001$; Table 2). Several nocturnal and daytime symptoms, including snoring, witnessed apneas, nocturnal dyspnea, daytime sleepiness, fatigue, and sleep-related accidents, were more prevalent in

Table 1. Demographic characteristics and anthropometric measures according to OSA severity

| Variable | Moderate-to-severe OSA n = 8393 | No/mild OSA n = 4322 | P value |
|---|------------------------------------|-------------------------|---------|
| Age, years | 51.8±11.7 | 46.9±12.3 | <0.001 |
| Female sex, % | 26.7 | 40.9 | <0.001 |
| Elderly (≥65 years), % | 14.2 | 7.8 | <0.001 |
| BMI, kg/m ² | 32.7±6.0 | 29.6±5.6 | <0.001 |
| Obesity (BMI ≥30 kg/m ²), % | 63.8 | 40.7 | <0.001 |
| Neck circumference, cm | 42.0±5.3 | 39.3±5.1 | <0.001 |
| Waist circumference, cm | 111.1±15.4 | 102.1±13.7 | <0.001 |
| Hip circumference, cm | 113.1±12.6 | 109.2±29.9 | <0.001 |

OSA: obstructive sleep apnea, BMI: body mass index

Table 2. Polysomnographic features, sleep architecture, and sleep-related symptoms according to OSA severity

| Variable | Moderate-to-severe OSA | No/mild OSA | P value |
|---|------------------------|-------------|---------|
| Polysomnographic and sleep architecture parameters | | | |
| PSG-AHI | 43.5±24.6 | 7.4±4.1 | <0.001 |
| ODI | 42.8±44.2 | 8.0±9.5 | <0.001 |
| REM-AHI | 43.3±27.0 | 16.6±26.4 | <0.001 |
| Supine AHI | 56.9±27.7 | 15.8±15.0 | <0.001 |
| Nadir SpO ₂ , % | 76.4±11.5 | 85.8±7.3 | <0.001 |
| Time with SpO ₂ <90%, min | 56.4±81.4 | 22.0±51.6 | <0.001 |
| N1 sleep, % | 6.9±9.1 | 4.9±6.7 | <0.001 |
| N3 sleep, % | 21.6±17.3 | 25.3±17.6 | <0.001 |
| REM sleep, % | 13.6±9.1 | 14.8±8.0 | <0.001 |
| Arousal index | 26.2±25.5 | 14.1±15.8 | <0.001 |
| Sleep-related symptoms and daytime outcomes | | | |
| Difficulty falling asleep | 18.4 | 16.7 | 0.031 |
| Sleep latency ≥30 min | 17.7 | 24.3 | <0.001 |
| Difficulty maintaining sleep | 15.4 | 14.4 | 0.204 |
| Total sleep time <6 h | 24.0 | 24.2 | 0.746 |
| Sleep efficiency <85% | 51.8 | 51.0 | 0.410 |
| Night sweats | 27.7 | 18.0 | <0.001 |
| Nocturia | 27.6 | 18.1 | <0.001 |
| Morning headache | 19.2 | 13.2 | <0.001 |
| Daytime sleepiness | 46.8 | 30.8 | <0.001 |
| Daytime tiredness | 46.8 | 33.6 | <0.001 |
| Fatigue | 46.7 | 33.6 | <0.001 |
| ESS score | 6.14±6.25 | 4.95±5.47 | <0.001 |
| ESS ≥11 | 25.8 | 17.7 | <0.001 |
| Difficulty in concentration | 19.6 | 16.4 | <0.001 |
| Sleep-related accident | 2.8 | 1.9 | 0.002 |

OSA: obstructive sleep apnea, PSG: polysomnography, AHI, apnea–hypopnea index, ODI: oxygen desaturation index, SpO₂: peripheral oxygen saturation, N1: stage N1 sleep, N3: stage N3 sleep, REM: rapid eye movement, ESS: Epworth Sleepiness Scale

patients with moderate-to-severe OSA. Although ESS scores and the prevalence of EDS (ESS ≥11) were higher in this group, subjective sleepiness showed limited discriminatory value when considered alongside objective disease characteristics (Table 2).

Comorbidities

Patients with moderate-to-severe OSA had a higher prevalence of cardiometabolic comorbidities, including HT, DM, CAD, HF, and chronic obstructive pulmonary disease, as well as depression and restless legs syndrome (all *P* < 0.001; Table 3). No significant between-group differences were observed for arrhythmia, cerebrovascular disease, asthma, hypothyroidism, or malignancy.

Factors Independently Associated with Moderate-to-Severe OSA

In multivariable logistic regression analyses (Table 4, Figure 2), increasing age, male sex, and higher BMI remained strong independent predictors of moderate-to-severe OSA across all models. After full adjustment, snoring, witnessed apneas, and nocturnal dyspnea were independently associated with moderate-to-severe OSA, whereas ESS score and nocturia were not. Cardiometabolic comorbidities did not retain independent associations with disease severity in the fully adjusted model.

DISCUSSION

Principal Findings

In this large, nationwide, multicenter sleep clinic cohort, moderate-to-severe OSA had a distinct clinical profile characterized by older age, male sex, and increased general and central adiposity. These demographic and anthropometric features remained the strongest independent predictors of

disease severity, even after comprehensive adjustment for symptoms and comorbidities. In contrast, subjective daytime sleepiness showed limited discriminatory value once objective risk factors and nocturnal symptoms were considered.

Demographic and Anthropometric Correlates of Obstructive Sleep Apnea Severity

The strong associations between advancing age, male sex, and moderate-to-severe OSA observed in the present study are consistent with prior population-based and clinic-based investigations.^{2,3,10} Age-related changes in upper airway anatomy, neuromuscular control, and ventilatory stability, together with sex-specific differences in fat distribution and airway collapsibility, are likely to underlie these associations.^{2,3,10,19}

Obesity emerged as a central determinant of disease severity, in line with extensive evidence linking increased body mass to upper airway narrowing and collapsibility. Beyond BMI, patients with moderate-to-severe OSA had larger neck, waist, and hip circumferences, underscoring the importance of central and peripheral adiposity. Prior imaging and physiological studies have demonstrated that fat accumulation in cervical and abdominal regions contributes to reduced lung volumes and mechanical loading of the upper airway, thereby exacerbating airway instability during sleep.²⁰⁻²² Collectively, these findings reinforce the clinical relevance of anthropometric assessment when evaluating OSA severity in routine practice.

Sleep Architecture, Hypoxemia, and Symptom Burden

Patients with moderate-to-severe OSA demonstrated greater respiratory event burden, more pronounced nocturnal hypoxemia, and increased sleep fragmentation, consistent with earlier polysomnographic studies linking disease severity to disrupted sleep continuity.²³ The observed shift toward lighter sleep stages and relative reduction in slow-wave and REM sleep

Table 3. Cardiometabolic, respiratory, and neuropsychiatric comorbidities and medication use according to OSA severity

| Variable | Moderate-to-severe OSA | No/mild OSA | P value |
|-----------------------------------|------------------------|-------------|---------|
| Hypertension/antihypertensive use | 35.5 | 23.5 | <0.001 |
| Diabetes mellitus | 18.0 | 11.7 | <0.001 |
| Hyperlipidemia | 6.6 | 4.2 | <0.001 |
| Coronary artery disease | 5.2 | 2.7 | <0.001 |
| Heart failure | 3.8 | 1.9 | <0.001 |
| COPD | 4.5 | 3.1 | <0.001 |
| Arrhythmia | 4.2 | 3.9 | 0.356 |
| Stroke/TIA | 0.8 | 0.6 | 0.311 |
| Depression | 15.3 | 12.2 | <0.001 |
| Restless legs syndrome | 14.7 | 11.6 | <0.001 |
| Psychiatric disorders (overall) | 6.1 | 6.5 | 0.498 |
| Asthma | 8.2 | 9.1 | 0.090 |
| Hypothyroidism | 4.0 | 4.6 | 0.108 |
| Cancer | 0.4 | 0.4 | 0.752 |
| Immunosuppressive drug use | 0.3 | 0.6 | 0.028 |
| Antiepileptic drug use | 0.9 | 1.1 | 0.505 |

OSA: obstructive sleep apnea, COPD: chronic obstructive pulmonary disease, TIA, transient ischemic attack

aligns with experimental and clinical data showing preferential suppression of restorative sleep in the presence of recurrent respiratory events and arousals.^{23,24}

Indices of nocturnal hypoxemia appear to play a particularly important role in shaping the clinical symptom burden. Prior work has suggested that measures such as oxygen desaturation index and cumulative hypoxemic exposure may correlate more closely with daytime impairment than AHI alone.²⁵ In agreement with this concept, patients with moderate-to-severe OSA in the present study reported higher rates of daytime sleepiness, fatigue, impaired concentration, and sleep-related accidents, supporting the clinical relevance of hypoxemia-driven sleep disruption.^{25,26}

Subjective Sleepiness and Disease Severity

Despite higher ESS scores and a greater prevalence of EDS among patients with more severe OSA, subjective sleepiness did not remain independently associated with moderate-to-severe disease after multivariable adjustment. This finding corroborates previous observations that subjective sleepiness

alone is an imperfect marker of OSA severity and may be influenced by interindividual differences in arousal threshold, sleep perception, comorbid conditions, and adaptive mechanisms.^{25,27} These results highlight the limitations of relying solely on subjective sleepiness when stratifying disease severity and underscore the importance of integrating objective risk factors with nocturnal symptom profiles.

Comorbidities and Obstructive Sleep Apnea Severity

Moderate-to-severe OSA was associated with a higher prevalence of cardiometabolic comorbidities, including HT, DM, CAD, and HF, consistent with extensive epidemiological evidence linking OSA severity to cardiometabolic disease burden.^{4,7,9} The increased prevalence of chronic obstructive pulmonary disease among patients with more severe OSA aligns with prior reports describing the overlap syndrome and its association with more severe nocturnal hypoxemia and adverse cardiopulmonary outcomes.²⁸

However, most comorbid conditions did not retain independent associations with disease severity in fully adjusted models,

Table 4. Multivariable logistic regression analysis of factors associated with obstructive sleep apnea across sequentially adjusted models

| | OR | 95% CI | P value |
|--|-------|-------------|---------|
| Model 1. Demographic and anthropometric variables | | | |
| Age (per year) | 1.041 | 1.038–1.045 | <0.001 |
| Male sex | 3.196 | 2.915–3.505 | <0.001 |
| BMI (kg/m ²) | 1.112 | 1.104–1.121 | <0.001 |
| Model 2. Model 1 + sleep-related symptoms and ESS | | | |
| Age (per year) | 1.045 | 1.040–1.049 | <0.001 |
| Male sex | 3.023 | 2.718–3.362 | <0.001 |
| BMI (kg/m ²) | 1.104 | 1.094–1.114 | <0.001 |
| Snoring | 2.355 | 2.120–2.617 | <0.001 |
| Witnessed apneas | 1.865 | 1.645–2.114 | <0.001 |
| Nocturnal dyspnea | 1.258 | 1.103–1.435 | <0.001 |
| Nocturia | 0.992 | 0.881–1.118 | 0.897 |
| ESS score | 1.007 | 0.999–1.015 | 0.097 |
| Model 3. Fully adjusted model | | | |
| Age (per year) | 1.045 | 1.040–1.050 | <0.001 |
| Male sex | 3.037 | 2.729–3.379 | <0.001 |
| BMI (kg/m ²) | 1.104 | 1.094–1.114 | <0.001 |
| Snoring | 2.353 | 2.118–2.615 | <0.001 |
| Witnessed apneas | 1.863 | 1.643–2.113 | <0.001 |
| Nocturnal dyspnea | 1.260 | 1.104–1.437 | <0.001 |
| Nocturia | 0.994 | 0.882–1.121 | 0.928 |
| ESS score | 1.007 | 0.999–1.015 | 0.096 |
| COPD | 0.871 | 0.676–1.123 | 0.287 |
| Coronary artery disease | 0.962 | 0.741–1.249 | 0.770 |
| Hypertension/antihypertensive use | 1.003 | 0.892–1.127 | 0.964 |
| Diabetes mellitus | 1.018 | 0.885–1.172 | 0.799 |

AHI: apnea–hypopnea index, BMI: body mass index, CI: confidence interval, COPD: chronic obstructive pulmonary disease, ESS: Epworth Sleepiness Scale, OR: odds ratio, OSA: obstructive sleep apnea

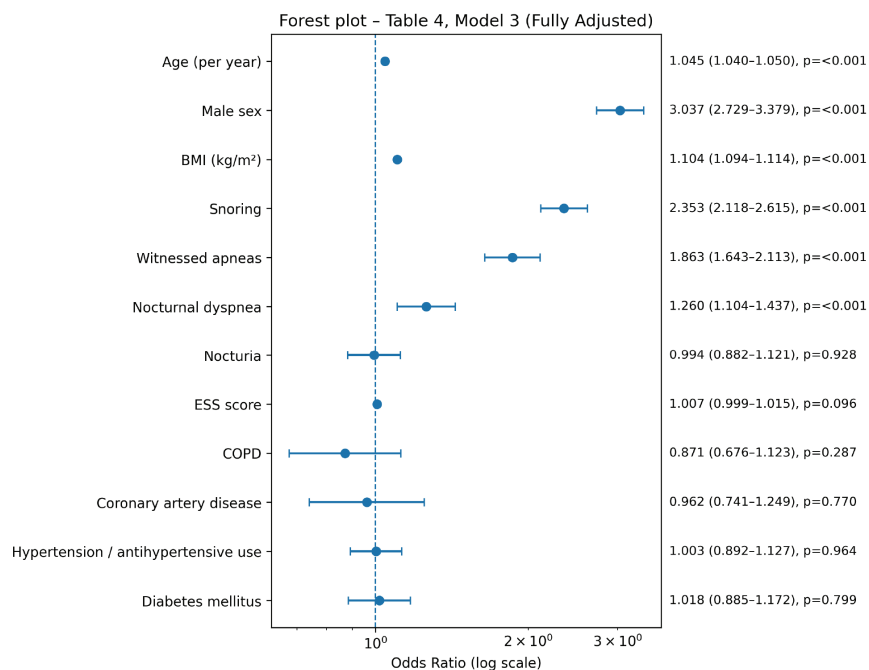


Figure 2. Multivariable regression analysis of the parameters related to moderate-to-severe OSA

OSA: obstructive sleep apnea, BMI: body mass index, ESS: Epworth Sleepiness Scale, COPD: chronic obstructive pulmonary disease

suggesting that their observed relationships with OSA may be largely mediated through shared risk factors such as age, sex, and obesity. With respect to neuropsychiatric conditions, the higher prevalence of depression and restless legs syndrome is consistent with earlier reports,²⁹⁻³¹ whereas the absence of differences in overall psychiatric morbidity underscores the heterogeneity of neuropsychiatric manifestations in OSA.

Clinical Implications

The present findings have important implications for clinical practice. Classic nocturnal symptoms, together with demographic and anthropometric risk factors, provided greater discriminatory value for identifying moderate-to-severe OSA than subjective sleepiness alone did. These results support a comprehensive, risk-based approach to OSA assessment that integrates objective clinical characteristics with symptom profiles, rather than reliance on daytime sleepiness as a primary indicator of disease severity.

Strengths and Limitations

Key strengths of this study include the large sample size, nationwide multicenter design, and standardized data collection within a well-established registry. Several limitations merit consideration. The cross-sectional design precludes causal inference, and the sleep clinic-based population may limit generalizability to community settings. Symptom reporting and comorbidity data were based on patient report and physician documentation, introducing potential misclassification. Residual confounding by unmeasured factors cannot be excluded, and the lack of longitudinal follow-up precludes assessment of disease progression or treatment effects.

CONCLUSION

In this large multicenter sleep clinic cohort, moderate-to-severe OSA was associated with a distinct demographic, anthropometric, and clinical profile characterized by older age, male sex, greater adiposity, more severe nocturnal hypoxemia, and increased sleep fragmentation. While subjective sleepiness was more prevalent in patients with more severe disease, objective risk factors and classic nocturnal symptoms demonstrated greater discriminatory value. These findings emphasize the importance of integrating demographic, anthropometric, and symptom-based information for the identification and risk stratification of clinically significant OSA in real-world practice.

*On behalf of the TURKAPNE Study Group (Alphabetical Order):

Ahmet Ursavaş¹, Ali Nihat Annakkaya², Alperen Aksakal³, Aydın Balci⁴, Ayfer Utkusavaş⁵, Aylin Özsancağ Uğurlu⁶, Ayşe Deniz Elmalı⁷, Baran Balcan⁸, Başak Gönen⁹, Bilkay Serez Kaya⁹, Burcu Baran¹⁰, Burcu Oktay Arslan¹¹, Canan Gündüz Gürkan¹², Caner Çınar¹³, Demet İlhan Algın¹⁴, Derya Karadeniz¹⁵, Dilara Mermi Dibek⁷, Dursun Dursunoğlu¹⁶, Duygu Özöl¹², Ebru Çakır Edis⁹, Ebru Duygu⁵, Ege Güleç Balbay², Ersin Günay^{4,17}, Fuat Erel¹⁸, Funda Aksu¹⁹, Gökhan Kırbas²⁰, Gülçin Benbir Şenel¹⁵, Gülgün Çetintaş Afşar¹², Gülin Sünter²¹, Hadice Selimoğlu Şen²⁰, Hamza Ogun²², Hasan Akça²³, Hikmet Fırat¹⁷, Hilal Türkmen Kaya²⁴, Işıl Yazıcı Gençdal²⁵, İbrahim Öztura²⁶, İlker Yılmam⁹, Kadriye Ağan²¹, Mehmet Ali Habeşoğlu²⁷, Mehmet Karadağ¹, Melike Banu Yücegeç¹⁷, Metin Akgün^{3,28}, Muhammed Emin Akkoyunlu²⁹, Mustafa Saygın³⁰, Nejat Altıntaş³¹, Nurhan Sarıoğlu¹⁸, Oğuz Osman Erdinç¹⁴, Onur Bulut³², Oya İtil³², Oya Öztürk²⁵, Önder Öztürk²⁴, Özge Aydın Güçlü¹, Özlem Erçen Diken³³, Pınar Bekdik Şirinocak³⁴, Pınar Yıldız Gülhan², Sadık Ardiç³⁵, Selma Fırat¹⁹, Sema Saraç¹², Semih Arbatlı⁸,

Sevgi Ferik²⁶, Sezgi Şahin Duyar¹⁹, Sinem Berik Safçı³³, Sinem N. Sökücü³⁶, Süreyya Yılmaz²⁰, Tunahan Anber²³, Uluğ Bey Hayri³⁷, Ülkü Dübüş Hoş⁷, Ümmühan Okur³⁸, Vasfiye Kabeloğlu²⁵, Yeliz Çelik⁸, Zahide Yılmaz³⁴, Zeynep Zeren Uçar¹¹

¹Department of Pulmonary Medicine, Bursa Uludağ University Faculty of Medicine, Bursa, Türkiye

²Department of Pulmonary Medicine, Düzce University Faculty of Medicine, Düzce, Türkiye

³Department of Pulmonary Medicine, Atatürk University Faculty of Medicine, Erzurum, Türkiye

⁴Department of Pulmonary Medicine, Afyon Health Sciences University Faculty of Medicine, Afyon, Türkiye

⁵Department of Pulmonary Medicine, University of Health Sciences Türkiye, Mehmet Akif Ersoy Thoracic and Cardiovascular Surgery Training and Research Hospital, İstanbul, Türkiye

⁶Department of Pulmonary Medicine, Başkent University Faculty of Medicine, İstanbul, Türkiye

⁷Clinic of Neurology, University of Health Sciences Türkiye, Başakşehir Çam and Sakura City Hospital, İstanbul, Türkiye

⁸Department of Pulmonary Medicine, Koç University Faculty of Medicine, İstanbul, Türkiye

⁹Department of Pulmonary Medicine, Trakya University Faculty of Medicine, Edirne, Türkiye

¹⁰Department of Pulmonary Medicine, Erciyes University Faculty of Medicine, Kayseri, Türkiye

¹¹Clinic of Pulmonary Medicine, University of Health Sciences Türkiye, Dr. Suat Seren Chest Diseases and Chest Surgery Training and Research Hospital, İzmir, Türkiye

¹²Clinic of Pulmonary Medicine, University of Health Sciences Türkiye, Süreyyapasa Chest Diseases Training and Research Hospital, İstanbul, Türkiye

¹³Department of Pulmonary Medicine, Marmara University Faculty of Medicine, İstanbul, Türkiye

¹⁴Department of Neurology, Eskişehir Osmangazi University Faculty of Medicine, Eskişehir, Türkiye

¹⁵Department of Neurology, İstanbul University Cerrahpaşa-Cerrahpaşa Faculty of Medicine, İstanbul, Türkiye

¹⁶Department of Cardiology, Pamukkale University Faculty of Medicine, Denizli, Türkiye

¹⁷Department of Pulmonary Medicine, University of Health Sciences Türkiye, Etlik City Hospital, Ankara, Türkiye

¹⁸Department of Pulmonary Medicine, Balıkesir University Faculty of Medicine, Balıkesir, Türkiye

¹⁹Clinic of Pulmonary Medicine, Atatürk Sanatorium Training and Research Hospital, Ankara, Türkiye

²⁰Department of Pulmonary Medicine, Dicle University Faculty of Medicine, Diyarbakır, Türkiye

²¹Department of Neurology, Marmara University Faculty of Medicine, İstanbul, Türkiye

²²Department of Pulmonary Medicine, Bezmialem Vakıf University Faculty of Medicine, İstanbul, Türkiye

²³Department of Pulmonary Medicine, Pamukkale University Faculty of Medicine, Denizli, Türkiye

²⁴Department of Pulmonary Medicine, Süleyman Demirel University Faculty of Medicine, Isparta, Türkiye

²⁵Clinic of Neurology, Bakırköy Prof. Dr. Mazhar Osman Mental Health and Neurological Diseases Training and Research Hospital, İstanbul, Türkiye

²⁶Department of Neurology, Dokuz Eylül University Faculty of Medicine, İzmir, Türkiye

²⁷Department of Pulmonary Medicine, Başkent University Faculty of Medicine, Adana, Türkiye

²⁸Department of Pulmonary Medicine, Ağrı İbrahim Çeçen University Faculty of Medicine, Ağrı, Türkiye

²⁹Department of Pulmonary Medicine, Medipol University Faculty of Medicine, İstanbul, Türkiye

³⁰Department of Physiology, Süleyman Demirel University Faculty of Medicine, Isparta, Türkiye

³¹Department of Pulmonary Medicine, Tekirdağ Namık Kemal University Faculty of Medicine, Tekirdağ, Türkiye

³²Department of Pulmonary Medicine, Dokuz Eylül University Faculty of Medicine, İzmir, Türkiye

³³Clinic of Pulmonary Medicine, University of Health Sciences Türkiye, Adana City Hospital, Adana, Türkiye

³⁴Clinic of Pulmonary Medicine, University of Health Sciences Türkiye, Derince Training and Research Hospital, Kocaeli, Türkiye

³⁵Clinic of Pulmonary Medicine, Koru Hospital, Ankara, Türkiye

³⁶Clinic of Pulmonary Medicine, University of Health Sciences Türkiye, Yedikule Chest Diseases and Thoracic Surgery Training and Research Hospital, İstanbul, Türkiye

³⁷Department of Pulmonary Medicine, Tekirdağ İrmet Hospital, Tekirdağ, Türkiye

³⁸Department of Pulmonary Medicine, Akdeniz University Faculty of Medicine, Antalya, Türkiye

Ethics

Ethics Committee Approval: All procedures were performed in accordance with internationally accepted ethical standards. The study protocol received approval from the Ethics Committee of the Medical Faculty of Marmara University, İstanbul (approval no: 09.2016.311, date: 05.09.2016).

Informed Consent: Written informed consent was obtained from all participants prior to data collection.

Footnotes

Authorship Contributions

Concept: Y.P., Ö.K.B., Design: Y.P., Ö.K.B., Data Collection or Processing: B.B., A.P., E.K., M.S.T., Ö.K.B., Ş.A., A.Ç., N.D., N.A.Y., Y.P., TURKAPNE Study Group, Analysis or Interpretation: B.B., Literature Search: B.B., Writing: B.B.

Conflict of Interest: Metin Akgün, MD, serves as Editor-in-Chief of Thoracic Research and Practice. He is also a member of the TURKAPNE Study Group and contributed to data collection for this study. In line with the journal's editorial conflict of interest policy, he was fully excluded from all editorial and peer review processes related to this manuscript. He had no access to reviewer identities, reviewer reports, editorial evaluations, or the final decision-making process.

Canan Gündüz Gürkan, MD, serves as an Editor of Thoracic Research and Practice. She is also a member of the TURKAPNE Study Group and contributed to data collection for this study. She was not involved in any stage of the peer review or editorial decision-making process for this manuscript and had no access to reviewer information or reports.

Ege Güleç Balbay, MD, serves as an Editor of Thoracic Research and Practice. He is also a member of the TURKAPNE Study Group and contributed to data collection for this study. He had no role in the peer review process or editorial evaluation of this manuscript and had no access to reviewer identities or reports.

The peer review and editorial decision-making processes for this manuscript were conducted exclusively by the other Editor-in-Chief of the journal, who had no involvement in the study and no conflict of interest with the authors or the study group. The conflicted Editor-in-Chief was completely blinded to the process. The handling editor and reviewers were assigned

independently, and a strict double-blind peer review process was maintained. The final decision was made solely by the non-conflicted Editor-in-Chief based on the reviewers' evaluations and the journal's editorial standards.

No conflict of interest was declared by the remaining authors.

















Financial Disclosure: Financed by Turkish Thoracic Society.

REFERENCES

- Benjafield AV, Ayas NT, Eastwood PR, et al. Estimation of the global prevalence and burden of obstructive sleep apnoea: a literature-based analysis. *Lancet Respir Med.* 2019;7(8):687-698. [\[Crossref\]](#)
- Young T, Palta M, Dempsey J, Skatrud J, Weber S, Badr S. The occurrence of sleep-disordered breathing among middle-aged adults. *N Engl J Med.* 1993;328(17):1230-1235. [\[Crossref\]](#)
- Peppard PE, Young T, Barnet JH, Palta M, Hagen EW, Hla KM. Increased prevalence of sleep-disordered breathing in adults. *Am J Epidemiol.* 2013;177(9):1006-1014. [\[Crossref\]](#)
- Peppard PE, Young T, Palta M, Skatrud J. Prospective study of the association between sleep-disordered breathing and hypertension. *N Engl J Med.* 2000;342(19):1378-1384. [\[Crossref\]](#)
- Marin JM, Carrizo SJ, Vicente E, Agusti AG. Long-term cardiovascular outcomes in men with obstructive sleep apnoea-hypopnoea with or without treatment with continuous positive airway pressure: an observational study. *Lancet.* 2005;365(9464):1046-1053. [\[Crossref\]](#)
- Yaggi HK, Concato J, Kernan WN, Lichtman JH, Brass LM, Mohsenin V. Obstructive sleep apnea as a risk factor for stroke and death. *N Engl J Med.* 2005;353(19):2034-2041. [\[Crossref\]](#)
- Punjabi NM, Caffo BS, Goodwin JL, et al. Sleep-disordered breathing and mortality: a prospective cohort study. *PLoS Med.* 2009;6(8):e1000132. [\[Crossref\]](#)
- Somers VK, White DP, Amin R, et al. Sleep apnea and cardiovascular disease: an American Heart Association/American College of Cardiology Foundation Scientific Statement from the American Heart Association Council for High Blood Pressure Research Professional Education Committee, Council on Clinical Cardiology, Stroke Council, and Council on Cardiovascular Nursing. *J Am Coll Cardiol.* 2008;52(8):686-717. [\[Crossref\]](#)
- Tasali E, Ip MS. Obstructive sleep apnea and metabolic syndrome: alterations in glucose metabolism and inflammation. *Proc Am Thorac Soc.* 2008;5(2):207-217. [\[Crossref\]](#)
- Punjabi NM. The epidemiology of adult obstructive sleep apnea. *Proc Am Thorac Soc.* 2008;5(2):136-143. [\[Crossref\]](#)
- Sassani A, Findley LJ, Kryger M, Goldlust E, George C, Davidson TM. Reducing motor-vehicle collisions, costs, and fatalities by treating obstructive sleep apnea syndrome. *Sleep.* 2004;27(3):453-458. [\[Crossref\]](#)
- Garbarino S, Guglielmi O, Sanna A, Mancardi GL, Magnavita N. Risk of occupational accidents in workers with obstructive sleep apnea: systematic review and meta-analysis. *Sleep.* 2016;39(6):1211-1218. [\[Crossref\]](#)
- Johns MW. A new method for measuring daytime sleepiness: the Epworth Sleepiness Scale. *Sleep.* 1991;14(6):540-545. [\[Crossref\]](#)
- Gasa M, Tamisier R, Launois SH, et al. Residual sleepiness in sleep apnea patients treated by continuous positive airway pressure. *J Sleep Res.* 2013;22(4):389-397. [\[Crossref\]](#)
- Hedner J, Grote L, Bonsignore M, et al. The European Sleep Apnoea Database (ESADA): report from 22 European sleep laboratories. *Eur Respir J.* 2011;38(3):635-642. [\[Crossref\]](#)
- Grote L, Hedner J, Peter JH. Sleep-related breathing disorder is an independent risk factor for uncontrolled hypertension. *J Hypertens.* 2000;18(6):679-685. [\[Crossref\]](#)
- Peker Y, Başoğlu ÖK, Fırat H. Rationale and design of the Turkish sleep apnea database - TURKAPNE: a national, multicenter, observational, prospective cohort study. *Thorac Res Pract.* 2018;19(3):136-140. [\[Crossref\]](#)
- Sateia MJ. International classification of sleep disorders-third edition: highlights and modifications. *Chest.* 2014;146(5):1387-1394. [\[Crossref\]](#)
- Eikermann M, Jordan AS, Chamberlin NL, et al. The influence of aging on pharyngeal collapsibility during sleep. *Chest.* 2007;131(6):1702-1709. [\[Crossref\]](#)
- Schwab RJ, Gupta KB, Gefter WB, Metzger LJ, Hoffman EA, Pack AI. Upper airway and soft tissue anatomy in normal subjects and patients with sleep-disordered breathing. Significance of the lateral pharyngeal walls. *Am J Respir Crit Care Med.* 1995;152(5 Pt 1):1673-1689. [\[Crossref\]](#)
- Malhotra A, White DP. Obstructive sleep apnoea. *Lancet.* 2002;360(9328):237-245. [\[Crossref\]](#)
- Edwards BA, Wellman A, Sands SA, et al. Obstructive sleep apnea in older adults is a distinctly different physiological phenotype. *Sleep.* 2014;37(7):1227-1236. [\[Crossref\]](#)
- Shahveisi K, Jalali A, Moloudi MR, Moradi S, Maroufi A, Khazaie H. Sleep architecture in patients with primary snoring and obstructive sleep apnea. *Basic Clin Neurosci.* 2018;9(2):147-156. [\[Crossref\]](#)
- Berry RB, Gleeson K. Respiratory arousal from sleep: mechanisms and significance. *Sleep.* 1997;20(8):654-675. [\[Crossref\]](#)
- Kainulainen S, Töyräs J, Oksenberg A, et al. Severity of desaturations reflects OSA-related daytime sleepiness better than AHI. *J Clin Sleep Med.* 2019;15(8):1135-1142. [\[Crossref\]](#)
- Lal C, Weaver TE, Bae CJ, Strohl KP. Excessive daytime sleepiness in obstructive sleep apnea. Mechanisms and clinical management. *Ann Am Thorac Soc.* 2021;18(5):757-768. [\[Crossref\]](#)
- Kapur VK, Auckley DH, Chowdhuri S, et al. Clinical practice guideline for diagnostic testing for adult obstructive sleep apnea: an American Academy of Sleep Medicine Clinical Practice Guideline. *J Clin Sleep Med.* 2017;13(3):479-504. [\[Crossref\]](#)
- Marin JM, Soriano JB, Carrizo SJ, Boldova A, Celli BR. Outcomes in patients with chronic obstructive pulmonary disease and obstructive sleep apnea: the overlap syndrome. *Am J Respir Crit Care Med.* 2010;182(3):325-331. [\[Crossref\]](#)
- Harris M, Glozier N, Ratnavadivel R, Grunstein RR. Obstructive sleep apnea and depression. *Sleep Med Rev.* 2009;13(6):437-444. [\[Crossref\]](#)
- André S, Andreozzi F, Van Overstraeten C, et al. Cardiometabolic comorbidities in obstructive sleep apnea patients are related to disease severity, nocturnal hypoxemia, and decreased sleep quality. *Respir Res.* 2020;21(1):35. [\[Crossref\]](#)
- Pinto JA, Ribeiro DK, Cavallini AF, Duarte C, Freitas GS. Comorbidities associated with obstructive sleep apnea: a retrospective study. *Int Arch Otorhinolaryngol.* 2016;20(2):145-150. [\[Crossref\]](#)

Review

The Impact of the Exposome on Epithelial Barriers: New Approach Methodologies for Translational Research

 Pelin Saglam-Metiner^{1,3},  Ebru Calkan-Yildirim^{1,4},  Basar Dogan^{1,2},  R. Dilara Vaizoglu¹,  Cigdem Elif Celik¹,  Ozlem Goksel^{1,5},  Ozlem Yesil-Celiktas^{1,2,6},  Levent Pelit^{1,4},  Yasin Kaymaz^{1,2},  Henrik Kløverpris⁷⁻⁹,  Douglas S. Kwon¹⁰,  Carla F. Kim^{11,12},  Petros Koutrakis¹³,  Cezmi Akdis¹⁴,  Omer H. Yilmaz¹⁵,  Tuncay Goksel^{1,5}

¹Translational Pulmonary Research Center (EgeSAM), Ege University Faculty of Medicine, İzmir, Türkiye

²Department of Bioengineering, Ege University Faculty of Engineering, İzmir, Türkiye

³İzmir Biomedicine and Genome Center (IBG), İzmir, Türkiye

⁴Department of Chemistry, Ege University Faculty of Science, İzmir, Türkiye

⁵Department of Pulmonary Medicine, Ege University Faculty of Medicine, İzmir, Türkiye

⁶ODTÜ MEMS Center, Ankara, Türkiye

⁷Department of Immunology and Microbiology, University of Copenhagen, Copenhagen, Denmark

⁸Africa Health Research Institute, Durban, South Africa

⁹School of Laboratory Medicine and Medical Sciences, University of KwaZulu-Natal, College of Health Sciences, Durban, South Africa

¹⁰Ragon Institute of Mass General Brigham, Massachusetts Institute of Technology and Harvard, Cambridge, MA, USA

¹¹Stem Cell Program, Division of Hematology, Oncology and Pulmonary, Respiratory Diseases, Department of Pediatrics, Boston Children's Hospital, Massachusetts, USA

¹²Department of Genetics, Harvard Medical School, Massachusetts, USA

¹³Department of Environmental Health, Harvard T.H. Chan School of Public Health, Boston, MA, USA

¹⁴Swiss Institute of Allergy and Asthma Research (SIAF), University of Zurich, Davos, Switzerland

¹⁵Department of Biology, The David H. Koch Institute for Integrative Cancer Research, Massachusetts Institute of Technology, Cambridge, MA, USA

Cite this article as: Saglam-Metiner P, Calkan-Yildirim E, Dogan B, et al. The impact of the exposome on epithelial barriers: new approach methodologies for translational research. *Thorac Res Pract.* 2026;27(3):182-194

ABSTRACT

Environmental exposures experienced throughout life, collectively referred to as the exposome, play a fundamental role in shaping epithelial barrier integrity, repair capacity, and vulnerability to disease. These exposures encompass a broad spectrum of chemical, physical, biological, and lifestyle-related factors. Despite growing recognition of their importance, a key unresolved challenge is understanding how single exposures and, more importantly, complex real-world exposure mixtures jointly disrupt epithelial organization, stem and progenitor cell niches, and immune-epithelial communication across different organs. This review consolidates current evidence on environmentally relevant exposomes that directly affect epithelial barrier function and examines their consequences for tissue architecture, niche stability, and frontline defense mechanisms. We further discuss recent advances in new approach methodologies, including organ-specific epithelial barrier models, organoids, organ-on-a-chips, and interconnected multi-organ platforms. By synthesizing evidence across organ systems, we highlight convergent biological processes, such as oxidative stress, inflammatory signaling, disruption of intercellular junctions, and impaired epithelial survival or regeneration, as shared pathways linking environmental stressors to barrier failure. We hope that this review will help bridge exposure science, epithelial biology, and bioengineered human-based models to define critical knowledge gaps and key translational priorities for the field.

KEYWORDS: Epithelial barrier, environmental exposome, NAMs, organ-axis models

Received: 19.01.2026

Revision Requested: 02.03.2026

Last Revision Received: 14.03.2026

Accepted: 26.03.2026

Epub: 14.04.2026

Publication Date: 12.05.2026

Corresponding author: Tuncay Goksel, MD, e-mail: tuncaygoksel@gmail.com

INTRODUCTION

Epithelial barrier integrity has emerged as a fundamental determinant of immune homeostasis and disease susceptibility; the epithelial barrier hypothesis proposes that progressive disruption of barrier integrity by environmental stressors drives chronic inflammation and disease.¹ The human body is in continuous interaction with a wide range of environmental stimuli from the earliest stages of life until death. This complex and dynamic network of interactions is captured by the concept of the exposome, which encompasses all environmental exposures experienced across the lifespan and provides a critical framework for understanding the origins of human disease and for identifying potential therapeutic strategies.² According to the European Academy of Allergy and Clinical Immunology guidelines, the exposome—which integrates indoor and outdoor factors, such as air, water, and soil pollution, wildfires, dust storms, nutrition, pathogens, and radiation, with internal biological processes including metabolism, inflammation, DNA damage responses, and oxidative stress—fundamentally shapes the trajectory of health and disease.³⁻⁶

The principal epithelial tissues of the human body include those that line the respiratory tract, the gastrointestinal system, and the skin. Beyond their structural roles, epithelial barriers regulate molecular transport, activate immune responses, and help maintain microbial tolerance, thereby coordinating frontline defense mechanisms against environmental challenges.⁷⁻⁹ According to the epithelial barrier hypothesis, increasing environmental pressures associated with climate change and extreme atmospheric conditions have intensified exposure to a broad spectrum of agents that compromise barrier integrity. These include airborne pollutants, particulate matter (PM), volatile organic compounds (VOCs), ozone, household chemicals, micro- and nanoplastics (MNPs), aeroallergens, bioaerosols, pollen, diesel exhaust emissions, and dietary components such as food emulsifiers that directly damage epithelial barriers.¹⁰⁻¹² Such exposures rarely occur in isolation; rather, they manifest as complex mixtures that collectively disrupt the tightly regulated architecture of epithelial tissues across multiple organ systems. The emergence of an increasingly aggressive and difficult-to-control exposome is largely driven by rapid technological advancement and modern lifestyle factors, including the widespread consumption of ultra-processed foods and the routine use of chemically complex

household cleaning and cosmetic products. In parallel, the exponential growth of electronic waste and its largely informal recycling have introduced a poorly regulated and inequitable source of environmental exposure at the global level.¹³ Notably, this complex exposome landscape coincides with a marked global rise in chronic non-communicable diseases, including obesity, cardiovascular disorders, cancer, respiratory diseases such as asthma, autoimmune conditions, mental health issues, and neurodegenerative disorders, including Alzheimer's disease, as well as preterm birth in infants.^{3,14-16} Accumulating epidemiological and experimental evidence links this trend to cumulative exposure (exposome) and its long-term effects on epithelial barrier integrity and immune regulation. Addressing the complexity of exposome-driven epithelial dysfunction requires experimental systems that extend beyond reductionist approaches. In this context, *in vitro* organotropic and microphysiological models have emerged as indispensable tools for mechanistic and translational research. New approach methodologies (NAMs), including organoids and organ-on-a-chip (OoC) platforms, enable reconstruction of three-dimensional (3D) *in vivo*-like architecture and modeling of functional epithelial barriers under biologically relevant exposure conditions.^{17,18} Importantly, this technological shift is being reinforced by evolving regulatory frameworks; recent U.S. Food and Drug Administration (FDA) initiatives, including the FDA Modernization Act reforms and subsequent NAMs-oriented guidance, which were further expanded by updates such as Act 3.0, approved in early 2026 are accelerating the adoption of human-relevant experimental systems by encouraging the integration of artificial intelligence, organoid-based assays, and microphysiological platforms.¹⁹

In this review, we provide a comprehensive overview of environmental exposomes related to epithelial function and the physiological roles of epithelial barriers examine how *in vitro* microphysiological tools are used to interrogate the complexity of the exposome-driven interactome. We then survey the established and emerging molecular mechanisms underlying epithelial barrier damage and discuss how these processes influence disease initiation and progression. Building on this framework, we synthesize evidence across organ systems to examine how single exposures and complex, real-world exposure mixtures disrupt epithelial organization, niche stability, and immune-epithelial communication, to highlight convergent pathways linking environmental stressors to barrier dysfunction, and to explore how next-generation NAMs can be used to move the field from descriptive associations toward mechanistic and predictive understanding (Figure 1).

ENVIRONMENTAL EXPOSOMES RELEVANT TO EPITHELIAL FUNCTION

Epithelial tissues constitute the primary interface of the human body with the external environment and are therefore continuously exposed to a wide range of environmental stressors. The concept of the environmental exposome has provided a comprehensive framework to understand how lifelong exposure to chemical, physical, and biological factors influences epithelial barrier integrity, tissue regeneration, and disease susceptibility.²⁰ Rather than acting as passive barriers, epithelial surfaces actively sense environmental cues and

Main Points

- Lifelong environmental exposures collectively shape epithelial barrier integrity, repair capacity, and susceptibility to disease.
- Complex real-world exposome mixtures disrupt epithelial organization, stem cell niches, and immune-epithelial interactions across organs.
- Oxidative stress, inflammation, and junctional dysfunction represent common pathways linking environmental stressors to epithelial barrier failure.
- Human-relevant new approach methodologies, including organoids and organ-on-a-chip platforms, enable mechanistic and translational investigations into exposome-driven epithelial dysfunction.

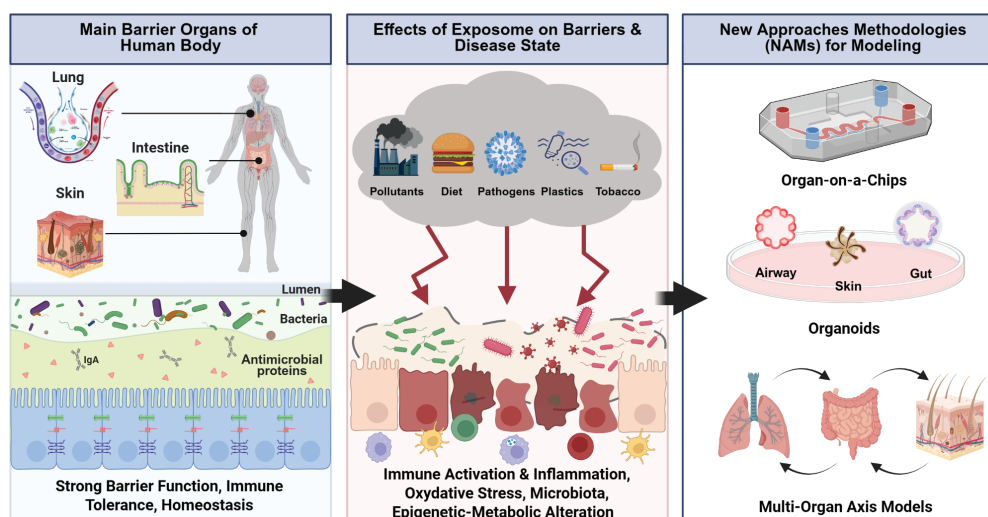


Figure 1. Overview of how environmental exposures compromise healthy epithelial integrity to drive chronic inflammation, and the application of NAMs as OoC and organoids to model these interactions. Created with BioRender.com

NAMs: new approach methodologies, OoC: organ-on-a-chip

translate them into molecular and cellular responses that shape immune activation, metabolic adaptation, and repair processes. The biological consequences of this co-exposure reality are therefore rarely captured by single-agent experimental paradigms, which may substantially underestimate the cumulative and often synergistic impact of the real-world exposome.

Airborne PM is among the most extensively studied exposome components affecting epithelial function. While PM_{2.5} mass concentration has historically served as a regulatory metric, accumulated evidence suggests that epithelial toxicity is driven primarily by particle composition and chemical reactivity rather than by particle mass alone.²¹ Studies have demonstrated that specific PM_{2.5} species and ultrafine particle fractions are associated with distinct metabolomic signatures, reflecting differential biological reactivity linked to metal-rich and organic aerosol components.²² In our previous study, we comparatively evaluated the impact of respirable inorganic <PM_{2.5} silica particles on airway epithelial barrier integrity using a biomimetic airway epithelial barrier-on-chip platform and *ex vivo* human bronchial tissue slices under static and dynamic conditions. Short-term exposure to extremely high concentrations of PM_{2.5} disrupted epithelial permeability, adhesion, junctional markers, and induced robust proinflammatory responses, particularly under dynamic flow, demonstrating the translational relevance of lung-on-chip systems for modeling environmentally realistic particulate exposures.¹² Additionally, Kaya and Yesil-Celiktas,²³ developed a human lung epithelium-on-a-chip platform incorporating a flexible, transparent ionic liquid-based membrane and a mechanically actuated air-liquid interface to recapitulate breathing-associated mechano-stress. PM_{0.5} silica particle exposure under dynamic conditions, in combination with mechanical strain, modulates epithelial viability, cytotoxicity, and proinflammatory signaling, emphasizing the importance of biomechanical cues in exposome-relevant lung toxicity assessment.²³

These findings underscore that epithelial responses to PM exposure depend on source-related physicochemical properties, which modulate oxidative stress pathways, inflammatory signaling, and cellular metabolism.²⁴ Moreover, at the epithelial surface, PM exposure has been shown to disrupt barrier integrity through oxidative stress-dependent mechanisms. Studies have demonstrated that PM induces the generation of reactive oxygen species (ROS), leading to tight junction (TJ) disassembly and increased epithelial permeability, thereby facilitating pathogen invasion and sustained inflammatory responses.^{25,26} Such barrier dysfunction is particularly relevant in airway epithelia, where chronic exposure to ambient particles may impair mucosal defense and predispose to infectious and inflammatory airway diseases.²⁷

In addition, VOCs represent a major component of the exposome, especially in indoor environments. Certain VOCs, such as formaldehyde, directly impair epithelial barrier function by inducing oxidative stress and disrupting TJ protein organization.²⁸ In human airway epithelial models, formaldehyde exposure has been shown to increase ROS production and compromise barrier integrity, highlighting the vulnerability of epithelial tissues to gaseous chemical stressors.²⁹ These effects are often exacerbated in the presence of co-exposures, reinforcing the concept that epithelial injury arises from cumulative and interactive environmental insults. In line with this perspective, exposome-oriented analytical studies have demonstrated that indoor VOC mixtures, including BTEX (benzene, toluene, ethylbenzene, xylenes), can be sensitively detected by advanced monitoring strategies, enabling a more accurate assessment of epithelial exposure burdens.³⁰

Beyond air pollutants, the exposome also encompasses household chemicals, detergents, surfactants, and other daily-use compounds that come into direct contact with epithelial surfaces.³¹ These agents exhibit a high affinity for lipid membranes and TJ complexes, leading to increased epithelial permeability and altered immune signaling. Integrative reviews

led by Celebi Sozener et al.⁷ and Mitamura et al.³² from Akdis group, have synthesized compelling evidence that chronic exposure to such environmental agents drives epithelial barrier breakdown, promotes alarmin release, and facilitates type 2-skewed immune responses. This body of work culminated in the formulation of the “*epithelial barrier hypothesis*”, which proposes that sustained barrier disruption represents a unifying mechanism linking environmental exposures to the rising prevalence of allergic, autoimmune, and chronic inflammatory diseases.¹

Recently, MNPs have emerged as a novel and increasingly relevant class of environmental contaminants with direct implications for epithelial health. Due to their small size and high surface reactivity, these particles can interact intimately with epithelial cells, inducing oxidative stress, apoptosis, and disruption of TJs.³³ Experimental evidence demonstrates that MNPs compromise the intestinal epithelial barrier function through ROS-mediated mechanisms, leading to increased permeability and epithelial cell death.³⁴ Broader reviews suggest that microplastic exposure perturbs epithelial–microbiome interactions and metabolic homeostasis, potentially contributing to chronic inflammatory and systemic disease processes.³⁵

Epithelial surfaces are continuously exposed not only to chemical pollutants but also to pollen, fungal spores, bacterial fragments, viruses, endotoxins, and complex aerosol mixtures formed by their interactions.^{5,36,37} Pollen and fungal spores are recognized as potent biological agents capable of directly modulating epithelial barrier function through their associated proteins, lipids, polysaccharides, and secondary metabolites.³⁷ In particular, it has been reported that pollen- and fungal-derived aerosol fractions interacting with environmental stressors induce distinct alterations in metabolomic profiles, resulting in metabolic reprogramming of epithelial cells and activation of inflammation-related signaling pathways.³⁸ Collectively, these findings underscore that bioaerosols should be considered not only in the context of allergy and infection but also within the broader framework of exposome-driven chronic inflammation, epithelial regeneration, and disease susceptibility.

Collectively, these findings highlight that environmental exposomes relevant to epithelial function exert their effects through shared mechanistic pathways, including oxidative stress, barrier disruption, immune activation, and metabolic remodeling. The biological impact of environmental exposures is shaped not only by exposure intensity but also by chemical composition, co-exposure patterns, and tissue-specific susceptibility. Understanding how diverse exposome components converge on epithelial barriers is therefore essential for elucidating the origins of chronic disease and for developing preventive strategies that reflect the complexity of real-world environmental exposures.

EPITHELIAL BARRIERS AND THEIR PHYSIOLOGICAL ROLES

Epithelial barriers are continuous cellular interfaces that line the skin and mucosal surfaces, including the gastrointestinal, respiratory, and urogenital tracts, where they physically separate host tissues from the external environment while permitting controlled exchange with it.³⁹ Across organs,

epithelial barriers share a conserved architectural framework consisting of polarized epithelial cells interconnected by specialized intercellular junctional complexes that define apical-basolateral organization and paracellular sealing. The junctional apparatus comprises TJs, adherens junctions (AJs), and desmosomes, which together establish epithelial cohesion and mechanical resilience.⁴⁰ TJs are formed by claudins, occludins, and junctional adhesion molecules, which are linked to cytoplasmic scaffolding proteins such as zonula occludens-1 (ZO-1), ZO-2, and ZO-3, creating a selectively permeable seal at the apical border.⁴¹ AJs, built around E-cadherin-catenin complexes, stabilize cell-cell adhesion and support epithelial polarity, while desmosomes reinforce tissue integrity under mechanical stress.⁴²

Barrier architecture is further specialized according to tissue function. In the gastrointestinal tract, a single-layered epithelium is overlaid by a mucus layer rich in gel-forming mucins that spatially segregates luminal contents from epithelial cells.⁴¹ In contrast, the skin barrier relies on a stratified, cornified epithelium in which terminally differentiated keratinocytes form the stratum corneum, a structure essential for preventing transepidermal water loss and chemical penetration.⁴³ These tissue-specific adaptations illustrate that epithelial barrier structure is tightly aligned with physiological demands rather than uniform across organs.⁴⁴

Epithelial barriers are dynamic systems sustained by continuous cell turnover driven by tissue-resident stem cell populations. In the intestine, epithelial renewal is organized along the crypt–villus axis, where intestinal stem cells located at crypt bases generate differentiated lineages, including absorptive enterocytes, goblet cells, enteroendocrine cells, and Paneth cells.⁴⁵ In barrier tissues affected by chronic inflammation, stem cell function and differentiation programs are altered, which are associated with impaired regeneration and barrier fragility. These observations indicate that epithelial stem cell niches contribute to barrier physiology beyond their role in epithelial renewal.^{7,46} A core physiological function of epithelial barriers is the regulation of selective permeability, permitting the exchange of nutrients, ions, and gases while restricting the passage of pathogens, toxins, and allergens.⁴⁷ TJs serve as dynamic regulators of paracellular transport, adjusting permeability in response to physiological cues rather than functioning as static seals. Disruption of junctional organization results in increased epithelial permeability, commonly referred to as barrier leakiness, which facilitates the translocation of microbes and antigens into subepithelial tissues.⁴⁸ Experimental and clinical studies have reported that increased epithelial permeability frequently accompanies and, in some contexts, precedes chronic inflammatory conditions in different tissues, suggesting that barrier dysfunction may contribute to inflammatory pathogenesis.^{49–51} Environmental agents, including detergents, emulsifiers, and airborne pollutants, have been shown experimentally to disrupt TJ integrity, reduce transepithelial electrical resistance, and induce a heterogeneous distribution of junctional proteins in epithelial models.⁵² These findings highlight barrier integrity as a vulnerable and actively regulated physiological property.^{10,36}

Epithelial barriers function as immunologically active tissues that directly participate in host defense. Epithelial cells express pattern recognition receptors that detect microbial products and environmental signals, activating intracellular pathways such as nuclear factor kappa B (NF- κ B), inflammasomes, and autophagy to reinforce barrier defenses.⁵³ Upon barrier perturbation, epithelial cells release alarmins, including thymic stromal lymphopoietin (TSLP), interleukin-25 (IL-25), and IL-33, which initiate coordinated immune responses by activating dendritic cells, innate lymphoid cells, and macrophages.^{54,55} This epithelial-driven signaling links physical barrier disruption to immune activation and tissue remodeling. In the gut, macrophages are key effector cells in epithelial barrier maintenance. Tissue-resident macrophages secrete IL-10 and growth factors such as epidermal growth factor and transforming growth factor-beta, which stabilize TJs and promote epithelial repair following injury. These mechanisms are experimentally supported and contribute to the restoration of barrier integrity during post-inflammatory and post-infectious states.⁴⁴

Epithelial barriers are central regulators of tissue homeostasis through their role in controlling host-microbiota interactions.^{56,57} The mucus layer and epithelial antimicrobial peptides spatially confine commensal microbes and prevent direct contact with the epithelium. Microbial metabolites, including short-chain fatty acids and tryptophan derivatives, modulate epithelial metabolism, TJ expression, and inflammatory tone, reinforcing barrier function under homeostatic conditions.^{58,59} Barrier disruption is associated with microbial dysbiosis and increased transepithelial microbial translocation, which can amplify immune activation and further compromise barrier integrity. Such feed-forward interactions have been described in allergic, autoimmune, and metabolic conditions, emphasizing the broad physiological relevance of epithelial barrier function.⁶⁰ Taken together, epithelial barriers function as integrated systems coordinating structural containment, selective permeability, immune signaling, and metabolic interactions. Beyond passive protection, epithelial barriers contribute to the regulation of stem cell niches, immune responses, and host-microbiota interactions.^{61,62} Together, these observations establish epithelial surfaces not merely as passive physical boundaries, but as metabolically active, immunologically instructive tissues whose integrity is continuously negotiated with the surrounding environment.^{63,64}

MECHANISMS OF EXPOSOME-INDUCED EPITHELIAL BARRIER DISRUPTION

The exposome compromises epithelial barrier integrity through both direct mechanisms of cellular injury and indirect effects on immune responses, microbiota composition, epigenetic regulation, and metabolic processes. Numerous studies have demonstrated that the environmental exposome disrupts epithelial structure and function across various barrier surfaces, including the skin, respiratory tract, and gastrointestinal system.^{16,65} This disruption occurs through complex biological pathways involving oxidative stress, activation of inflammatory signaling, weakening of intercellular junctional complexes, dysbiosis, and epigenetic alterations in epithelial and immune cells.⁶⁶ Taken together, these pathways form an interconnected

biological network in which oxidative and inflammatory signals initiate epithelial injury, while microbial, metabolic, and epigenetic alterations contribute to the maintenance and progression of barrier dysfunction over time.^{43,67,68}

One of the major mechanisms underlying epithelial barrier dysfunction is the destabilization of TJ and AJ complexes, which maintain epithelial cohesion. Experimental studies have demonstrated that pesticide exposure impairs epithelial barrier integrity by disrupting the organization and function of intercellular junctions. Exposure to chlorpyrifos and imidacloprid has been shown to compromise intestinal epithelial barrier properties through alterations in key TJ components, including occludin, claudins, and the adaptor protein ZO-1, resulting in increased paracellular permeability.^{69,70} Similarly, deltamethrin exposure has been reported to modulate epithelial barrier function by altering monolayer integrity and permeability, indicating a functional disturbance of junctional complexes.⁷¹ Surfactants and detergents disrupt epithelial barrier integrity primarily by perturbing membrane lipid protein interactions, thereby promoting degradation and mislocalization of TJ components. Experimental studies employing primary human airway epithelial cultures have demonstrated that household cleaning products, including dishwashing detergents and rinse aids, directly injure epithelial cells and induce pronounced junctional breakdown, characterized by disrupted ZO-1 and occludin continuity, reduced barrier resistance, and increased paracellular permeability at concentrations relevant to daily exposure.⁷²⁻⁷⁴ MNPs further compromise epithelial stability by interacting with the apical membrane and disrupting membrane protein organization, thereby weakening barrier integrity.⁴³ Beyond these surface-level effects, MNPs have been shown to translocate across both airway and intestinal epithelia and, during epithelial passage, trigger oxidative stress and inflammatory signaling, which further amplify junctional disruption and may contribute to systemic exposure.^{20,75}

Air pollutants such as PM_{2.5}, PM₁₀, diesel exhaust particles, and ozone similarly impair epithelial barrier function by activating cytoskeletal contraction pathways, resulting in destabilization of tight and AJ complexes and enhanced epithelial permeability.^{70,76} Long-term environmental monitoring studies have demonstrated that PM concentrations frequently exceed guideline thresholds in urban and industrialized regions, underscoring the relevance of chronic low-dose exposure scenarios.⁷⁷ Recent source-apportionment analyses indicate that PM_{2.5} derived from industrial and traffic emissions is enriched in transition metals such as nickel, vanadium, and zinc, as well as in carbonaceous fractions (elemental and organic carbon), which are strongly associated with oxidative stress-driven epithelial injury and barrier dysfunction.⁷⁸

Another mechanism contributing to epithelial barrier dysfunction is oxidative stress, which has been consistently observed across epithelial models following diverse environmental exposures. Experimental evidence from human epithelial models demonstrates that pesticide exposure induces excessive intracellular ROS generation, leading to mitochondrial dysfunction and activation of intrinsic apoptotic pathways, characterized by increased Bcl-2-associated X protein/B-cell lymphoma 2 ratios and caspase-3/9 activation.⁷⁹

Air pollutants similarly provoke ROS-dependent epithelial injury, resulting in disruption of junctional organization and increased epithelial permeability, thereby linking oxidative stress to functional barrier impairment.⁵⁰ In parallel, oxidative stress-driven mitochondrial dysfunction has been shown to compromise epithelial barrier function by reducing cellular energy availability and weakening barrier integrity, even in the absence of overt junctional protein loss.⁸⁰

Environmental exposures frequently trigger the release of epithelial-derived alarmins, including IL-33, IL-25, and TSLP, which initiate potent type 2 inflammatory responses at barrier surfaces. Experimental studies in human epithelial models have demonstrated that the release of epithelial alarmins is closely associated with impaired barrier integrity, characterized by disrupted TJ organization and increased epithelial permeability.^{64,81} These alarmins activate dendritic cells, T helper 2 cells, and group 2 innate lymphoid cells, leading to increased production of IL-4, IL-5, and IL-13 cytokines, which further destabilize TJs and promote mucus hypersecretion, thereby deepening barrier dysfunction.⁸²⁻⁸⁵ Sublethal epithelial damage has been shown to promote the release of nuclear alarmins such as high-mobility group box 1 (HMGB1), which functions as a central danger-associated molecular pattern amplifying inflammatory signaling following epithelial stress. HMGB1-mediated damage-associated molecular pattern signaling has been implicated in sustaining epithelial-immune crosstalk and perpetuating inflammatory feedback loops, thereby linking epithelial injury to chronic, type 2-skewed inflammation and progressive weakening of barrier function across tissues.^{43,84-87} Climate change-related increases in pollen burden further compromise epithelial defense mechanisms. Elevated pollen exposure suppresses type III interferon lambda production, an essential antiviral mechanism, thereby increasing susceptibility to virus-induced epithelial injury and potentially augmenting alarmin release during allergen encounter.⁶⁵ Processed foods increase exposomal pressure. Emulsifiers such as polysorbate-20 and polysorbate-80 weaken epithelial cohesion, increase paracellular leakiness, and induce inflammatory responses within the gut.^{88,89} In addition, advanced glycation end products generated during high-temperature processing of ultra-processed foods activate epithelial danger-signaling pathways, disrupt TJ integrity, and increase susceptibility to allergic sensitization.⁴⁶

Alterations in gut microbiota represent an additional consequence of exposome exposure. Pesticides, including imidacloprid and chlorpyrifos, alter the microbial composition by reducing beneficial *Lactobacillus* spp. and promoting the expansion of *Escherichia coli* pathobionts. These compositional changes are associated with reduced production of short-chain fatty acids, which are essential metabolites for epithelial energy balance and immune regulation, and may impair Aryl hydrocarbon receptor-dependent signaling pathways involved in mucosal homeostasis. Barrier disruption facilitates the translocation of microbial products, such as lipopolysaccharide, which has been associated with enhanced NF- κ B-mediated inflammatory signaling in epithelial and immune cells.^{50,66,90} Beyond these compositional alterations, the gut microbiota actively regulate epithelial barrier permeability by continuously modulating TJ architecture. Interactions between commensal

bacteria, their metabolites, and epithelial cells influence the expression, localization, and assembly of junctional proteins, including claudins, occludin, and ZO-1, thereby dynamically controlling paracellular permeability. Dysbiosis-associated depletion of short-chain fatty-acid-producing bacteria compromises epithelial energy metabolism and TJ reassembly, resulting in increased epithelial permeability and a heightened susceptibility to inflammatory stress.⁹¹ Importantly, epithelial barrier breach enables sustained activation of innate microbial sensing pathways, including Toll-like receptor-myeloid differentiation factor 88 (MyD88) signaling, establishing a feed-forward epithelial-immune-microbiota loop that stabilizes chronic inflammation and reinforces long-term barrier dysfunction, as demonstrated in mucosal tissues.⁶⁸

Exposome-associated epigenetic and metabolic alterations further compromise epithelial integrity. Environmental toxicants induce DNA methylation changes, histone modifications, and chromatin remodeling that affect epithelial differentiation, barrier formation, and immune gene regulation.⁹² Metabolic dysfunction in immune cells has also been implicated in secondary epithelial stress and injury. In individuals living with human immunodeficiency virus, reduced peroxisome proliferator-activated receptor gamma expression in colon-resident cytotoxic T lymphocytes (CD8+ T-cells) impairs fatty acid oxidation and mitochondrial function, increasing their uptake of epithelial lipids and amplifying epithelial stress responses and apoptotic susceptibility.⁶⁷ Notably, single-cell transcriptomic and integrative bioinformatics analyses provide critical insights into how exposome-related stressors shape cellular heterogeneity, immune crosstalk, and tissue regeneration. High-resolution omics approaches reveal that chronic microenvironmental cues induce stable, disease-associated transcriptional programs in immune cells, particularly macrophage subsets characterized by enhanced lipid metabolism, responses to hypoxia, and immunoregulatory signatures. The persistence and expansion of these transcriptional states reflect long-term metabolic and transcriptional remodeling within stressed tissues, which may indirectly compromise epithelial barrier integrity and repair by sustaining inflammatory and metabolic pressure on epithelial cells, thereby contributing to disease-associated tissue remodeling.^{93,94}

Collectively, these findings demonstrate that the exposome reshapes oxidative, inflammatory, microbial, epigenetic, and metabolic pathways within epithelial and immune cells, establishing a persistent and multifactorial mechanism that undermines epithelial barrier integrity across organ systems.

ORGAN-SPECIFIC EPITHELIAL BARRIER MODELS: NAMS AND ORGAN-AXIS APPROACHES

Traditional *in vitro* cell culture and *in vivo* animal models have significant limitations in recapitulating human epithelial barrier function, multi-organ communication, and long-term responses to environmental exposures.^{95,96} These limitations have driven the adoption of NAMS as the methodological backbone of modern exposome research, offering human-relevant platforms that bridge reductionist cell culture and ethically constrained animal experimentation^{17,73,97,98} These systems may integrate

cutting-edge bioengineering tools: microfluidics, genetically engineered cell sources, biomaterials, and tissue-specific architecture, enabling the study of epithelial barriers under conditions that closely mimic *in vivo* physiology.⁹⁹⁻¹⁰²

OoC platforms represent advanced micro-bioengineering technologies that enable high-quality *in vitro* modeling of human organ functions by recapitulating the mechanical and chemical microenvironment through microfluidic and tissue engineering approaches. These systems offer considerable potential for evaluating disease mechanisms, predicting drug efficacy and toxicity, and capturing patient-specific responses. However, they still face several challenges related to scalability, standardization, reproducibility, real-time measurement, and regulatory acceptance, which are currently being addressed through bioengineering-based strategies.^{100,103,104} OoC platforms, such as lung-on-a-chip, skin-on-a-chip, gut-on-a-chip, and blood-brain barrier-on-a-chip, recreate key structural and functional features of real tissues using one or more cell types from a specific tissue, including spatio-temporal structure, TJ formation, cellular polarity, mechanical stretch, and vascularization.^{12,97,101,102,105-108} OoC platforms have also been developed for the retina, liver, kidney, placenta, and other organs, providing tools to investigate organ-specific responses to environmental stressors. These models are particularly valuable for exposome research because they allow controlled studies of the effects of chemical, physical, and biological exposures on barrier integrity and function.^{98,109,110}

In recent years, organoids, self-organizing “stem cell-derived miniature tissues”, which function as 3D *in vitro* culture systems derived from tissue stem cells, progenitor cells, or induced pluripotent stem cells (iPSCs), have enabled studies that reflect human genetic variation and person-to-person differences, and have become essential tools for remodeling human organ physiology, epithelial barriers, regeneration, and disease processes.^{95,111,112} Organoid-based systems can recapitulate the cellular diversity, architecture, and many functional aspects of native tissues reproduce the histopathology, molecular profiles, and responses to therapies of their primary counterparts, and offer substantial advantages over traditional 2D immortalized cell culture and patient-derived xenograft mouse models.^{112,113} In addition to existing organoid models for all organ systems, recent advances in lung, intestinal, brain, and liver organoid models underscore the increasing importance of 3D human-relevant systems for studying tissue homeostasis, regeneration, and disease. Lung parenchymal tissue or bronchoalveolar lavage fluid-derived airway and alveolar organoids enable detailed interrogation of epithelial progenitor states, lineage plasticity, and early oncogenic events,^{112,114} while intestinal organoids provide mechanistic insights into stem cell metabolism, niche signaling, and diet-driven tumorigenesis.^{111,115,116} In parallel, unguided, guided, and assembled brain organoids recapitulate key features of human neurodevelopment, including enriched cellular diversity, functional neuronal networks, and progressive tissue maturation¹¹⁷⁻¹¹⁹ and liver organoids faithfully model hepatic heterogeneity, multi-zonal architecture, and disease-specific molecular traits with high translational relevance.^{120,121}

While organoids alone offer great promise, their capabilities are further enhanced when combined with OoC technologies, resulting in systems termed “organoid-on-chip” (OrgoC)

that provide controllable microphysiological environments for mechanistic toxicology, including the assessment of environmental exposures and exposome effects on human tissues.^{73,122} OrgoC approaches further enhance physiological relevance by combining the multicellular complexity of organoids with the dynamic control of microfluidic systems. These platforms aim to emulate not only the cellular and architectural complexity of tissues but also the dynamic microenvironment: flow, shear stress, oxygen/nutrient gradients, vascularization, and multi-compartment barrier interfaces.¹⁰¹

Multi-organ or organ-axis platforms enable investigation of organ-to-organ communication, systemic metabolite exchange, and the effects of barrier impairment. Recent studies demonstrate that these models can capture complex scenarios, including environmental pollutant-induced organ barrier disruption and consequent neuroinflammatory responses.^{96,108,123} Among these systems, the brain-lung-liver-intestine axis constitutes a critical multi-organ network orchestrating systemic responses to environmental and chemical insults.¹²⁴ Inhaled pollutants can trigger inflammatory and oxidative signaling within the lung epithelium, with mediators subsequently disseminated via the circulation to distal organs such as the liver and brain, thereby eliciting secondary organ-specific effects.^{125,126} Likewise, orally ingested MNPs or pharmaceutical compounds undergo intestinal absorption and hepatic biotransformation, processes that may generate bioactive metabolites capable of crossing physiological barriers and influencing central nervous system function.¹²⁷ Critically, single-organ models are inherently unable to capture what happens downstream of an initial exposure event; when the lung epithelium responds to an inhaled pollutant, the resulting inflammatory mediators enter the systemic circulation and may elicit secondary responses in distal organs such as the liver, gut, or brain, producing effects that a lung model alone will miss entirely.^{128,129} Multi-organ axis platforms allow observation of these propagated cross-organ consequences within a single connected human-relevant system, revealing systemic vulnerabilities that single-organ models cannot structurally detect.¹³⁰

Despite the recognized importance of mixture-based exposures, most NAM studies to date have employed single-agent or binary exposure designs, which inadequately reflect the complexity of real-world environmental conditions.^{131,132} Translating this complexity into experimental NAM platforms is methodologically feasible. For example, differentiated primary human nasal epithelial cells cultured at ALI have been used to model multi-allergen exposures, including birch, timothy grass, and ragweed pollen, delivered as aqueous extracts, suspensions, or particle aerosols, using dedicated aerosolization systems.¹³³ Similarly, ALI-based epithelial models have enabled the study of complex environmental co-exposures such as fungal spores combined with grass pollen allergens, demonstrating how epithelial barrier responses can be interrogated under environmentally relevant multi-agent exposure conditions.¹³⁴ Beyond aeroallergens, co-exposure protocols combining PM with VOCs, dietary contaminants, or microbial components can be implemented within existing organoid and OoC platforms to generate ecologically relevant exposure scenarios; emerging evidence already demonstrates that exposures to mixtures elicit biological responses qualitatively distinct from those produced

by individual agents alone.¹³⁵ Considerations of dose realism and temporal dynamics are equally critical, as acute high-dose designs capture fundamentally different biology than the chronic, low-level, and sequential exposure patterns that define human environmental experience. Key unresolved challenges include the lack of standardized mixture protocols across platforms, the difficulty of attributing specific biological effects to individual constituents within a mixture, and the poorly understood role of synergistic and antagonistic pollutant interactions at epithelial surfaces.¹³⁰ Addressing these challenges through the integration of multi-omics profiling and computational toxicology with NAM-based mixture experiments represents a tractable path forward, the translational implications of which are discussed further in Section 6.¹¹⁰

The choice of NAM platform should be guided by the experimental question at hand. Organoids are best suited to questions concerning stem cell dynamics, progenitor niche regulation, or long-term differentiation trajectories, where the system's self-organizing capacity is a key advantage.^{136,137} OoC platforms, by contrast, are preferred when the design requires real-time barrier monitoring, fluid shear stress, cyclic mechanical stretch, or gas-liquid interfacing conditions that static cultures cannot replicate.^{138,139} Multi-organ axis systems become necessary when the scientific question demands cross-organ communication, for instance, when investigating whether a pollutant absorbed in the lung epithelium triggers secondary neuroinflammatory or hepatic responses via the circulation.^{140,141} OrgoC platforms, next-generation human organ avatars, can potentially reflect the complex, detailed human-relevant organ structures and immune cell circulation within fluid flow.¹⁴² Despite these advances in NAMs, reproducing the full cellular diversity across laboratories, long-term culture stability, immune cell interactions, scalability, and organ-to-organ connections remains technically demanding.^{18,143} Standardization of design across platforms, media formulations, biological validation, regulatory qualification, and read-out metrics is still limited, particularly in multi-organ systems.¹⁴⁴ Together, these gaps define the methodological frontier of the field. Nevertheless, human iPSC-derived NAMs and NAMs based on CRISPR/Cas9 gene-editing technology offer the potential to incorporate genetic variability, thereby supporting personalized toxicology and disease modeling.^{19,145}

Organ-specific OoC, OrgoC, barrier-on-chip, multi-organ-on-a-chip, and body-on-chip platforms provide physiologically relevant, human-based models to study the effects of the exposome on epithelial integrity, regeneration, and disease. They bridge the gap between traditional *in vitro* and *in vivo* approaches, enabling mechanistic insights into both local barrier disruption and systemic organ-axis interactions. Cutting-edge development and validation of these models will be critical to fully realize their potential in environmental health and translational research.

CONCLUSION AND FUTURE PERSPECTIVES

Environmental exposomes function as complex and interacting mixtures that converge on shared oxidative, inflammatory, metabolic, microbial, and epigenetic pathways, ultimately

affecting epithelial integrity, regenerative capacity, and disease susceptibility across multi-organ systems. This perspective reframes epithelial barriers as dynamic environmental sensors and integrators that actively determine tissue resilience and systemic vulnerability. Despite increasing recognition of exposome complexity, much of the existing literature remains constrained by single-agent or short-term exposure models that poorly reflect real-world conditions. Addressing this gap will require a decisive shift toward studying multicomponent, low-dose, and temporally dynamic exposure mixtures, including chemical pollutants, bioaerosols, dietary contaminants, and microbiome-modulating agents in combination rather than in isolation. In this context, next-generation NAMs, particularly organoids, OoC, OrgoC, and multi-organ axis platforms, offer powerful opportunities to model human-relevant exposure scenarios. By integrating epithelial barriers with immune, vascular, and stromal compartments, these systems enable mechanistic interrogation of exposure-driven crosstalk across interconnected organ axes. However, further methodological advances are needed to standardize chronic and sequential exposure paradigms and to capture cumulative and non-linear effects.

Future progress will also depend on the ability to trace exposome components and their transformation products across epithelial barriers into systemic compartments, primarily in the lung-gut-skin organ-axis models. The integration of traceable exposure strategies with high-content imaging, labelling strategies, multi-omics, and computational modeling will be critical for linking exposure dose, barrier penetration, intracellular fate, and functional outcomes. Ultimately, the convergence of exposome science with advanced NAMs holds significant promise for moving beyond associative findings toward causal, predictive, and translational insights that can inform environmental risk assessment, regulatory frameworks, and personalized prevention strategies.

Footnotes

Authorship Contributions

Concept: P.S.M., T.G., Design: P.S.M., B.D., Literature Search: All authors, Writing: All authors.

Conflict of Interest: Tuncay Goksel, MD, serves as Editor for Thoracic Research and Practice. He had no involvement in the peer review of this article and had no access to information regarding its peer review. The other authors have no disclosures.

Financial Disclosure: This scientific collaboration was supported by the Scientific and Technological Research Council of Türkiye (TUBITAK), Science Fellowships and Grant Programs (BIDEB) 2223-B Domestic Scientific Event Organization Support Program, and also, in particular, by the Presidency of the Republic of Türkiye Strategy and Budget Department (2019K12-149080), and MIT Global - MISTI (MIT International Science and Technology Initiatives) Project-Seed Fund. The first author, P.S.M., also gratefully acknowledges the TUBITAK-BIDEB 2218 National Postdoctoral Research Scholarship Project (123C325).

REFERENCES

- Akdis CA. Does the epithelial barrier hypothesis explain the increase in allergy, autoimmunity and other chronic conditions? *Nat Rev Immunol.* 2021;21(11):739-751. [\[Crossref\]](#)
- Zare Jeddi M, Galea KS, Ashley-Martin J, et al. Guidance on minimum information requirements (MIR) from designing to reporting human biomonitoring (HBM). *Environ Int.* 2025;202:109601. [\[Crossref\]](#)
- Akdis CA, Nadeau KC. Human and planetary health on fire. *Nat Rev Immunol.* 2022;22(11):651-652. [\[Crossref\]](#)
- Agache I, Annesi-Maesano I, Cecchi L, et al. EAACI guidelines on environmental science for allergy and asthma: the impact of short-term exposure to outdoor air pollutants on asthma-related outcomes and recommendations for mitigation measures. *Allergy.* 2024;79(7):1656-1686. [\[Crossref\]](#)
- Agache I, Annesi-Maesano I, Cecchi L, et al. EAACI Guidelines on environmental science for allergy and asthma-recommendations on the impact of indoor air pollutants on the risk of new-onset asthma and on asthma-related outcomes. *Allergy.* 2025;80(3):651-676. [\[Crossref\]](#)
- Sarigiannis D, Karakitsios S, Anesti O, et al. Advancing translational exposomics: bridging genome, exposome and personalized medicine. *Hum Genomics.* 2025;19(1):48. [\[Crossref\]](#)
- Celebi Sozener Z, Ozdel Ozturk B, Cerci P, et al. Epithelial barrier hypothesis: effect of the external exposome on the microbiome and epithelial barriers in allergic disease. *Allergy.* 2022;77(5):1418-1449. [\[Crossref\]](#)
- Meng J, Xiao H, Xu F, She X, Liu C, Canonica GW. Systemic barrier dysfunction in type 2 inflammation diseases: perspective in the skin, airways, and gastrointestinal tract. *Immunol Res.* 2025;73(1):60. [\[Crossref\]](#)
- Kouthouridis S, Saha P, Ludlow M, Truong BYN, Zhang B. Late-stage placental barrier model for transport studies of prescription drugs during pregnancy. *Lab Chip.* 2025;25(13):3168-3184. [\[Crossref\]](#)
- Yazici D, Pat Y, Mitamura Y, Akdis CA, Ogulur I. Detergent-induced eosinophilic inflammation in the esophagus: a key evidence for the epithelial barrier theory. *Allergy.* 2023;78(6):1422-1424. [\[Crossref\]](#)
- Vermeulen R, Schymanski EL, Barabási AL, Miller GW. The exposome and health: where chemistry meets biology. *Science.* 2020;367(6476):392-396. [\[Crossref\]](#)
- Goksel O, Sipahi MI, Yanasik S, et al. Comprehensive analysis of resilience of human airway epithelial barrier against short-term PM2.5 inorganic dust exposure using *in vitro* microfluidic chip and *ex vivo* human airway models. *Allergy.* 2024;79(11):2953-2965. [\[Crossref\]](#)
- Ádám B, Göen T, Scheepers PTJ, et al. From inequitable to sustainable e-waste processing for reduction of impact on human health and the environment. *Environ Res.* 2021;194:110728. [\[Crossref\]](#)
- Maitre L, Bustamante M, Hernández-Ferrer C, et al. Multi-omics signatures of the human early life exposome. *Nat Commun.* 2022;13(1):7024. [\[Crossref\]](#)
- Pero-Gascon R, Hemeryck LY, Poma G, et al. FLEXiGUT: rationale for exposomics associations with chronic low-grade gut inflammation. *Environ Int.* 2022;158:106906. [\[Crossref\]](#)
- Park HH, Armstrong MJ, Gorin FA, Lein PJ. Air pollution as an environmental risk factor for alzheimer's disease and related dementias. *Med Res Arch.* 2024;12(10):5825. [\[Crossref\]](#)
- Atalay-Sahar E, Yildiz-Ozturk E, Ozgur S, et al. Novel approach methodologies in modeling complex bioaerosol exposure in asthma and allergic rhinitis under climate change. *Expert Rev Mol Med.* 2025;27:e13. [\[Crossref\]](#)
- Zhang X, Liu H, Cheng H, et al. *In vitro* biomimetic models for respiratory diseases: progress in lung organoids and lung-on-a-chip. *Stem Cell Res Ther.* 2025;16(1):415. [\[Crossref\]](#)
- Patra D, Sayed IM, Mukherjee S, et al. Integrating human intestinal organoids into FDA's new approach methodologies for drug discovery. *Adv Sci (Weinh).* 2026:e22276. [\[Crossref\]](#)
- Losol P, Sokolowska M, Hwang YK, et al. Epithelial barrier theory: the role of exposome, microbiome, and barrier function in allergic diseases. *Allergy Asthma Immunol Res.* 2023;15(6):705-724. [\[Crossref\]](#)
- Kelly FJ, Fussell JC. Size, source and chemical composition as determinants of toxicity attributable to ambient particulate matter. *Atmos Environ.* 2012;60:504-526. [\[Crossref\]](#)
- Nassan FL, Wang C, Kelly RS, et al. Ambient PM_{2.5} species and ultrafine particle exposure and their differential metabolomic signatures. *Environ Int.* 2021;151:106447. [\[Crossref\]](#)
- Kaya B, Yesil-Celiktas O. Ionic liquid-based transparent membrane-coupled human lung epithelium-on-a-chip demonstrating PM0.5 pollution effect under breathing mechanostress. *Bio-Design Manuf.* 2024;7(5):624-636. [\[Crossref\]](#)
- Engels SM, Kamat P, Pafilis GS, et al. Particulate matter composition drives differential molecular and morphological responses in lung epithelial cells. *PNAS Nexus.* 2023;3(1):pgad415. [\[Crossref\]](#)
- Hong Z, Guo Z, Zhang R, et al. Airborne fine particulate matter induces oxidative stress and inflammation in human nasal epithelial cells. *Tohoku J Exp Med.* 2016;239(2):117-125. [\[Crossref\]](#)
- Liu J, Chen X, Dou M, et al. Particulate matter disrupts airway epithelial barrier via oxidative stress to promote *Pseudomonas aeruginosa* infection. *J Thorac Dis.* 2019;11(6):2617-2627. [\[Crossref\]](#)
- Xian M, Ma S, Wang K, et al. Particulate matter 2.5 causes deficiency in barrier integrity in human nasal epithelial cells. *Allergy Asthma Immunol Res.* 2020;12(1):56-71. [\[Crossref\]](#)
- Albano GD, Montalbano AM, Gagliardo R, Anzalone G, Profita M. Impact of air pollution in airway diseases: role of the epithelial cells (cell models and biomarkers). *Int J Mol Sci.* 2022;23(5):2799. [\[Crossref\]](#)
- Wolkoff P. Indoor air humidity, air quality, and health - an overview. *Int J Hyg Environ Health.* 2018;221(3):376-390. [\[Crossref\]](#)
- Bolat S, Demir S, Ezer H, et al. MOF-801 based solid phase microextraction fiber for the monitoring of indoor BTEX pollution. *J Hazard Mater.* 2024;466:133607. [\[Crossref\]](#)
- Rinaldi AO, Li M, Barletta E, et al. Household laundry detergents disrupt barrier integrity and induce inflammation in mouse and human skin. *Allergy.* 2024;79(1):128-141. [\[Crossref\]](#)
- Mitamura Y, Ogulur I, Pat Y, et al. Dysregulation of the epithelial barrier by environmental and other exogenous factors. *Contact Dermatitis.* 2021;85(6):615-626. [\[Crossref\]](#)
- Li L, Lv X, He J, et al. Chronic exposure to polystyrene nanoplastics induces intestinal mechanical and immune barrier dysfunction in mice. *Ecotoxicol Environ Saf.* 2024;269:115749. [\[Crossref\]](#)
- Liang B, Zhong Y, Huang Y, et al. Underestimated health risks: polystyrene micro- and nanoplastics jointly induce intestinal barrier dysfunction by ROS-mediated epithelial cell apoptosis. *Part Fibre Toxicol.* 2021;18(1):20. [\[Crossref\]](#)
- Bora SS, Gogoi R, Sharma MR, et al. Microplastics and human health: unveiling the gut microbiome disruption and chronic disease risks. *Front Cell Infect Microbiol.* 2024;14:1492759. [\[Crossref\]](#)

36. Damialis A, Gilles S, Sofiev M, et al. Higher airborne pollen concentrations correlated with increased SARS-CoV-2 infection rates, as evidenced from 31 countries across the globe. *Proc Natl Acad Sci U S A*. 2021;118(12):e2019034118. [\[Crossref\]](#)
37. Humbal C, Gautam S, Trivedi U. A review on recent progress in observations, and health effects of bioaerosols. *Environ Int*. 2018;118:189-193. [\[Crossref\]](#)
38. Zaidman NA, O'Grady KE, Patil N, et al. Airway epithelial anion secretion and barrier function following exposure to fungal aeroallergens: role of oxidative stress. *Am J Physiol Cell Physiol*. 2017 Jul;313(1):C68-C79. [\[Crossref\]](#)
39. Blundell C, Tess ER, Schanzer AS, et al. A microphysiological model of the human placental barrier. *Lab Chip*. 2016;16(16):3065-3073. [\[Crossref\]](#)
40. Lu HF, Zhou YC, Yang LT, et al. Involvement and repair of epithelial barrier dysfunction in allergic diseases. *Front Immunol*. 2024;15:1348272. [\[Crossref\]](#)
41. Yao Y, Shang W, Bao L, Peng Z, Wu C. Epithelial-immune cell crosstalk for intestinal barrier homeostasis. *Eur J Immunol*. 2024;54(6):e2350631. [\[Crossref\]](#)
42. Lialios P, Alimperti S. Role of E-cadherin in epithelial barrier dysfunction: implications for bacterial infection, inflammation, and disease pathogenesis. *Front Cell Infect Microbiol*. 2025;15:1506636. [\[Crossref\]](#)
43. Pat Y, Yazici D, D'Avino P, et al. Recent advances in the epithelial barrier theory. *Int Immunol*. 2024;36(5):211-222. [\[Crossref\]](#)
44. Meng EX, Verne GN, Zhou Q. Macrophages and gut barrier function: guardians of gastrointestinal health in post-inflammatory and post-infection responses. *Int J Mol Sci*. 2024;25(17):9422. [\[Crossref\]](#)
45. Spit M, Koo BK, Maurice MM. Tales from the crypt: intestinal niche signals in tissue renewal, plasticity and cancer. *Open Biol*. 2018;8(9):180120. [\[Crossref\]](#)
46. Zhang Q, Yu G, Jiang Y, et al. Dietary advanced glycation end-products promote food allergy by disrupting intestinal barrier and enhancing Th2 immunity. *Nat Commun*. 2025;16(1):4960. [\[Crossref\]](#)
47. Horowitz A, Chanez-Paredes SD, Haest X, Turner JR. Paracellular permeability and tight junction regulation in gut health and disease. *Nat Rev Gastroenterol Hepatol*. 2023;20(7):417-432. [\[Crossref\]](#)
48. Braskett M, Goleva E, Bronova I, et al. Lipidomic analysis of esophageal epithelia reveals a distinctive sphingolipid profile in eosinophilic esophagitis. *Allergy*. 2025;80(10):2849-2860. [\[Crossref\]](#)
49. Baur X, Akdis CA, Budnik LT, et al. Immunological methods for diagnosis and monitoring of IgE-mediated allergy caused by industrial sensitizing agents (IMExAllergy). *Allergy*. 2019;74(10):1885-1897. [\[Crossref\]](#)
50. Sun Y, Zhang J, Song W, Shan A. Vitamin E alleviates phoxim-induced toxic effects on intestinal oxidative stress, barrier function, and morphological changes in rats. *Environ Sci Pollut Res Int*. 2018;25(26):26682-26692. [\[Crossref\]](#)
51. Korkmaz RÜ, Omony J, Tan X, et al. The therapeutic potential of farm dust extracts in a mouse model of eosinophilic inflammation. *Allergy*. 2026;81(4):1173-1192. [\[Crossref\]](#)
52. Bakirtas A, Kiykim A, Baskin AK, et al. A survey on environmental protective and risk factors and awareness related to epithelial barrier integrity, microbiome and allergic diseases. *Allergy*. 2026;81(3):930-933. [\[Crossref\]](#)
53. Constant DA, Nice TJ, Rauch I. Innate immune sensing by epithelial barriers. *Curr Opin Immunol*. 2021;73:1-8. [\[Crossref\]](#)
54. Hansi RK, Ranjbar M, Whetstone CE, Gauvreau GM. Regulation of airway epithelial-derived alarmins in asthma: perspectives for therapeutic targets. *Biomedicines*. 2024;12(10):2312. [\[Crossref\]](#)
55. Zhao M, Ren K, Xiong X, et al. Epithelial STAT6 O-GlcNAcylation drives a concerted anti-helminth alarmin response dependent on tuft cell hyperplasia and Gasdermin C. *Immunity*. 2022;55(4):623-638.e5. Erratum in: *Immunity*. 2022;55(7):1327. [\[Crossref\]](#)
56. Sugita K, Soyka MB, Wawrzyniak P, et al. Outside-in hypothesis revisited: the role of microbial, epithelial, and immune interactions. *Ann Allergy Asthma Immunol*. 2020;125(5):517-527. [\[Crossref\]](#)
57. Goswami S, Zhang Q, Celik CE, Reich EM, Yilmaz ÖH. Dietary fat and lipid metabolism in the tumor microenvironment. *Biochim Biophys Acta Rev Cancer*. 2023;1878(6):188984. [\[Crossref\]](#)
58. Okumura R, Takeda K. The role of the mucosal barrier system in maintaining gut symbiosis to prevent intestinal inflammation. *Semin Immunopathol*. 2024;47(1):2. [\[Crossref\]](#)
59. Ornelas A, Dowdell AS, Lee JS, Colgan SP. Microbial metabolite regulation of epithelial cell-cell interactions and barrier function. *Cells*. 2022;11(6):944. [\[Crossref\]](#)
60. Yazici D, Ogulur I, Pat Y, et al. The epithelial barrier: the gateway to allergic, autoimmune, and metabolic diseases and chronic neuropsychiatric conditions. *Semin Immunol*. 2023;70:101846. [\[Crossref\]](#)
61. Neurath MF, Artis D, Becker C. The intestinal barrier: a pivotal role in health, inflammation, and cancer. *Lancet Gastroenterol Hepatol*. 2025;10(6):573-592. [\[Crossref\]](#)
62. Kløverpris HN, Leslie A, Goulder P. Role of HLA adaptation in HIV evolution. *Front Immunol*. 2016;6:665. [\[Crossref\]](#)
63. Venter C, Meyer RW, Greenhawt M, et al. Role of dietary fiber in promoting immune health-an EAACI position paper. *Allergy*. 2022;77(11):3185-3198. [\[Crossref\]](#)
64. Zeyneloglu C, Babayev H, Ogulur I, et al. The epithelial barrier theory proposes a comprehensive explanation for the origins of allergic and other chronic noncommunicable diseases. *FEBS Lett*. 2025;599(22):3208-3243. [\[Crossref\]](#)
65. Celebi Sözüner Z, Cevhertas L, Nadeau K, Akdis M, Akdis CA. Environmental factors in epithelial barrier dysfunction. *J Allergy Clin Immunol*. 2020;145(6):1517-1528. [\[Crossref\]](#)
66. Lima C, Falcão MAP, Rosa JGS, Disner GR, Lopes-Ferreira M. Pesticides and their impairing effects on epithelial barrier integrity, dysbiosis, disruption of the ahr signaling pathway and development of immune-mediated inflammatory diseases. *Int J Mol Sci*. 2022;23(20):12402. [\[Crossref\]](#)
67. Das Adhikari U, Froehle LM, Pipkin AN, et al. Immunometabolic defects of CD8+ T cells disrupt gut barrier integrity in people with HIV. *Cell*. 2025;188(20):5666-5679.e19. [\[Crossref\]](#)
68. Kayama H, Okumura R, Takeda K. Interaction between the microbiota, epithelia, and immune cells in the intestine. *Annu Rev Immunol*. 2020;38:23-48. [\[Crossref\]](#)
69. Tirelli V, Catone T, Turco L, Di Consiglio E, Testai E, De Angelis I. Effects of the pesticide clorpyrifos on an *in vitro* model of intestinal barrier. *Toxicol In Vitro*. 2007;21(2):308-313. [\[Crossref\]](#)
70. Zhao GP, Wang XY, Li JW, et al. Imidacloprid increases intestinal permeability by disrupting tight junctions. *Ecotoxicol Environ Saf*. 2021;222:112476. [\[Crossref\]](#)
71. Ilboudo S, Fouche E, Rizzati V, Toé AM, Gamet-Payrastre L, Guissou PI. *In vitro* impact of five pesticides alone or in

- combination on human intestinal cell line Caco-2. *Toxicol Rep.* 2014;1:474-489. [\[Crossref\]](#)
72. Ogulur I, Pat Y, Aydin T, et al. Gut epithelial barrier damage caused by dishwasher detergents and rinse aids. *J Allergy Clin Immunol.* 2023;151(2):469-484. [\[Crossref\]](#)
 73. Wang H, Ning X, Zhao F, Zhao H, Li D. Human organoids-on-chips for biomedical research and applications. *Theranostics.* 2024;14(2):788-818. [\[Crossref\]](#)
 74. Xian M, Wawrzyniak P, Rückert B, et al. Anionic surfactants and commercial detergents decrease tight junction barrier integrity in human keratinocytes. *J Allergy Clin Immunol.* 2016;138(3):890-893.e9. [\[Crossref\]](#)
 75. Donkers JM, Höppener EM, Grigoriev I, et al. Advanced epithelial lung and gut barrier models demonstrate passage of microplastic particles. *Microplastics and Nanoplastics.* 2022;2(1):6. [\[Crossref\]](#)
 76. Karaguzel D, Walewska A, Sarac BE, et al. Heat-not-burn tobacco aerosols induce immune dysregulation and barrier disruption comparable to conventional cigarettes. *Allergy.* 2026;81(3):781-795. [\[Crossref\]](#)
 77. Koutrakis P, Sax SN, Sarnat JA, et al. Analysis of PM₁₀, PM_{2.5}, and PM_{2.5-10} concentrations in Santiago, Chile, from 1989 to 2001. *J Air Waste Manag Assoc.* 2005;55(3):342-351. [\[Crossref\]](#)
 78. Kim S, Yi SM, Kim H, et al. Heterogeneity in the health effects of PM_{2.5} sources across the major metropolitan cities, South Korea: significance of region-specific management. *Environ Res.* 2024;263(Pt 3):120230. [\[Crossref\]](#)
 79. Niu C, Wang C, Wu G, et al. Toxic effects of the emamectin benzoate exposure on cultured human bronchial epithelial (16HBE) cells. *Environ Pollut.* 2020;257:113618. [\[Crossref\]](#)
 80. Guerbette T, Rioux V, Bostoën M, et al. Saturated fatty acids differently affect mitochondrial function and the intestinal epithelial barrier depending on their chain length in the *in vitro* model of IPEC-J2 enterocytes. *Front Cell Dev Biol.* 2024;12:1266842. [\[Crossref\]](#)
 81. Steelant B, Farré R, Wawrzyniak P, et al. Impaired barrier function in patients with house dust mite-induced allergic rhinitis is accompanied by decreased occludin and zonula occludens-1 expression. *J Allergy Clin Immunol.* 2016;137(4):1043-1053.e5. [\[Crossref\]](#)
 82. Wawrzyniak P, Wawrzyniak M, Wanke K, et al. Regulation of bronchial epithelial barrier integrity by type 2 cytokines and histone deacetylases in asthmatic patients. *J Allergy Clin Immunol.* 2017;139(1):93-103. [\[Crossref\]](#)
 83. Sugita K, Steer CA, Martinez-Gonzalez I, et al. Type 2 innate lymphoid cells disrupt bronchial epithelial barrier integrity by targeting tight junctions through IL-13 in asthmatic patients. *J Allergy Clin Immunol.* 2018;141(1):300-310.e11. [\[Crossref\]](#)
 84. Berni Canani R, Caminati M, Carucci L, Eguluz-Gracia I. Skin, gut, and lung barrier: physiological interface and target of intervention for preventing and treating allergic diseases. *Allergy.* 2024;79(6):1485-1500. [\[Crossref\]](#)
 85. D'Avino P, Kim J, Li M, et al. Distinct roles of IL-4, IL-13, and IL-22 in human skin barrier dysfunction and atopic dermatitis. *Allergy.* 2026;81(2):480-497. [\[Crossref\]](#)
 86. Plewa P, Pokwicka J, Bakinowska E, Kiełbowski K, Pawlik A. The Role of alarmins in the pathogenesis of asthma. *Biomolecules.* 2025;15(7):996. [\[Crossref\]](#)
 87. Dsilva A, Wagner A, Itan M, et al. Distinct roles for thymic stromal lymphopoietin (TSLP) and IL-33 in experimental eosinophilic esophagitis. *Allergy.* 2025;80(11):3095-3107. [\[Crossref\]](#)
 88. Rondinella D, Raoul PC, Valeriani E, et al. The detrimental impact of ultra-processed foods on the human gut microbiome and gut barrier. *Nutrients.* 2025;17(5):859. [\[Crossref\]](#)
 89. Pat Y, Yazici D, Zeyneloglu C, et al. Cellular stress, inflammation and barrier damage in gut epithelial cells caused by aspartame. *Allergy.* 2026;81(3):884-901. [\[Crossref\]](#)
 90. Giambò F, Teodoro M, Costa C, Fenga C. Toxicology and microbiota: how do pesticides influence gut microbiota? A review. *Int J Environ Res Public Health.* 2021;18(11):5510. [\[Crossref\]](#)
 91. Allam-Ndoul B, Castonguay-Paradis S, Veilleux A. Gut microbiota and intestinal trans-epithelial permeability. *Int J Mol Sci.* 2020;21(17):6402. [\[Crossref\]](#)
 92. Vieujean S, Caron B, Haghnejad V, et al. Impact of the exposome on the epigenome in inflammatory bowel disease patients and animal models. *Int J Mol Sci.* 2022;23(14):7611. [\[Crossref\]](#)
 93. Keremitçi D, Tuna Ö, Houdjedj A, Kazan H, Kaymaz Y. Transcriptional states of lung cancer microenvironment reveal macrophage subtype dynamics linked to disease progression. *J Immunol.* 2025;214(12):3273-3282. [\[Crossref\]](#)
 94. Unver N, Uluturk S, Tavukcuoglu E, Duymaz Yilmaz E, Kaymaz Y, Esendagli G. The impact of aspirin on PD-L1 expression and alteration of M2 polarization in non-small cell lung cancer. *Inflamm Res.* 2025;74(1):124. [\[Crossref\]](#)
 95. Saglam-Metiner P, Gulce-Iz S, Biray-Avci C. Bioengineering-inspired three-dimensional culture systems: organoids to create tumor microenvironment. *Gene.* 2019;686:203-212. [\[Crossref\]](#)
 96. Saglam-Metiner P, Goksel O, Goksel T, Yilmaz OH, Erdal E, Yesil-Celiktas O. Bioengineered humanoid-on-chip platforms: tools for evaluating the effects of environmental exposure on human physiological barriers. *Thorac Res Pract.* 2025;26(Suppl 1):1-3. [\[Crossref\]](#)
 97. Dogan B, Saglam-Metiner P, Goksel T, Yesil-Celiktas O. A NAMS-based microphysiological system for metastasis and mechanobiology studies. *Thorac Res Pract.* 2025;26(Suppl 1):4-6. [\[Crossref\]](#)
 98. Koornneef S, Horne FJ, Thio HB, et al. Advances in organ-on-a-chip technology to examine the impact of air pollutants on epithelial barrier tissues. *Environ Res.* 2025;285(Pt 1):122289. [\[Crossref\]](#)
 99. Filiz Y, Arslan Y, Duran E, et al. Decellularized plant-derived vasculature-on-a-chip interacting with breast cancer spheroids to evaluate a dual-drug therapy. *Appl Mater Today.* 2024;36(October 2023):102015. [\[Crossref\]](#)
 100. Filiz Y, Esposito A, De Maria C, Vozzi G, Yesil-Celiktas O. A comprehensive review on organ-on-chips as powerful preclinical models to study tissue barriers. *Prog Biomed Eng (Bristol).* 2024;6(4). [\[Crossref\]](#)
 101. Saglam-Metiner P, Duran E, Sabour-Takanlou L, Biray-Avci C, Yesil-Celiktas O. Differentiation of neurons, astrocytes, oligodendrocytes and microglia from human induced pluripotent stem cells to form neural tissue-on-chip: a neuroinflammation model to evaluate the therapeutic potential of extracellular vesicles derived from mesenchymal stem cells. *Stem Cell Rev Rep.* 2024;20(1):413-436. [\[Crossref\]](#)
 102. Saglam-Metiner P, Yanasik S, Odabasi YC, et al. ICU patient-on-a-chip emulating orchestration of mast cells and cerebral organoids in neuroinflammation. *Commun Biol.* 2024;7(1):1627. [\[Crossref\]](#)
 103. Ingber DE. Human organs-on-chips for disease modelling, drug development and personalized medicine. *Nat Rev Genet.* 2022;23(8):467-491. [\[Crossref\]](#)


104. Izadifar Z, Charrez B, Almeida M, et al. Organ chips with integrated multifunctional sensors enable continuous metabolic monitoring at controlled oxygen levels. *Biosens Bioelectron.* 2024;265:116683. [\[Crossref\]](#)
105. Yildiz-Ozturk E, Saglam-Metiner P, Yesil-Celiktas O. Lung carcinoma spheroids embedded in a microfluidic platform. *Cytotechnology.* 2021;73(3):457-471. [\[Crossref\]](#)
106. Kim K, Jeong S, Sung GY. Effect of periodical tensile stimulation on the human skin equivalents by magnetic stretching skin-on-a-chip (MSSC). *Biochip J.* 2022;16(4):501-514. [\[Crossref\]](#)
107. Nguyen HT, Rissanen SL, Peltokangas M, et al. Highly scalable and standardized organ-on-chip platform with TEER for biological barrier modeling. *Tissue Barriers.* 2024;12(4):2315702. [\[Crossref\]](#)
108. Ding X, Xu N, Zhang W, Wang P. Integrated microfluidic three-organ chip for real-time toxicity analysis of fluorotelomer alcohols in the gut-vascular-nerve axis. *Lab Chip.* 2025;25(23):6170-6176. [\[Crossref\]](#)
109. Abdessalam S, Hardy TJ, Pershina D, Yoon JY. A comparative review of organ-on-a-chip technologies for micro- and nanoplastics versus other environmental toxicants. *Biosens Bioelectron.* 2025;282:117472. [\[Crossref\]](#)
110. Sillé FCM, Smirnova L, Hartung T. Microphysiological systems as a pillar of the Human Exposome Project. *J Biol Chem.* 2025;301(11):110782. [\[Crossref\]](#)
111. Shay JES, Yilmaz ÖH. Dietary and metabolic effects on intestinal stem cells in health and disease. *Nat Rev Gastroenterol Hepatol.* 2025;22(1):23-38. [\[Crossref\]](#)
112. Li J, Dang SM, Sengupta S, et al. Organoid modeling reveals the tumorigenic potential of the alveolar progenitor cell state. *EMBO J.* 2025;44(6):1804-1828. [\[Crossref\]](#)
113. Yu B, Zhou D, Wang F, Chen X, Li M, Su J. Organoids for tissue repair and regeneration. *Mater Today Bio.* 2025;33:102013. [\[Crossref\]](#)
114. Liu MY, Chen B, Borji M, et al. Human airway and alveolar organoids from BAL fluid. *Am J Respir Crit Care Med.* 2024;209(12):1501-1504. [\[Crossref\]](#)
115. Mead BE, Hattori K, Levy L, et al. Screening for modulators of the cellular composition of gut epithelia via organoid models of intestinal stem cell differentiation. *Nat Biomed Eng.* 2022;6(4):476-494. [\[Crossref\]](#)
116. Imada S, Khawaled S, Shin H, et al. Short-term post-fast refeeding enhances intestinal stemness via polyamines. *Nature.* 2024;633(8031):895-904. [\[Crossref\]](#)
117. Lancaster MA, Renner M, Martin CA, et al. Cerebral organoids model human brain development and microcephaly. *Nature.* 2013;501(7467):373-379. [\[Crossref\]](#)
118. Saglam-Metiner P, Devamoglu U, Filiz Y, et al. Spatio-temporal dynamics enhance cellular diversity, neuronal function and further maturation of human cerebral organoids. *Commun Biol.* 2023;6(1):173. [\[Crossref\]](#)
119. Paşca SP, Arlotta P, Bateup HS, et al. A framework for neural organoids, assembloids and transplantation studies. *Nature.* 2025;639(8054):315-320. [\[Crossref\]](#)
120. Akbari S, Sevinç GG, Ersoy N, et al. Robust, long-term culture of endoderm-derived hepatic organoids for disease modeling. *Stem Cell Reports.* 2019;13(4):627-641. [\[Crossref\]](#)
121. Reza HA, Santangelo C, Iwasawa K, et al. Multi-zonal liver organoids from human pluripotent stem cells. *Nature.* 2025;641(8065):1258-1267. Erratum in: *Nature.* 2025;642(8067):E16. [\[Crossref\]](#)
122. Hu C, Yang S, Zhang T, et al. Organoids and organoids-on-a-chip as the new testing strategies for environmental toxicology-applications & advantages. *Environ Int.* 2024;184:108415. [\[Crossref\]](#)
123. Brandauer K, Schweinitzer S, Lorenz A, et al. Advances of dual-organ and multi-organ systems for gut, lung, skin and liver models in absorption and metabolism studies. *Lab Chip.* 2025;25(6):1384-1403. [\[Crossref\]](#)
124. Balistreri CR, Magro D, Jadavji NM. Insights into the toxic effects of micro-nano-plastics on the human brain and their relationship with the onset of neurological diseases: a narrative review. *Ageing Res Rev.* 2025;111:102836. [\[Crossref\]](#)
125. Bovard D, Sandoz A, Luettich K, et al. A lung/liver-on-a-chip platform for acute and chronic toxicity studies. *Lab Chip.* 2018;18(24):3814-3829. [\[Crossref\]](#)
126. Giammona A, Terribile G, Rainone P, et al. Effects of particulate air pollution exposure on lung-brain axis and related miRNAs modulation in mouse models. *Front Cell Dev Biol.* 2025;13:1526424. [\[Crossref\]](#)
127. Guo Y, Chen X, Gong P, Li G, Yao W, Yang W. The gut-organ-axis concept: advances the application of gut-on-chip technology. *Int J Mol Sci.* 2023;24(4):4089. [\[Crossref\]](#)
128. Gillan JL, Jaeschke L, Kuebler WM, Grune J. Immune mediators in heart-lung communication. *Pflügers Arch.* 2025;477(1):17-30. [\[Crossref\]](#)
129. Schimek K, Frentzel S, Luettich K, et al. Human multi-organ chip co-culture of bronchial lung culture and liver spheroids for substance exposure studies. *Sci Rep.* 2020;10(1):7865. [\[Crossref\]](#)
130. Li B, Tang Y, Huang Z, Ma L, Song J, Xue L. Synergistic innovation in organ-on-a-chip and organoid technologies: reshaping the future of disease modeling, drug development and precision medicine. *Protein Cell.* 2025:pwaf058. [\[Crossref\]](#)
131. Bridgeman L, Pamies D, Frangiamone M. Human organoids to assess environmental contaminants toxicity and mode of action: towards New Approach Methodologies. *J Hazard Mater.* 2025;497:139562. [\[Crossref\]](#)
132. Fadeel B, Alexander J, Antunes SC, et al. Editorial: five grand challenges in toxicology. *Front Toxicol.* 2025;6:1533238. [\[Crossref\]](#)
133. Eggestein A, Urban S, Hümmer E, et al. Towards real life exposure: nasal epithelial cell stimulation with pollen particle aerosols. *Environ Res.* 2025;286(Pt 1):122762. [\[Crossref\]](#)
134. Eggestein A, Rauer D, Herrmann SM, et al. A walk in the park: influence of natural co-exposure to grass pollen and fungal spores on nasal mycobiome and cytokine responses. *Clin Exp Allergy.* 2026. [\[Crossref\]](#)
135. Fredoc-Louison J, Cherièrè M, Rival B, De Araujo S, François S, Dekali S. Beyond cytotoxicity: pollutant mixtures elicit unconventional epithelial-fibroblast signaling in a human lung air-liquid interface co-culture model. *Front Toxicol.* 2025;7:1722968. [\[Crossref\]](#)
136. Zhao Z, Chen X, Dowbaj AM, et al. Organoids. *Nat Rev Methods Primers.* 2022;2:94. [\[Crossref\]](#)
137. Artegiani B, Hendriks D. Organoids from pluripotent stem cells and human tissues: when two cultures meet each other. *Dev Cell.* 2025;60(4):493-511. [\[Crossref\]](#)
138. Caragnano G, Monteduro AG, Rizzato S, Giannelli G, Maruccio G. Biological barrier models-on-chips: a novel tool for disease research and drug discovery. *Biosensors (Basel).* 2025;15(6):338. [\[Crossref\]](#)

139. Schellberg BG, Koppes RA, Koppes AN. Recent advances in integrated organ-chip sensing toward robust and user-friendly systems. *J Biomed Mater Res A*. 2025;113(2):e37876. [\[Crossref\]](#)
140. Picollet-D'hahan N, Zuchowska A, Lemeunier I, Le Gac S. Multiorgan-on-a-chip: a systemic approach to model and decipher inter-organ communication. *Trends Biotechnol*. 2021;39(8):788-810. [\[Crossref\]](#)
141. Abokor FA, Al Yazeedi S, Baher JZ, Cheung C, Sin DD, Osei ET. Exploring multi-organ crosstalk via the TissUse HUMIMIC chip system: lessons learnt so far. *Biotechnol Bioeng*. 2025;122(11):2951-2966. [\[Crossref\]](#)
142. Saglam-Metiner P, Yildirim E, Dincer C, Basak O, Yesil-Celiktas O. Humanized brain organoids-on-chip integrated with sensors for screening neuronal activity and neurotoxicity. *Mikrochim Acta*. 2024;191(1):71. [\[Crossref\]](#)
143. Skardal A. Grand challenges in organoid and organ-on-a-chip technologies. *Front Bioeng Biotechnol*. 2024;12:1366280. [\[Crossref\]](#)
144. Portela JMD, Paul P, Moriarty O, et al. Review on organs-on-chips for medicines safety assessment: a European regulatory perspective. *ALTEX*. 2026;43(1):98-112. [\[Crossref\]](#)
145. Maguire E, Winston J, Ellwood SH, et al. Modeling common Alzheimer's disease with high and low polygenic risk in human iPSC: a large-scale research resource. *Stem Cell Reports*. 2025;20(8):102570. [\[Crossref\]](#)



Letter to the Editor

Comment on: Letter to the Editor Regarding CT-based Prediction of Lung Cancer Histology

 Fani Tsolaki

Department of Medical Sciences, Aristotle University of Thessaloniki, Thessaloniki, Greece

Cite this article as: Tsolaki F. Comment on: Letter to the editor regarding CT-based prediction of lung cancer histology. *Thorac Res Pract.* 2026;27(3):195-195

KEYWORDS

COPD, diagnostic methods, lung cancer

Received: 09.03.2026

Accepted: 15.03.2026

Publication Date: 12.05.2026

DEAR EDITOR,

I perused the interesting article by Adrianta et al.¹ published in your esteemed journal regarding the CT-defined emphysema morphology as a predictor for histological subtypes of lung cancer. The authors concluded that certain morphological patterns can be associated with distinct histological subtypes (e.g., centrilobular emphysema with adenocarcinoma). The benefits of developing this method are evident in cases where adequate biopsy specimen retrieval is not possible.

In this context, I would like to comment on the technique of micro-computed tomography,² which is a different method, sharing however the same rationale: to reach a histological diagnosis without pathological examination, based on specialized imaging modalities. The development of micro-computed tomography to the extent that its cost will be permissive and its radiation levels safe for the human organism will hopefully bring important novel applications in the diagnosis of malignant disease aiming at accurate diagnosis without the need for interventional or surgical tissue retrieval.

Footnotes

Conflict of Interest: No conflict of interest was declared by the author.

Financial Disclosure: The author declared that this study received no financial support.

REFERENCES




1. Adrianta FA, Erawati DR, Pratiwi SD, Setijowati N. CT-defined emphysema morphology as a predictor for histological subtypes of lung cancer: a single-center retrospective study. *Thorac Res Pract.* 2026;27(2):103-108. [\[Crossref\]](#)
2. Katsamenis OL, Olding M, Warner JA, et al. X-ray micro-computed tomography for nondestructive three-dimensional (3D) X-ray histology. *Am J Pathol.* 2019;189(8):1608-1620. [\[Crossref\]](#)

Corresponding author: Fani Tsolaki, MD, MSc, PhD, e-mail: ftsola@auth.gr



Letter to the Editor

Response to: Letter to the Editor Regarding CT-based Prediction of Lung Cancer Histology

 Fadlan Adima Adrianta¹,  Dini Rachma Erawati¹,  Suryanti Dwi Pratiwi²,  Nanik Setijowati³

¹Department of Radiology, Faculty of Medicine, Universitas Brawijaya, Dr. Saiful Anwar Regional General Hospital, Malang, Indonesia

²Department of Pulmonology and Respiratory Medicine, Faculty of Medicine, Universitas Brawijaya, Dr. Saiful Anwar Regional General Hospital, Malang, Indonesia

³Department of Public Health and Preventive Medicine, Faculty of Medicine, Universitas Brawijaya, Malang, Indonesia

Cite this article as: Adrianta FA, Erawati DR, Pratiwi SD, Setijowati N. Response to: letter to the editor regarding CT-based prediction of lung cancer histology. *Thorac Res Pract.* 2026;27(3):196-197

KEYWORDS

Lung cancer, emphysema, computed tomography, imaging biomarkers, radiomics

Received: 31.03.2026

Accepted: 05.04.2026

Publication Date: 12.05.2026

DEAR EDITOR,

We sincerely thank the author for the thoughtful comments and for highlighting emerging imaging approaches regarding our recently published article entitled “CT-defined Emphysema Morphology as a Predictor for Histological Subtypes of Lung Cancer: A Single-center Retrospective Study.” We greatly appreciate the opportunity to further discuss the evolving role of imaging in the noninvasive characterization of lung cancer.

We fully agree with the author that advanced imaging techniques, such as micro-computed tomography (micro-CT), play an important role in bridging imaging and histopathology. Recent developments have demonstrated that micro-CT can provide nondestructive three-dimensional “X-ray histology” with micrometer-scale resolution, offering detailed microarchitecture which further can predict histological characteristic of lung disease.¹ In this regard, both approaches—micro-CT and clinical CT-based analysis—share an overarching goal: to enhance imaging’s ability to reflect underlying tumor biology and to potentially reduce reliance on invasive diagnostic procedures.

Although micro-CT is primarily applied in *ex vivo* settings under controlled experimental conditions, our study focused on routinely available clinical CT imaging to identify radiologic phenotypes associated with histological subtypes of lung cancer. From a practical clinical perspective, such approaches may offer immediate applicability, particularly in situations where tissue sampling is limited, contraindicated, or technically challenging.²

Within this broader framework, CT-based imaging biomarkers—such as emphysema morphology evaluated in our study—represent a complementary strategy in the continuum of imaging research. Increasingly, quantitative imaging approaches, including radiologic phenotyping and radiomics-based analyses, are being explored to further strengthen the link between imaging features and tumor biology.³⁻⁵ Future integration of high-resolution experimental imaging, quantitative imaging analysis, and radiologic–pathologic correlation may provide a more comprehensive understanding of lung cancer heterogeneity.

We thank the author for contributing to this important discussion and for emphasizing the potential of advanced imaging technologies to advance noninvasive diagnostic strategies.

Corresponding author: Fadlan Adima Adrianta, MD, e-mail: adimaadrianta@gmail.com

Footnotes**Authorship Contributions**

Concept: F.A.A., D.R.E., S.D.P., N.S., Design: F.A.A., D.R.E., S.D.P., N.S., Literature Search: F.A.A., D.R.E., S.D.P., N.S., Writing: F.A.A., D.R.E.

Conflict of Interest: No conflict of interest was declared by the authors.

Financial Disclosure: The authors declared that this study received no financial support.

REFERENCES

1. Katsamenis OL, Olding M, Warner JA, et al. X-ray micro-computed tomography for nondestructive three-dimensional (3D) X-ray histology. *Am J Pathol.* 2019;189(8):1608-1620. [\[Crossref\]](#)
2. Adrianta FA, Erawati DR, Pratiwi SD, Setijowati N. CT-defined emphysema morphology as a predictor for histological subtypes of lung cancer: a single-center retrospective study. *Thorac Res Pract.* 2026;27(2):103-108. [\[Crossref\]](#)
3. Lambin P, Rios-Velazquez E, Leijenaar R, et al. Radiomics: extracting more information from medical images using advanced feature analysis. *Eur J Cancer.* 2012;48(4):441-446. [\[Crossref\]](#)
4. Aerts HJWL, Velazquez ER, Leijenaar RTH, et al. Corrigendum: decoding tumour phenotype by noninvasive imaging using a quantitative radiomics approach. *Nat Commun.* 2014;5:4644. [\[Crossref\]](#)
5. Gillies RJ, Kinahan PE, Hricak H. Radiomics: images are more than pictures, they are data. *Radiology.* 2016;278(2):563-577. [\[Crossref\]](#)